INFORMATION TO USERS

This manuscript has been reproduced from the microfilm master. UMI films the text directly from the original or copy submitted. Thus, some thesis and dissertation copies are in typewriter face, while others may be from any type of computer printer.

The quality of this reproduction is dependent upon the quality of the copy submitted. Broken or indistinct print, colored or poor quality illustrations and photographs, print bleedthrough, substandard margins, and improper alignment can adversely affect reproduction.

In the unlikely event that the author did not send UMI a complete manuscript and there are missing pages, these will be noted. Also, if unauthorized copyright material had to be removed, a note will indicate the deletion.

Oversize materials (e.g., maps, drawings, charts) are reproduced by sectioning the original, beginning at the upper left-hand corner and continuing from left to right in equal sections with small overlaps.

Photographs included in the original manuscript have been reproduced xerographically in this copy. Higher quality 6" x 9" black and white photographic prints are available for any photographs or illustrations appearing in this copy for an additional charge. Contact UMI directly to order.

ProQuest Information and Learning
300 North Zeeb Road, Ann Arbor, MI 48106-1346 USA
800-521-0600

Reproduced with permission of the copyright owner. Further reproduction prohibited without permission.

NOTE TO USERS

This reproduction is the best copy available.

UMI®

Reproduced with permission of the copyright owner. Further reproduction prohibited without permission.

National Library of Canada
Bibliothèque nationale du Canada

Acquisitions and Bibliographic Services
Acquisitions et services bibliographiques

395 Wellington Street
Ottawa ON K1A 0N4
Canada

395, rue Wellington
Ottawa ON K1A 0N4
Canada

Your file Votre référence

Our file Notre référence

The author has granted a non-exclusive licence allowing the National Library of Canada to reproduce, loan, distribute or sell copies of this thesis in microform, paper or electronic formats.

L'auteur a accordé une licence non exclusive permettant à la Bibliothèque nationale du Canada de reproduire, prêter, distribuer ou vendre des copies de cette thèse sous la forme de microfiche/film, de reproduction sur papier ou sur format électronique.

The author retains ownership of the copyright in this thesis. Neither the thesis nor substantial extracts from it may be printed or otherwise reproduced without the author's permission.

L'auteur conserve la propriété du droit d'auteur qui protège cette thèse. Ni la thèse ni des extraits substantiels de celle-ci ne doivent être imprimés ou autrement reproduits sans son autorisation.

0-612-60873-5

Canada

Reproduced with permission of the copyright owner. Further reproduction prohibited without permission.

Self-Consistent Driven Bloch Oscillations in Excitonic Wannier-Stark Ladder

by

L. Yang

Submitted to the Department of Physics
in partial fuLfiUment of the requirements for the degree of

Master of Science

at the

LAKEHEAD UNIVERSITY

August 2001

(c) Lijun Yang, 2001

The author hereby grants to Lakehead University permission to reproduce and to distribute copies of this thesis document in whole or in part.

Signature of Author.....

Certified by.

Marc M. Dignam
Assistant Professor of Physics
Thesis upervisor

Accepted by.

[. Gallagher
Assistant Professor, Department Committee on Graduate Students

Reproduced with permission of the copyright owner. Further reproduction prohibited without permission.

Self-Consistent Driven Bloch Oscillations in Excitonic Wannier-Stark Ladder

by

L. Yang

Submitted to the Department of Physics
on 7 August 2001, in partial fulfillment of the
requirements for the degree of
Master of Science

Abstract

In this thesis, we present a theoretical model of Self-consistent driven Bloch oscillations (SCD BO) of different types of charge carriers in biased semiconductor superlattices photoexcited via ultra-short near-bandgap optical pulses. In this work, we wish to assess the influence of the unbound continuum excitonic states on the 1s excitons. This is modelled by calculating the full dynamics of 1s excitons and free electron-hole pairs, including the Coulomb interaction in a mean-field approximation. All the calculations are based on a recently-developed Quasi-bosonic treatment, by which we can study SCD BO to infinite order in optical field without loosing the crucial intraexcitonic electron-hole correlations. The interaction of 1s excitons with free electron-hole pairs is studied in both coherent and non-coherent systems. The numerical results obtained are found to be partially in agreement with the experimental results reported by *F. Lõser et al.* [Phys. Rev. Lett. **85**, 4763 (2000)]. However, we find several serious discrepancies that indicate that a more complete treatment may have to be adopted in future work. Despite this, the work in this thesis provides some useful insights to the coherent response of photoexcited semiconductor superlattices, and lays the ground work for future study.

Thesis Supervisor: Marc M. Dignam
Title: Assistant Professor of Physics

Reproduced with permission of the copyright owner. Further reproduction prohibited without permission.

Contents

Reproduced with permission of the copyright owner. Further reproduction prohibited without permission.

Reproduced with permission of the copyright owner. Further reproduction prohibited without permission.

List of Figures

Reproduced with permission of the copyright owner. Further reproduction prohibited without permission.

Reproduced with permission of the copyright owner. Further reproduction prohibited without permission.

List of Tables

Reproduced with permission of the copyright owner. Further reproduction prohibited without permission.

Acknowlegement

First of all, I would like to express my sincere gratitude to Dr. Marc M. Dignam for his great help in completing this thesis. I will treasure all the pleasant and unforgettable studying experiences with him during the past two years. I must say that I benefit quite a lot from his solid background on quantum mechanics and photonics. His rigorous working style will have a positive influence on the rest of my life. Without his help, I might have no chance to get access to the fields in which I am very interested. His patience, understanding and guidance account for every progress I made in my study period. I will never forget the friendly hospitality of him and his wife Suzanne upon my arrival in Canada and during my study period. Also, I will never forget the scene that he picked me up at airport at midnight, which made me, who never went out of his home country before, feel at home.

Many thanks to Dr. M. H. Hawton and Dr. V. V. Paranjape. I learned a lot from the courses they instructed and from many insightful discussions with them. I will remember their kindness to me for all my life.

I would like to thank Dr. M. C. Gallagher and Dr. W. J. Keeler for all their help in my study period in Lakehead University.

I am grateful for the friendly help from graduate students J. M. Lachaine and M. Sawler.

I greatly appreciate all the help from the Department of Physics in Queen's University, where I have spent one year as a visiting graduate student. Particularly, I want to thank Bing Wang for all his help before and after I arrived at Queen's University.

Finally, I wish to extend my thanks to my wife Jie An for her undertaking all the work in bringing up our daughter Bingying Yang in China when I am away.

Reproduced with permission of the copyright owner. Further reproduction prohibited without permission.

Chapter 1

Introduction

The behavior of electrons in periodic potentials in the presence of external DC and AC electric fields has attracted a lot of attention over the past 60 years or so. One of the important effects studied in this area was Bloch Oscillations (BO). BO involve the dynamic behavior of electrons in a periodic potential in the presence of a uniform, static electric field. They were first predicted by Zener in 1934 based on Bloch's work [1, 2].

A simple semiclassical model can account for the basic features of Bloch oscillations. In this model, the time evolution of the position and wave vector of an electron in a given band are determined by the following semiclassical equations of motion [3]:

$$\dot{\mathbf{r}} = \mathbf{v}(\mathbf{k}) = \frac{1}{\hbar}\frac{\partial \varepsilon(\mathbf{k})}{\partial \mathbf{k}}, \tag{1.1}$$

$$\hbar\dot{\mathbf{k}} = -e\left[\mathbf{E}(\mathbf{r},t) + \frac{1}{c}\mathbf{v}(\mathbf{k}) \times \mathbf{H}(\mathbf{r},t)\right], \tag{1.2}$$

where $\mathbf{E}(\mathbf{r},t)$ and $\mathbf{H}(\mathbf{r},t)$ are the external electric and magnetic fields and $\varepsilon(\mathbf{k})$ is the dispersion relation for the given band. Consider now the 1D case with a uniform, static electric field $\mathbf{E} = F_0\hat{\mathbf{z}}$ and no magnetic field. If we assume a tight-binding dispersion relation of the form

$$\varepsilon(k_z) = \varepsilon_0 - \frac{\Delta}{2}\cos(k_z d), \tag{1.3}$$

Reproduced with permission of the copyright owner. Further reproduction prohibited without permission.

where Δ is the bandwidth. Then Eqs. (1.1) and (1.2) can be rewritten as

$$\dot{z}=v_z(k_z)=\frac{\Delta d}{2\hbar}\sin(k_z d), \tag{1.4}$$

$$\hbar\dot{k}_z=-eF_0. \tag{1.5}$$

Solving Eq. (1.5), we have,

$$k_z=k_0-\frac{eF_0 t}{\hbar}. \tag{1.6}$$

Substituting Eq. (1.6) into Eq. (1.4) gives

$$\begin{aligned}\dot{z} &= v_z(k_z)\\ &= \frac{\Delta d}{2\hbar}\sin\left(k_0 d-\frac{edF_0 t}{\hbar}\right)\\ &\equiv -\frac{\Delta d}{2\hbar}\sin\left(\omega_B t-k_0 d\right),\end{aligned} \tag{1.7}$$

where

$$\omega_B\equiv\frac{edF_0}{\hbar} \tag{1.8}$$

is called Bloch frequency. Finally, the time-dependent function $z(t)$ can be obtained by solving Eq. (1.7), i. e.,

$$\begin{aligned}z &= z_0+\frac{\Delta d}{2\hbar\omega_B}\cos(\omega_B t-k_0 d)\\ &\equiv z_0+L\cos(\omega_B t-k_0 d),\end{aligned} \tag{1.9}$$

where $L\equiv\frac{\Delta d}{2\hbar\omega_B}=\frac{\Delta}{2eF_0}$ is the so called Wannier-Stark localization length. It can be seen from Eq. (1.9) that in configuration space, the electron is localized, oscillating back and forth from its initial position to an end point, with the distance between the two points being inversely proportional to the field strength.

The semiclassical model provides an intuitive way of understanding the basic principles of BO and is useful in estimating the most important features of a system before complete analysis is followed. However, at high fields, the validity of a semiclassical approach to derive the electronic motion is doubtful. *James* argued [4], already in 1949, that in a solid an electric

Reproduced with permission of the copyright owner. Further reproduction prohibited without permission.

field would break the continuum of band states into a series of levels with an equidistant energy separation proportional to the field. When the separation between these states is larger than their broadening, then a quantum-mechanical approach rather than a semiclassical approach is necessary [5]. A Semiclassical model will also encounter problems when it is used to describe the BO in superlattices [6].

Beyond the above semiclassical model, BO correspond actually to the behavior of a wavepacket that consists of a superposition of stationary states of the electron in the static field. These stationary states are known as the Wannier-Stark ladder (WSL). After *James*, *Wannier* later studied systematically the motion of electrons in a periodic potential of period d in the presence of a constant electric field [7], showing that if $\psi(z)$ is a solution of the Schrödinger equation with energy E_0, then $\psi(z-nd)$ is also a solution of the equation, with energy E_0+neF_0d, where F_0 is the applied constant electric field and n is an integer. This set of solutions constitute the WSL of energy levels, whose separation, eF_0d, can be written in terms of the Bloch frequency ω_B as defined in Eq. (1.8), i. e., $eF_0d \equiv \hbar\omega_B$. Thus in BO the wavepacket is oscillating in configuration space with the intrinsic Bloch frequency ω_B, given by the energy separation of WSL levels.

From above arguments, it can be seen that the determination of the WSL states of a system is the most important basis for the study of BO. The knowledge people have about BO is virtually always in parallel with those about the WSL. In Chapter 2, we will review the approaches for determining the WSL.

We should mention here the definition and calculation of the polarization of bulk crystalline materials that is related to the BO discussed above. When periodic boundary conditions are used, the polarization is actually not well defined [8, 9]. This difficulty can be overcome by using the prescription of Blount for interband polarization, which is the usual approach for the seminconductor optical interaction. In addition, for neutral particles such as excitons discussed in this thesis, the matrix elements for intraband polarization become well defined. Electron-hole separation is well defined even if their center of mass is not.

Now let's turn our attention to the experimental evidence for the WSL and BO. Although the WSL was predicted way back to 1949, it was not experimentally observed until late 1980's. Several experiments in 1960's and 1970's [10, 11, 12, 13] were explained in terms of the formation

Reproduced with permission of the copyright owner. Further reproduction prohibited without permission.

of Stark ladders in bulk semiconductors. However, their results were not conclusive due to the smallness of the observed effects. The main problem with the bulk semiconductor is: for reasonable electric-field strength, scattering will destroy the coherences needed for forming either WSL or BO. This is all due to the small period of the crystal lattice, which is related inversely to the electric field for producing the BO. For a scattering time τ, the critical field that can produce BO is defined as $\frac{\hbar}{2\pi\tau ed}$, which is quite large a value (typically on the order of 10^6 kV/cm) [14] for typical crystal lattice constant d.

The situation in the early 1970's changed with the initial proposal by *Esaki* and *Tsu* that one could observe such effects in superlattices [15]. In semiconductor superlattices, because of their long periodicity and possible long scattering times, the critical fields could be orders of magnitude smaller [16, 17]. The first convincing demonstration of the existence of the WSL was obtained in photo-current experiments in GaAs-GaAlAs superlattices [18]. For a certain range of fields, the heavy-hole states in this material system are fully localized whereas the electron states are still partially extended. In the experiments, photo-current spectra were obtained by measuring the current as a function of the frequency of the applied CW light, which is nearly resonant with the bandgap. Because the current is proportional to the absorption, the current spectra is closely related to the absorption spectra of the system. Therefore, peaks occur in the photo-current at frequencies corresponding to the transitions from a $n = 0$ hole state to $n = 0, \pm 1, \pm 2...$ states, with the strength of a current peak being proportional to the electron-hole overlap. Thus the well-defined photo-current spectra, where the spectral lines would be equidistant in energy with separation being the Stark energy, $\hbar\omega_B$, constitute the evidence for the existence of a WSL. Other optical interband transitions involving WSL states have also been observed using optical techniques such as electro-reflectance [19] and direct absorption [20]. However, theoretical models based on single-particles can not explain such experimental phenomena as the sharp peaks in the photo-current, unequal ladder spacing, and absorption asymmetry which actually arise from the excitonic effect neglected in the non-interacting pictures. Thus to account for the carriers in this system requires a more complete theoretical model which includes excitonic effects, i. e., electron-hole Coulomb interaction [21]. The excitonic WSL will be discussed in detail in Chapter 2.

After the initial theoretical proposals for the observation of BO in superlattices by *Bastard*

Reproduced with permission of the copyright owner. Further reproduction prohibited without permission.

[22] and *Plessen* [23] etc., the first observations of BO by four-wave mixing in superlattices were made by *Feldmann et al.* and *Leo et al.* in 1992 [24, 25], about four years after the first conclusive observation of the WSL. Other approaches for observing BO include the measurement of the terahertz radiation given off by the oscillating dipole [26], and the observation of a shift of the Wannier-Stark ladder states due to the self-induced intraband dipole field [27, 28].

There are a number of approaches for treating the dynamics of electrons and holes in photoexcited semiconductor superlattices. One of the most common and successful approaches involves the Semiconductor Bloch Equations (SBEs) [29] - [35]. These equations enable one to treat the nonlinear optical responses in the presence of constant electric fields under full inclusion of the Coulomb interaction. In other words, the SBEs make it possible to evaluate the coherent effects to all orders in the optical field and include the Coulomb interaction. Within a density matrix formalism, this model reduces the infinite hierarchy via a Hartree-Fock decoupling scheme to only two-point correlations. Three important observables, electron densities, hole densities and polarizations can be obtained by solving the SBEs.

However, SBEs can run into problems due to the use of the random phase approximation (RPA). This approximation does not comprise systematic control criteria for the approximation with respect to the key experimentally controllable parameter: optical field strength [36, 37, 38]. Although descriptions neglecting higher order contributions are sometimes in good agreement with the experiments [39, 40, 41], there are still other experiments clearly marking the limits of SBEs treatment [42, 43, 44]. All these limitations are due to the fact that SBEs are based on an ill-controlled Hartree-Fock approximation. With SBEs, problems arise even to second-order in the optical field. The factorization procedure due to RPA results in incorrect decay rates and quantitatively incorrect behavior in the calculation of the intraband current [45]. Thus, although SBEs were initially derived to evaluate the coherent effects to any order in optical field, the factorization of higher order correlations into polarization and number parts by RPA makes the method in good agreement generally with only the lowest order optical response. Beyond the first order response, e.g. in the study of intraband polarization in superlattices, SBEs may encounter problems. This limitation of SBEs arises in essence from the RPA–like factorization, the validity of which needs justification in many cases. This will be discussed in some detail in Chapter 3.

Reproduced with permission of the copyright owner. Further reproduction prohibited without permission.

To overcome the difficulties encountered by the SBEs, an alternative approach called Dynamically Controlled Truncation (DCT), was derived by Axt *et al* [36, 37, 38]. While SBEs try to describe the coherent response to infinite order in optical field but lose correlations by factorization, DCT makes a compromise by maintaining correct correlations but describing the coherent response of a semiconductor to a prescribed order of the optical field. The idea of DCT relies on the observation that a complete calculation of the nonlinear optical response of a semiconductor to any prescribed order in the driving field can be achieved by considering only a finite set of electronic correlation functions [36, 37, 38]. SBEs and DCT predict similar results in many experimental situations. However, severe deviations or even contradictory results may occur in some cases when SBEs and DCT are employed respectively [44]. One important example is in fact the second-order response of a semiconductor superlattice in a static electric field, which is the system considered here. These different predictions are a direct consequence of the Hartree-Fock approximation in the SBEs, which replaces the long-lived fourth-order density-like source for the excitonic contributions in the equations of motion by a short-lived second-order transition-like amplitude. This replacement causes the loss of correlation within an electron-hole pair.

While DCT is very successful in accounting for experimental phenomena that SBEs can not explain, it has two main limitations. First, it is usually derived in a basis of non-interacting electrons and holes eigenstates in the absence of a DC field with some sort of phenomenological decay/dephasing. However, in the absence of the optical field, the eigenstates to which the system will relax are the excitonic states in a DC field. Thus, the non-interacting basis will not model the phenomenological dephasing in an appropriate way. The other limitation of DCT is: although it can be used to describe the coherent response to any order in optical field, in practice it has to be terminated to a prescribed finite order so as to maintain the correct correlation.

Based on SBEs, *Dignam* developed a set of equations of motion describing the coherent dynamics of excitons in a semiconductor superlattice in the presence of both constant and time-dependent electric fields [34]. Rather than employing the k_z-state basis as usually done in SBEs, the equations of motion is developed in a basis of single-particle one-band WSL states that make the basic physical effect of the terahertz field especially transparent. This was the

Reproduced with permission of the copyright owner. Further reproduction prohibited without permission.

first attempt trying to address the dynamics of such a system where both constant and AC fields are applied.

To address the problem with the non-interacting electrons and holes basis, *Hawton* and *Nelson* [45] developed a theory of quasibosonic excitons that is based on use of exciton creation operators to describe interband and intraband polarization. The resulting expansion in powers of the optical field is analogous to DCT but takes a simpler form. This was applied to the biased superlattice in an external terahertz field by *Lachaine et al.* [46]. *Dignam* and *Hawton* further developed a theory [47], also within the same excitonic basis and with bosonic treatment, that can describe the coherent response to infinite order in optical field but retain the crucial intraexcitonic electron-hole correlations. In Chapter 3, this theory will be briefly described.

Excitonic BO in photoexcited semiconductor superlattices are in essence the relative oscillatory motion of electron-hole pairs. According to the classical electromagnetic theory, these accelerated charge carriers will generate intraband polarization in the superlattice. The electric fields generated by this intraband polarization, which is in the terahertz regime, will inevitably influence the relative motion of electrons and holes that generate the fields. The first experiment showing the existence of terahertz radiation due to intraband polarization was made by *Waschke et al* [26]. Other experiments also showed that the self-induced terahertz fields would shift the energy level of the original WSL [27, 28].

Recently, experimental work has been done trying to address the problem of the Shapiro effect which is the analog of the corresponding effect in Josephson junctions. In the experiment, the BO were found to be accompanied by a coherent quasi-DC current that was attributed to the interaction of the charge carriers with the self-induced field [48]. This was observed by a quasi-linear change in the intraband polarization. The theoretical treatment of this effect in Ref. [48] required the transfer of energy between the coherent 1s excitons and a background incoherent plasma. This involved a vastly simplified semiclassical model for the plasma that clearly needs improvement. In an attempt to better understand the dynamics of the interaction of the coherent excitons with the continuum plasma, we here use a full quantum-mechanical model for both the 1s excitons and the continuum states.

In order to give a realistic description of BO in photoexcited semiconductor superlattices with the self-induced fields, a theoretical approach that can model both static and AC electric

Reproduced with permission of the copyright owner. Further reproduction prohibited without permission.

fields is necessary. As it turns out, the electric fields generated by charge carriers other than 1s excitons play a more important role in the interaction. In this thesis, we will try to model the influence of the unbound continuum excitonic states on the 1s excitons. This is one step further forward trying to describe the coherent effects in superlattices in a more realistic way. The excitons are to be self-consistent driven by the terahertz fields due to the polarization of excitons and unbound continuum excitonic states. The study of the interaction of excitons with self-induced fields requires the inclusion of at least 3rd order or above response to an optical field in the equations of motion [47]. We will treat the self-induced electric fields in a self-consistent way, which is equivalent to treating the response to infinite order in the optical field. The BO and its interaction with self-induced fields, hereafter referred to as self-consistent driven (SCD) BO , will be studied in detail in Chapter 4 and 5. This is different from the theoretical treatment for the system as in Refs. [34, 46], where the external terahertz field rather than the system-self-induced field, is applied. The work in this thesis will provide a basis for a more complete, realistic description for the BO in photoexcited semiconductor superlattices.

The plan of this thesis is as follows. A brief introduction to the approaches for calculating the WSL in semiconductor superlattices will be given in Chapter 2. The methods based on single-particle and excitonic pictures are to be introduced respectively. The calculated excitonic WSL states will be employed as the basis in solving problems concerning the dynamics of excitons and free electron-hole pairs in later chapters. In Chapter 3, the theoretical treatment of the excitonic dynamics in photoexcited semiconductor superlattices is presented. The time-dependent behavior of electrons and holes, rather than the stationary states discussed in Chapter 2, will be discussed in detail. First, the approaches involving SBEs are reviewed, and their shortcomings discussed in the context of determining the nonlinear optical response of a semiconductor superlattice in applied along-axis static and terahertz electric fields. Then, excitonic dynamics using the quasibosonic treatment is introduced and taken as the theoretical background for our SCD Bloch oscillations. In Chapter 4, the Hamiltonian for the free electron-hole pairs in the superlattice potential in the presence of the external optical, DC and terahertz electric fields will be derived. Then, the equations of motion for electron-hole pairs are obtained by using Heisenberg equations of motion. This constitutes the background for studying the influence of free pairs on excitons. In Chapter 5, the interaction between excitons

Reproduced with permission of the copyright owner. Further reproduction prohibited without permission.

and free electron-hole pairs will be studied in detail. The SCD effect, in which the electric fields due to charge carriers interact with these carriers themselves, is the main subject. The SCD phenomena in the coherent regime will be studied first and then followed by the more realistic cases in which there is dephasing. Energy conservation in the coherent regime and energy exchange in cases where there is dephasing, together with the driving effect of self-induced electric fields will be studied in SCD phenomena. Finally, in Chapter 6, we will summarize and give the conclusions of the thesis.

Reproduced with permission of the copyright owner. Further reproduction prohibited without permission.

Chapter 2

Wannier-Stark Ladder(WSL) in A Semiconductor Superlattice

2.1 Introduction

As already mentioned in Chapter 1, the study of the WSL is closely related to the study of Bloch Oscillations (BO). Calculating the stationary WSL states in a semiconductor superlattice is the most essential part in studying the dynamics of electrons and holes in this system. Only after these states are properly understood can we study dynamic behavior of electrons and holes on these states.

The effect of a static electric field on electronic states in solids is quite an old topic and has been studied theoretically since late 1940's [4, 7, 49]. However, the topic was intensively studied [50]-[62] only after the initial proposal of the superlattice by Esaki and Tsu in early 1970's [15]. After the first observation of a WSL in superlattices [18], several other experiments also unambiguously showed the existence of a WSL [19, 20, 63, 64, 65, 66].

A brief introduction to the approaches for calculating the WSL in semiconductor superlattices is presented in this chapter. The methods based on a single-particle picture and on an excitonic picture are introduced separately in two sections. The calculated excitonic and non-interacting electron-hole WSL states will be employed as the basis in solving problems concerning the dynamics of excitons and free pairs in later chapters.

Reproduced with permission of the copyright owner. Further reproduction prohibited without permission.

2.2 Calculating the Wannier-Stark Ladder in A Single-particle Picture

The method for calculating the WSL of superlattices belongs to the category of effective mass theory [67], or envelope function approximation, which is suitable for dealing with slowly-varying local potentials such as those in semiconductor superlattices, quantum wells, etc. This allows us to deal with the effects of the band-edge discontinuities at heterojunctions without worrying about the potential fluctuations that occur on the atomic scale.

The earliest calculation of WSL for superlattices was borrowed from the simple theory originally developed for bulk crystals [68] which can account for most features of the Stark-localization phenomenon in superlattices. For semiconductor superlattices, it was predicted long ago that a strong electric field would localize an electron within a period [69, 70]. A tight-binding formalism for the superlattice envelope wavefunctions also predicted the field-induced localization of the states and was used to calculate the electro-absorption, which revealed a blue shift of the absorption edge between the zero and high-field limits and oscillations periodic in the inverse of the field [50]. These general results were also obtained by employing other formalisms such as a variational calculation [71], a finite Kronig-Penney model with a superimposed linearly varying potential [72], and a split-time scheme [73].

In the early stages, most theoretical work for calculating WSL had been done in the single-particle picture, i.e. no effect of Coulomb interaction between electrons and holes was included. When working within the envelope function approximation and neglecting band nonparabolicities and valence-band mixing, it has been shown that [49, 74], within one-miniband (first superlattice minibands in either conduction or valence band) approximation, the eigenstates for non-interacting electrons in a static electric field, F_o, are spatially localized in the z-direction and have equal energy spacings of eF_od, where d is the period of the superlattice. The corresponding wavefunctions for the conduction band and valence band electrons in a static along-axis electric field have the forms [34]

$$\psi_n^{c,v}(\mathbf{r},\mathbf{k}) = \frac{1}{\sqrt{A}} e^{i\mathbf{k}\cdot\rho} \chi_n^{c,v}(z) u_o^{c,v}(\mathbf{r}), \tag{2.1}$$

where c (v) refers to conduction (valence) band electrons, $\mathbf{r}$ is a three-dimensional position

Reproduced with permission of the copyright owner. Further reproduction prohibited without permission.

vector, $\boldsymbol{\rho}$ is the corresponding two-dimensional position vector in the (x,y) plane, $\mathbf{k}$ is the two-dimensional in-plane wave vector, A is the in-plane normalization area, and the $u_o^{c,v}(\mathbf{r})$ are the periodic portions of the bulk Bloch functions at the conduction and valence band extrema respectively (assumed to be the same for both materials in the superlattice). The functions, $\chi_n^{c,v}(z) = \chi_n^{e,h}(z)$, are so-called WSL states, which are the eigenstates of the one-dimensional Hamiltonians,

$$H^{e,h}(z) = \frac{\partial}{\partial z}\frac{-\hbar^2}{2m_z^{e,h}(z)}\frac{\partial}{\partial z} + U^{e,h}(z) - q_{e,h}F_o z, \tag{2.2}$$

in the single-miniband approximation, where $m_z^{e,h}(z)$ is the layer-dependent along-axis effective mass for the electrons or holes, $U^{e,h}(z)$ is the superlattice potential experienced by the electrons or holes due to bandgap discontinuities (with $U^{e,h}(z) = 0$ in the wells), $q_e = -e$ and $q_h = e$ are the charges of the electrons and holes respectively, and e is the modulus of the charge on an electron. Within the one-miniband approximation, these WSL eigenstates can be expanded in the basis of miniband Wannier states, $a^\lambda(z)$, localized at different sites :

$$\chi_n^e(z) = \sum_m C_{m-n}^e a^c(z - md), \tag{2.3}$$

$$\chi_n^h(z) = \sum_m C_{m-n}^h a^v(z - md), \tag{2.4}$$

where the expansion coefficients satisfy the summation relations [34]:

$$\sum_n C_n^{e*} C_{n+p}^e = \delta_{p,0}, \tag{2.5}$$

$$\sum_n n C_n^{e*} C_{n+p}^e = \frac{-1}{eF_o d}\left[\varepsilon_p^e - \delta_{p,0}\varepsilon_0^e\right], \tag{2.6}$$

where $\varepsilon_p^e \equiv \frac{1}{N_z}\sum_{k_z} \varepsilon^e(k_z) e^{ik_z pd}$ is the p^{th} Fourier component of the along-axis energy dispersion, $\varepsilon^e(k_z)$, for the electron or hole miniband when applied static field $F_o = 0$.

In the nearest-neighbor tight-binding approximation, the WSL states in Eqs. (2.3) and (2.4) are replaced by the single-site groundstates and one finds that

$$C_{m-n}^{e,h} = J_{m-n}(\theta_{e,h}) \tag{2.7a}$$

Reproduced with permission of the copyright owner. Further reproduction prohibited without permission.

where $J_m(\theta_{e,h})$ is a Bessel function of the first kind of order m [34], and $\theta_{e,h} \equiv \Delta_{e,h}/2q_{e,h}F_o d$, where $\Delta_{e,h}$ is the bandwidth of the electron or hole miniband.

The single-particle WSL energies for electrons and holes are given respectively by

$$E^e_{n,\mathbf{k}} = E_{gap} + \frac{\hbar^2\mathbf{k}^2}{2m^e_{\|}(z)} + E^e_0 + eF_o nd \tag{2.8}$$

and

$$E^h_{n,\mathbf{k}} = \frac{\hbar^2\mathbf{k}^2}{2m^h_{\|}(z)} + E^h_0 - eF_o nd, \tag{2.9}$$

where E_{gap} is the bandgap of the bulk semiconductor in the wells, n is an integer, and $E_0^{e,h}$ are the $n = 0$ eigenenergies of the one-dimensional single-particle Hamiltonians, $H^{e,h}(z)$ of Eq. (2.2).

WSL based on the single-particle picture can account for many features in the optical transition experiment about semiconductor superlattices. We will use these states in Chapters 4 and 5 to treat the dynamics of continuum states. However, as already mentioned in Chapter 1, all experiments in which a Stark ladder has been identified have been performed on undoped semiconductor superlattices in which electrons and holes have been photoinjected. The resulting WSLs are therefore excitonic Stark ladders, rather than single-particle ladders. Moreover, WSL based on the single-particle picture can not account for some detailed effects in the optical transition experiment, such as the peaks in the absorption or photo-current spectra and the deviations from field linearity in the energy fan charts.

2.3 Excitonic WSL

In this section, we introduce the basic methods for calculating the excitonic WSL that include Coulomb interaction between electrons and holes. The consequences of the Coulomb interaction between an electron and a hole are particularly significant when an electric field is applied to a superlattice because of the strong modification of this interaction by the field. In the absence of the field, both electron and hole wavefunctions are delocalized and their interaction is similar to that in bulk semiconductors. However, under high fields the electron and hole wavefunctions are confined to single wells and their excitonic binding energies have been found to be greatly

Reproduced with permission of the copyright owner. Further reproduction prohibited without permission.

enhanced [63].

There are a variety of approaches for calculating excitonic WSL. For example, calculations that use numerically obtained electron and hole wavefunctions and one-parameter variational excitonic wavefunctions, with the basis limited to 1s exciton states, accounted well for the field-induced enhancement of the binding energy [75]. A simpler model, based on a tight-binding approach for the electronic wavefunctions, found a binding energy that varied quadratically with the confinement factor of the electrons [60]. An alternative formalism, using a scattering phase-shift treatment of the Stark states, has yielded results also in good agreement with experimental data [76]. A more elaborate calculation, in which the 1s exciton eigenstates of the superlattices are expanded in terms of localized exciton wavefunctions, has explained many of the low-field effects observed experimentally, e.g., the absorption asymmetry of the upper and lower branches of the Stark ladder and the nonlinear dependence of the excitonic Stark transitions on the strength of the field [21, 59]. This approach is to be used to calculate the excitonic WSL used in later chapters as the basis in studying dynamics of electrons and holes in semiconductor superlattices. A brief outline of this approach is presented next.

First, two important theories are used in the following calculation of exciton states in semiconductor superlattices: tight-binding theory and effective mass theory. The tight-binding method, which was used by F. Bloch in 1929 [1], is basically a method that uses the linear combination of atomic orbitals as the basis. The central idea of this method is the fact that in some cases, e.g. insulator and semiconductor, the electronic state of the solid is not so different from the electronic state of the free atom. Thus, according to the superposition principle in quantum mechanics, we may use the linear combination of these atomic states to approximate the electronic states in the corresponding solid. It is an especially good approximation for low orbitals that has not too large overlap between atomic orbitals [77]. In the following calculation, the eigenstates of the systems are expanded in terms of localized exciton wavefunctions, which is in the spirit of the tight-binding procedure. The second important theory employed in the following method is effective-mass theory, which is very useful in dealing with the problem where a slowly-varying local potential is involved.

Using the effective mass theory, the Hamiltonian for the envelope function describing an

Reproduced with permission of the copyright owner. Further reproduction prohibited without permission.

exciton in the presence of a static electric field may be written as [58, 59]

$$H(z_e, z_h, \boldsymbol{\rho}) = H_0(z_e, z_h, \boldsymbol{\rho}) + U^e(z_e) + U^h(z_h) + eF_0 z, \tag{2.10}$$

where $U^e(z_e)[U^h(z_h)]$ is the superlattice potential for the electron (hole) and H_0 takes the form

$$\begin{aligned} H_0(z_e, z_h, \boldsymbol{\rho}) \;=\; & -\frac{\hbar^2}{2m_{\|}}\frac{1}{\boldsymbol{\rho}}\frac{\partial}{\partial\boldsymbol{\rho}}\left[\boldsymbol{\rho}\frac{\partial}{\partial\boldsymbol{\rho}}\right] - \frac{\hbar^2}{2}\frac{\partial}{\partial z_e}\frac{1}{m^*_{ez}(z_e)}\frac{\partial}{\partial z_e} \\ & -\frac{\hbar^2}{2}\frac{\partial}{\partial z_h}\frac{1}{m^*_{hz}(z_h)}\frac{\partial}{\partial z_h} - \frac{e^2}{\epsilon(\boldsymbol{\rho}^2 + z^2)^{1/2}}. \end{aligned} \tag{2.11}$$

Here, z_e and z_h are the z coordinates of the electron and hole respectively, $z \equiv z_e - z_h$, $\boldsymbol{\rho}$ denotes the electron-hole separation in the xy plane. The layer-dependent transverse electron-hole-reduced effective mass $m_{\|}$ is defined by

$$\frac{1}{m_{\|}} \equiv \frac{1}{m_{e\|}(z_e)} + \frac{1}{m_{h\|}(z_h)}, \tag{2.12}$$

where $m_{e\|}(z_e)$ and $m_{h\|}(z_h)$ are the transverse electron and hole effective masses respectively. The layer-dependent effective mass for the electron and hole in the z direction is denoted by $m_{ez}(z_e)$ and $m_{hz}(z_h)$ respectively. Finally, ϵ is an average static dielectric constant of the structure, e is the modulus of the charge on an electron, and F_0 is the applied static electric field strength.

Note that the field term in Eq. (2.10) is dependent only on z. Thus the Hamiltonian $H(z_e, z_h, \boldsymbol{\rho})$ is invariant under simultaneous translation of the electron and hole coordinates by nd even in the presence of an applied electric field, where d is the superlattice period and n is an integer. This is equivalent to a translation of the exciton center of mass by nd. Therefore, the exciton wavefunction is not Stark localized but completely delocalized. This is not so surprising because the exciton is a neutral particle.

Using the above translation symmetry, the exciton envelope function can be written as [21]

$$\psi^q_n(z_e, z_h, \boldsymbol{\rho}) = \frac{1}{N_z}\sum_m e^{iqmd} W_n(\boldsymbol{\rho}, z_e - md, z_h - md) \tag{2.13}$$

where m is an integer, q is the exciton wave number in the z direction, and $W_n(\boldsymbol{\rho}, z_e, z_h)$ is an

Reproduced with permission of the copyright owner. Further reproduction prohibited without permission.

electric-field-dependent exciton Wannier function. The index n is a discrete quantum number of longitudinal motion that, in the high field limit, gives the approximate separation of the electron and hole in units of the SL period.

The problem now is to find expressions for the exciton Wannier functions $W_n(\boldsymbol{\rho}, z_e, z_h)$ in Eq. (2.13). Those states for which the exciton Wannier functions are well localized will be calculated because they are the states of interest, i.e., they are the ones which are optically created. *Dignam* and *Sipe* [21] expanded the Wannier functions $W_n(\boldsymbol{\rho}, z_e, z_h)$ in terms of the eigenstates of the electric-field-dependent two-well Hamiltonian. These eigenstates are obtained variationally by using the wave function

$$\Phi_l^{\gamma}(z_e, z_h, \boldsymbol{\rho}) \equiv \varphi_l^{\gamma}(\boldsymbol{\rho}) \mathrm{f}^e(z_e - ld) \mathrm{f}^h(z_h). \tag{2.14}$$

The state, $\Phi_l^{\gamma}(z_e, z_h, \boldsymbol{\rho})$, is an approximate eigenstate of a two-well Hamiltonian which only includes the band-edge potential for the hole well at $z_h = 0$ and the electron well at $z_e = ld$ along with the electron-hole Coulomb interaction. The quantum number γ (which could be 1s, 2p etc.) is the in-plane excitation quantum number for the two-well eigenstate. The functions $\mathrm{f}^e(z_e)$ and $\mathrm{f}^h(z_h)$ are the single-particle electron and hole 1D eigenstates respectively of isolated wells centered at $z = 0$. In practice, the $\varphi_l^{\gamma}(\boldsymbol{\rho})$ are variational functions with variational parameters that are determined by minimizing the energy of the given two-well exciton Hamiltonian as described in Ref. [21].

By expanding the Wannier functions $W_n(\boldsymbol{\rho}, z_e, z_h)$ in terms of the eigenfunction $\Phi_l^{\gamma}(z_e, z_h, \boldsymbol{\rho})$, the exciton envelope wavefunction in Eq. (2.13) is written as [21]

$$\psi_n^q(z_e, z_h, \boldsymbol{\rho}) = \frac{1}{N_z} \sum_{m,l} B_{l,\gamma}^{n,q} e^{iqmd} \Phi_l^{\gamma}(z_e - md, z_h - md, \boldsymbol{\rho}) \tag{2.15}$$

where $B_{l,\gamma}^{n,q}$ are expansion coefficients determined by diagonalizing the full exciton Hamiltonian in the two-well basis.

The excitonic envelope wavefunctions in Eq. (2.15) provide a more realistic description of the WSL in superlattices than the wavefunctions obtained within the single-particle picture. They can account for many detailed experimental aspects that the WSL states based on a single-particles picture can not explain. In this work, we will only consider the 1s excitons

Reproduced with permission of the copyright owner. Further reproduction prohibited without permission.

(γ =1s), for which [21]

$$\Phi_l^{1s}(z_e, z_h, \boldsymbol{\rho}) \equiv \left[\frac{2}{\pi}\right]^{1/2} \lambda e^{-\lambda\rho} \mathrm{f}^e(z_e - ld)\mathrm{f}^h(z_h), \tag{2.16}$$

where λ is the variational parameter which depends on l. Using the collective index μ to replace (n, q) and considering only 1s excitons, we obtain the exciton envelope function with zero center of mass motion (This is good approximation because we consider only excitons that are optically created.)

$$\psi^{\mu}(z_e, z_h, \boldsymbol{\rho}) = \frac{1}{N_z} \sum_{m,l} B^{\mu}_{l,1s} \Phi_l^{1s}(z_e - md, z_h - md, \boldsymbol{\rho}). \tag{2.17}$$

Considering only 1s excitons in a superlattice system can be justified by the fact that 1s excitons dominate the linear optical response, and are the only excitonic states with an appreciable binding energy. Some other more complete theories [78, 79, 80] that go beyond 1s excitons recently have been used to calculate the linear optical response. However, they are extremely complicated and are not suitable for calculating nonlinear dynamics.

Reproduced with permission of the copyright owner. Further reproduction prohibited without permission.

Chapter 3

Dynamics of Excitons Near Semiconductor Band Edge

3.1 Introduction

In this chapter, we present the theoretical treatment of the coherent effects in photoexcited semiconductor superlattices, where excitons are created by using ultrashort optical pulses with photon energies roughly equal to the bandgap energy. In other words, we will be studying the time-dependent behavior of electrons and holes rather than the stationary states discussed in Chapter 2. The stationary states determined in Chapter 2 will be employed as the basis states for solving equations of motion.

There have been a relatively large number of theoretical treatments of the coherent dynamics in semiconductor nanostructures over the past 15 years, with the most popular methods originated from the application of the Semiconductor Bloch Equations (SBEs) [29] - [35] . In recent years, some other approaches have been developed to try to overcome the limitations of these methods based on the SBEs. These approaches include those based on the Dynamically Controlled Truncation (DCT) technique [37, 38] and those based on the Quasi-Bosonic treatment of Hawton and Nelson [45, 47].

A brief review of the theoretical treatments of the coherent response of photoexcited semiconductor superlattices is given in Section 3.2. The SBEs approach is first discussed, and its shortcomings discussed in the context of determining the nonlinear optical response of a semi-

Reproduced with permission of the copyright owner. Further reproduction prohibited without permission.

conductor superlattice in applied along-axis static and terahertz electric fields. Then, the DCT approach to the coherent dynamics is briefly introduced. Its advantages in comparison with the SBEs and its disadvantages in the basis choice is discussed in detail. Finally, excitonic dynamics using the quasibosonic treatment is introduced in Section 3.3 [45, 47]. Apart from the applied terahertz field, the terahertz field induced by the polarization of charge carriers will also be included in this treatment. This final treatment, which is derived in a more appropriate basis and could be used to analyze the coherent response to any order in the optical field, constitutes the theoretical background for the SCD Bloch oscillations of Chapter 4 and 5.

3.2 Review of the Excitonic Dynamics in Semiconductor Superlattices

Although the linear optical response of a photoexcited semiconductor in the presence of static electric fields and Coulomb interaction has been relatively well understood for a long time, there were no complete theoretical treatments of the nonlinear coherent response for such a system until the early 1990's. Based on semiconductor Bloch equations (SBEs), *Koch* and *Meier et al.* developed a method to consistently describe the coherent optical phenomena in semiconductors [29] - [35]. The dynamic equations obtained, hereafter referred to as SBEs, include the Coulomb interaction in the Hartree-Fock approximation, and beyond, depending on the treatment of the carrier relaxation and dephasing processes. Beyond perturbation theory, SBEs make it possible to evaluate the coherent response to infinite order in the optical field. SBEs were derived from the following Hamiltonian, which is based on a two-band approximation[29, 31]

$$H = H_{s-p} + H_{coul} + H_{dip} \tag{3.1}$$

where H_{s-p}, H_{coul} and H_{dip} are single-particle, Coulomb and dipole interacting Hamiltonians and respectively take the forms,

$$H_{s-p} = \sum_{\mathbf{k}} \left[E_{c,\mathbf{k}} a^{\dagger}_{c,\mathbf{k}} a_{c,\mathbf{k}} + E_{v,\mathbf{k}} a^{\dagger}_{v,\mathbf{k}} a_{v,\mathbf{k}} \right], \tag{3.2}$$

Reproduced with permission of the copyright owner. Further reproduction prohibited without permission.

$$H_{coul} = \frac{1}{2} \sum_{\mathbf{k},\mathbf{k}',\mathbf{q}\neq 0} V_{\mathbf{q}} a^{\dagger}_{c,\mathbf{k}+\mathbf{q}} a^{\dagger}_{c,\mathbf{k}'-\mathbf{q}} a_{c,\mathbf{k}'} a_{c,\mathbf{k}} + a^{\dagger}_{v,\mathbf{k}+\mathbf{q}} a^{\dagger}_{v,\mathbf{k}'-\mathbf{q}} a_{v,\mathbf{k}'} a_{v,\mathbf{k}} + 2a^{\dagger}_{c,\mathbf{k}+\mathbf{q}} a^{\dagger}_{v,\mathbf{k}'-\mathbf{q}} a_{v,\mathbf{k}'} a_{c,\mathbf{k}} \tag{3.3}$$

and

$$H_{dip} = -\sum_{\mathbf{k}} \mu \mathbf{E}_{op}(\mathbf{t}) \left[a^{\dagger}_{c,\mathbf{k}} a_{v,\mathbf{k}} + a^{\dagger}_{v,\mathbf{k}} a_{c,\mathbf{k}} \right] - \sum_{\mathbf{k},\mathbf{k}',\lambda=c,v} \langle \lambda, \mathbf{k}' | ie\mathbf{F}(\mathbf{t}) \cdot \nabla_{\mathbf{k}} | \lambda, \mathbf{k}' \rangle a^{\dagger}_{\lambda',\mathbf{k}} a_{\lambda,\mathbf{k}}, \tag{3.4}$$

where $E_{c,\mathbf{k}}$ and $E_{v,\mathbf{k}}$ are single particle energies for electrons in conduction band and holes in valence band respectively; $V_{\mathbf{q}}$ is the Coulomb interacting potential; $a^{\dagger}_{\lambda,\mathbf{k}}$ and $a_{\lambda,\mathbf{k}}$ ($\lambda = c, v$) are electron and hole creation and annihilation operators which anticommute in the usual way; $\mathbf{E}_{op}(\mathbf{t})$ and $\mathbf{F}(\mathbf{t})$ are optical field and electrical field respectively; and finally, μ is the optical dipole element.

Using the above Hamiltonian Eq. (3.1), the SBEs can be used to describe the dynamics of populations $n_{c,v}(\mathbf{k},t)$ and interband polarization $\mathbf{P}(\mathbf{k},t)$ using the Heisenberg equation of motion [31]:

$$\begin{aligned} &\left\{ \frac{\partial}{\partial t} - \frac{e}{\hbar}\mathbf{F}(\mathbf{t}) \cdot \nabla_{\mathbf{k}} - \frac{i}{\hbar} \left[e_c(\mathbf{k},t) - e_v(\mathbf{k},t) \right] \right\} \mathbf{P}(\mathbf{k},t) \\ = \; & \frac{i}{\hbar} \left[n_c(\mathbf{k},t) - n_v(\mathbf{k},t) \right] \Omega(\mathbf{k},t) + \left[\frac{\partial \mathbf{P}(\mathbf{k},t)}{\partial t} \right]_{coll}, \end{aligned} \tag{3.5}$$

$$\left[\frac{\partial}{\partial t} - \frac{e}{\hbar}\mathbf{F}(\mathbf{t}) \cdot \nabla_{\mathbf{k}} \right] n_c(\mathbf{k},t) = -\frac{2}{\hbar} \mathrm{Im} \left[\Omega(\mathbf{k},t) \mathbf{P}^*(\mathbf{k},t) \right] + \left[\frac{\partial n_c(\mathbf{k},t)}{\partial t} \right]_{coll}, \tag{3.6}$$

and

$$\left[\frac{\partial}{\partial t} - \frac{e}{\hbar}\mathbf{F}(\mathbf{t}) \cdot \nabla_{\mathbf{k}} \right] n_v(\mathbf{k},t) = \frac{2}{\hbar} \mathrm{Im} \left[\Omega(\mathbf{k},t) \mathbf{P}^*(\mathbf{k},t) \right] + \left[\frac{\partial n_v(\mathbf{k},t)}{\partial t} \right]_{coll}. \tag{3.7}$$

Here, $n_c(\mathbf{k},t) \equiv \left\langle a^{\dagger}_{c,\mathbf{k}} a_{c,\mathbf{k}} \right\rangle$, $n_v(\mathbf{k},t) \equiv \left\langle a^{\dagger}_{v,\mathbf{k}} a_{v,\mathbf{k}} \right\rangle$, $\mathbf{P}(\mathbf{k},t) \equiv \left\langle a^{\dagger}_{v,\mathbf{k}} a_{c,\mathbf{k}} \right\rangle$; $e_c(\mathbf{k},t) = E_{c,\mathbf{k}} - \sum_{\mathbf{k}'} V(\mathbf{k},\mathbf{k}') n_c(\mathbf{k}',t)$ and $e_v(\mathbf{k},t) = E_{v,\mathbf{k}} - \sum_{\mathbf{k}'} V(\mathbf{k},\mathbf{k}') n_v(\mathbf{k}',t)$ are the Coulomb-renormalized energies of electrons and holes respectively, and $\Omega(\mathbf{k},t) = \mu \mathbf{E}_{op}(\mathbf{t}) + \sum_{\mathbf{k}'} V(\mathbf{k},\mathbf{k}') \mathbf{P}(\mathbf{k}',t)$ is the generalized Rabi frequency; $V(\mathbf{k},\mathbf{k}')$ is the Coulomb interaction. Note that in the derivation of the above equations of motion, a random phase approximation (RPA) [81, 82, 83] is made to

Reproduced with permission of the copyright owner. Further reproduction prohibited without permission.

split the four-operator terms into product of densities and interband polarizations, for example,

$$\left\langle a^{\dagger}_{v,\mathbf{k}'+\mathbf{q}} a^{\dagger}_{c,\mathbf{k}-\mathbf{q}} a_{c,\mathbf{k}'} a_{c,\mathbf{k}} \right\rangle \approx \mathbf{P}(\mathbf{k},t) n_c(\mathbf{k},t) \delta_{\mathbf{k}-\mathbf{q},\mathbf{k}'}. \tag{3.8}$$

The explicit terms in Eqs. (3.5), (3.6) and (3.7) denote the results obtained in the time-dependent Hartree-Fock approximation, whereas the terms with subscript *coll* refers to many-body collision terms beyond the Hartree-Fock approximation, and to other dephasing mechanism such as carrier-phonon scattering. Usually, these undetermined terms are simplified by adding phenomenological dephasing time constants. That is, the collision terms in Eqs. (3.5), (3.6) and (3.7) are replaced in practice by $\frac{\mathbf{P}(\mathbf{k},t)}{T_2}$, $\frac{\partial n_c(\mathbf{k},t)}{T_1}$ and $\frac{n_v(\mathbf{k},t)}{T_1}$ respectively.

Although SBEs were derived to evaluate the coherent effects to any orders in optical field, the factorization of higher order correlations into polarization and number parts by RPA makes the method in good agreement generally with only the lowest order optical response. Beyond the first order response, e.g. in the study of intraband polarization in superlattices, SBEs may encounter problems. For example, the factorization of higher order correlations into interband polarization and number parts makes some of the decay time constants wrong. The Coulomb coupling of the electron and hole within a pair in the SBEs decays faster than the intraband polarization [38], since factorization implies that intraband process decay twice as fast as interband processes [45]. Thus, the prediction by the SBEs that terahertz emission is characteristic of free electrons and holes rather than excitons is not in agreement with both theoretical prediction [21] and experimental results [38].

Axt *et al* developed an alternative approach called Dynamically Controlled Truncation (DCT) to address the problems the SBEs encountered [36, 37, 38]. While the SBEs try to describe the coherent response to infinite order in optical field but lose correlations by factorization, DCT makes a compromise by maintaining correct correlations but describing the coherent response of a semiconductor within a prescribed order of the optical field. The idea of the DCT technique relies on the observation that a complete calculation of the nonlinear optical response of a semiconductor to any prescribed order in the driving field can be achieved by considering only a finite set of electronic correlation functions [36, 37, 38]. Both DCT theory and SBEs can predict similar results for linear response of a superlattice. However, DCT can

Reproduced with permission of the copyright owner. Further reproduction prohibited without permission.

also explain the experimental results that SBEs can not explain [44].

DCT still has limitations because it is usually derived in a basis of electron-hole pairs created at a fixed lattice sites or in k_z-state basis but these basis are actually not appropriate to describe the coherent response in semiconductor superlattices. Thus, the use of phenomenological decay and dephasing terms in DCT theory can not be properly justified because the free electron states are not even close to being the eigenstates of the system (in the absence of terahertz and optical fields). *Dignam* [34] tried to address this problem by employing a basis of single-particle one-band WSL states [Eqs. (2.3) and (2.4)] in the presence of static electric field. Because these non-interacting states are much closer to the actual excitonic states, the physical significance of terms is much more transparent. Moreover, the electrons and holes are spatially localized in z direction in the WSL basis, the only states that are optically excited are those with an appreciable electron-hole overlap integral. Therefore, one need only calculate those WSL states for which the electron-hole overlap is significant.

In summary, SBEs are successful in accounting for the lowest-order coherent responses in a photoexcited semiconductor superlattice. Although it was originally developed to account for the higher order effects, it is not so successful due to the use of RPA. The crux is: while RPA successfully reduces the infinite hierarchy via a Hartree-Fock decoupling to much simplified polarization and number parts, it also removes some crucial electron-hole correlations. DCT, however, makes a compromise by maintaining correct correlations but describing the coherent response of a semiconductor within a prescribed order of the optical field. In practice, it will have to be terminated to a prescribed finite order so as to maintain the correct correlation. Moreover, the DCT is usually derived in a k_z-state basis that is not suitable for the photoexcited semiconductor superlattices. From above, it can be seen that, to give a more realistic picture of the dynamics of electrons and holes, we need an approach that has the following characteristics: can account for the nonlinear coherent response but not lose the correct correlations, and above all, the method should be derived in a more appropriate basis. This is the approach introduced in the next section with a quasibosonic treatment.

Reproduced with permission of the copyright owner. Further reproduction prohibited without permission.

3.3 Quasibosonic Exciton Dynamics and SCD Bloch Oscillations

3.3.1 Equations of Motion for Excitons in the Quasibosonic Treatment

In this section, the equations of motion for SCD Bloch oscillations are derived by using a quasibosonic treatment by *Hawton* and *Nelson* [45]. This is based on the fact that excitons are bosons at low densities and their creation and destruction operators satisfy the bosonic commutation relations to a first approximation [84]. The main idea behind this treatment is to use the excitonic states rather than the single-particle one-band WSL states as a basis. This quasibosonic picture of excitons provides us with a physically transparent treatment of optical processes of semiconductors near the band edge, and can be successfully applied with phenomenological dephasing up to third-order in optical field and beyond.

First, an exciton operator $B_\nu^\dagger$ which can create an exciton in v state (with zero center of mass momentum) can be introduced as a linear combination of a set of pair operators [45],

$$B_\nu^\dagger = \sum_{\mathbf{k}} \psi_{\nu,\mathbf{k}} B_{\mathbf{k}}^\dagger, \tag{3.9}$$

where $\psi_{\nu,\mathbf{k}}$ is the k-space representation of the exciton basis, $B_{\mathbf{k}}^\dagger$ is the quasi-bosonic pair operator obtained from Fermion operators (the product of electron and hole operator) by using Usui's transformation [85]. It can be shown that exciton operators satisfy the following commutation relations [45],

$$\left[B_{\nu_1}^\dagger, B_{\nu_2}^\dagger\right] = [B_{\nu_1}, B_{\nu_2}] = 0, \tag{3.10}$$

$$\left[B_{\nu_1}, B_{\nu_2}^\dagger\right] = \delta_{\nu_1,\nu_2} - 2\sum_{m1,m2} \chi_{m1,m2}^{n1,n2} B_{v_2}^\dagger, B_{v_1}^\dagger, \tag{3.11}$$

where

$$\chi_{m1,m2}^{n1,n2} \equiv \sum_{\mathbf{k}} \psi_{n_1,\mathbf{k}}^* \psi_{n_2,\mathbf{k}} \psi_{m_2,\mathbf{k}}^* \psi_{m_1,\mathbf{k}}, \tag{3.12}$$

and $\alpha_e \equiv m_e/M$, $\alpha_h \equiv m_h/M$, and m_e, m_h and M are the electron, hole and total masses respectively. The χ parameters in Eq. (3.12) describe phase-space filling and can be calculated for any particular exciton basis. Commutation relations (3.10) and (3.11), and the definition

Reproduced with permission of the copyright owner. Further reproduction prohibited without permission.

(3.12) are the basic relations that are needed to derive the equations of motion for excitons below.

It has been shown by *Dignam* and *Hawton* [47] that, with the above treatment the Hamiltonian for the exciton system can be written to a good approximation as

$$H^{ex} = H_o^{ex} - V\mathbf{E}^{ex} \cdot \mathbf{P}^{ex} + V\frac{\mathbf{P}_{intra}^{ex} \cdot \mathbf{P}_{intra}^{ex}}{2\epsilon_0 \epsilon}, \tag{3.13}$$

where

$$H_o^{ex} = \sum_{\mu} \hbar\omega_\mu B_\mu^\dagger B_\mu$$

is the energy of the excitons in the superlattice in the presence of the applied DC field, $B_\mu^\dagger$ and B_μ are excitonic creation and annihilation operators which create and destroy excitons in the μ^{th} state in the presence of an applied field F_0, $\mathbf{E}(t) = \mathbf{E}_{opt}(t) + \mathbf{E}_{THz}^{ext}(t)$ is the sum of the applied external optical and THz fields, and $\mathbf{P}^{ex} = \mathbf{P}_{intra}^{ex} + \mathbf{P}_{inter}^{ex}$ is the total polarization due to the excitons, where

$$\mathbf{P}_{intra}^{ex} = \frac{1}{V}\sum_{\mu,\nu} \mathbf{G}_{\mu,\nu}^{ex} B_\mu^\dagger B_\nu \tag{3.14}$$

is the intraband polarization and

$$\mathbf{P}_{inter}^{ex} = \frac{2}{V}\,\mathrm{Re}\left\{\sum_{\mu} \mathbf{M}_\mu^{ex} \left\langle B_\mu^\dagger \right\rangle\right\}. \tag{3.15}$$

is the interband polarization. $\mathbf{M}_\mu^{ex}$ is the interband dipole matrix element for the μ^{th} exciton and is given by [34]

$$\mathbf{M}_\mu^{ex} \equiv \mathbf{M}_o \frac{1}{\sqrt{N_z}} \int dz \psi^{\mu *}(z, z, 0), \tag{3.16}$$

where $\mathbf{M}_o$ is the bulk dipole matrix element between the conduction and valence bands and $\psi^\mu(z_e, z_h, \boldsymbol{\rho})$ is defined in Eq. (2.15). $\mathbf{G}_{\mu,\nu}^{ex}$ is the intraband dipole matrix element and takes the form

$$\mathbf{G}_{\mu,\nu}^{ex} = \left\langle \psi^\mu(z_e, z_h, \boldsymbol{\rho}) \left| -e(\mathbf{r}_e - \mathbf{r}_h) \right| \psi^\nu(z_e, z_h, \boldsymbol{\rho}) \right\rangle. \tag{3.17}$$

The calculation of these matrix elements has been discussed by previous authors [34, 46]. Finally, V is the volume of the system (assumed to be very large relative to the superlattice

Reproduced with permission of the copyright owner. Further reproduction prohibited without permission.

period and exciton Bohr radius) and ϵ is the dielectric constant of the semiconductor due to all the bound charges in the system. The exciton-exciton interaction in this Hamiltonian resides in the last term. The exact expression for this term is obtained if $\mathbf{P}^{ex}_{intra}$ is replaced by the exact polarization rather than the polarization in the dipole approximation, and the electron-hole Coulomb interaction within a given exciton is subtracted out. Because we are not concerned with exciton-exciton correlations in this work, we replace the exact polarization by the long-wavelength dipole approximation as in Eq. (3.15). This is essentially equivalent to treating exciton-exciton interactions in a mean-field approach. We emphasize, however, that the electron-hole interaction within an exciton is included in H_0^{ex}, and this allows for the electron-hole correlations which yield Wannier excitons in the usual way.

From this, one can derive the following equation of motion:

$$\begin{aligned} i\hbar\frac{dB^\dagger_\mu}{dt} + \hbar\omega_\mu B^\dagger_\mu &= \mathbf{E}_{opt}\cdot\left[\mathbf{M}^{ex*}_\mu - 2\sum_{\mu',\mu'',\mu'''}\mathbf{M}^{ex*}_{\mu'}X^{\mu',\mu}_{\mu'',\mu'''}B^\dagger_{\mu''}B_{\mu'''}\right] \\ &+\mathbf{E}^{ext}_{THz}(t)\cdot\left[\sum_{\mu'}\mathbf{G}^{ex}_{\mu',\mu}B^\dagger_{\mu'} - 2\sum_{\mu'\mu''\mu'''\mu''''}\mathbf{G}^{ex}_{\mu'',\mu'}X^{\mu',\mu}_{\mu''',\mu''''}B^\dagger_{\mu''}B^\dagger_{\mu'''}B_{\mu''''}\right] \\ &-\frac{1}{\epsilon_0\epsilon}\frac{1}{V}\sum_{\mu',\mu'',\mu'''}\mathbf{G}^{ex}_{\mu'',\mu'''}\cdot\mathbf{G}^{ex}_{\mu',\mu}B^\dagger_{\mu''}B_{\mu'''}B^\dagger_{\mu'} \\ &+\frac{2}{V}\sum_{\mu'\mu''\mu'''\mu''''\mu'''''\mu''''''}\mathbf{G}^{ex}_{\mu'',\mu'}\mathbf{G}^{ex}_{\mu''''',\mu''''}X^{\mu',\mu}_{\mu''',\mu'''}B^\dagger_{\mu'''''}B_{\mu''''}B^\dagger_{\mu''}B^\dagger_{\mu'''}B_{\mu'''''}. \end{aligned}$$

The terms containing the $X^{\mu',\mu}_{\mu'',\mu'''}$ are due to phase-space filling and arise from the commutation relations of excitonic operators as in Eq. (3.12). These terms have been shown to be small [47] relative to the other nonlinear terms, and hence can be safely ignored. In this approximation, the equation of motion simplifies to

$$i\hbar\frac{dB^\dagger_\mu}{dt} + \hbar\omega_\mu B^\dagger_\mu = \mathbf{E}_{opt}\cdot\mathbf{M}^{ex*}_\mu + \left[\mathbf{E}^{ext}_{THz} - \frac{\mathbf{P}^{ex}_{intra}}{\epsilon_0\epsilon}\right]\cdot\sum_{\mu'}\mathbf{G}^{ex}_{\mu',\mu}B^\dagger_{\mu'}.$$

It is seen here that the net effect of the exciton-exciton interactions in this dipole approximation is to replace the applied external field with the total THz field, which is given by the sum of

Reproduced with permission of the copyright owner. Further reproduction prohibited without permission.

the applied field and the excitonic intraband field

$$\mathbf{E}^{ex}_{intra} \equiv -\frac{\mathbf{P}^{ex}_{intra}}{\epsilon_0 \epsilon}. \tag{3.18}$$

However, we must remember that at this point $\mathbf{E}^{ex}_{intra}$ is in fact an operator which can be written in terms of the excitonic destruction and creation operators.

Now, taking the expectation value of the above equation, and adding a phenomenological interband dephasing time constant, T_μ, we obtain

$$\begin{aligned} i\hbar\frac{d\left\langle B^\dagger_\mu\right\rangle}{dt} + \hbar\left(\omega_\mu + \frac{i}{T_\mu}\right)\left\langle B^\dagger_\mu\right\rangle &= \mathbf{E}_{opt}\cdot\mathbf{M}^{ex*}_\mu + \mathbf{E}^{ext}_{THz}\cdot\sum_{\mu'}\mathbf{G}^{ex}_{\mu',\mu}\left\langle B^\dagger_{\mu'}\right\rangle \\ &\quad -\frac{1}{\epsilon_0\epsilon}\cdot\frac{1}{V}\sum_{\mu',\mu'',\mu'''}\mathbf{G}^{ex}_{\mu'',\mu'''}\cdot\mathbf{G}^{ex}_{\mu',\mu}\left\langle B^\dagger_{\mu''}B_{\mu'''}B^\dagger_{\mu'}\right\rangle. \end{aligned}$$

To solve this equation, we would in general have to have the equation of motion for $\left\langle B^\dagger_{\mu''}B_{\mu'''}B^\dagger_{\mu'}\right\rangle$. To avoid this difficulty, we employ the following approximate factorization:

$$\left\langle B^\dagger_{\mu''}B_{\mu'''}B^\dagger_{\mu'}\right\rangle = \left\langle B^\dagger_{\mu''}B_{\mu'''}\right\rangle\left\langle B^\dagger_{\mu'}\right\rangle.$$

This amounts to using the physical approximation

$$\left\langle \mathbf{P}^{ex}_{intra}B^\dagger_{\mu'}\right\rangle = \left\langle \mathbf{P}^{ex}_{intra}\right\rangle\left\langle B^\dagger_{\mu'}\right\rangle.$$

This approximation can be shown to be valid as long as the optical pulse duration is much less than the dephasing times [47], which it is for the situations discussed here. Note that this approximation is different from that used in the SBEs in that the electron-hole correlations within each exciton are included before the factorization. Using this factorization, we obtain:

$$i\hbar\frac{d\left\langle B^\dagger_\mu\right\rangle}{dt} + \hbar\left(\omega_\mu + \frac{i}{T_\mu}\right)\left\langle B^\dagger_\mu\right\rangle = \mathbf{E}_{opt}(t)\cdot\mathbf{M}^{ex*}_\mu + \left[\mathbf{E}^{ext}_{THz}(t) + \left\langle\mathbf{E}^{ex}_{intra}\right\rangle\right]\cdot\sum_{\mu'}\mathbf{G}^{ex}_{\mu',\mu}\left\langle B^\dagger_{\mu'}\right\rangle. \tag{3.19}$$

Reproduced with permission of the copyright owner. Further reproduction prohibited without permission.

The intraband equation of motion within the same set of approximations is then seen to be

$$\begin{aligned} i\hbar\frac{d\left\langle B_\mu^\dagger B_\nu\right\rangle}{dt} &= -\hbar\left(\omega_\mu-\omega_\nu+\frac{i}{T_{\mu\nu}}\right)\left\langle B_\mu^\dagger B_\nu\right\rangle+\mathbf{E}_{opt}\cdot\left[\mathbf{M}_\mu^{ex*}\left\langle B_\nu\right\rangle-\mathbf{M}_\nu^{ex}\left\langle B_\mu^\dagger\right\rangle\right] \\ &+\left[\mathbf{E}_{THz}^{ext}(t)+\left\langle\mathbf{E}_{intra}^{ex}\right\rangle\right]\sum_{\mu'}\left(\mathbf{G}_{\mu',\mu}\left\langle B_{\mu'}^\dagger B_\nu\right\rangle-\mathbf{G}_{\mu',\nu}^*\left\langle B_\mu^\dagger B_{\mu'}\right\rangle\right), \quad (3.20) \end{aligned}$$

where we have used the factorization $\left\langle\mathbf{P}_{intra}^{ex}B_{\mu'}^\dagger B_\nu\right\rangle=\left\langle\mathbf{P}_{intra}^{ex}\right\rangle\left\langle B_{\mu'}^\dagger B_\nu\right\rangle$. Thus, the problem of determining the intraband polarization dynamics reduces to solving the above two sets of equations where $\left\langle\mathbf{E}_{intra}^{ex}\right\rangle$ is defined in Eq. (3.18).

In later chapters, because we are only interested in the driving effect from the fields due to charge carriers, i.e. SCD Bloch oscillations, we will omit the applied Terahertz portion, $\mathbf{E}_{THz}^{ext}(t)$, and retain only $\left\langle\mathbf{E}_{intra}^{ex}\right\rangle$. Note that Eqs. (3.19) and (3.20) are to infinite order in optical field, and hence are in spirit similar to the SBEs. That is, like SBEs, one does not have to use perturbation theory. However, because they employ an exciton basis and treat intraband and interband processes separately, they do not have the same problems encountered by the SBEs.

3.3.2 Dimensionless Equations for Excitons:

To move to dimensionless equations that do not contain the factors such as Volume in the definition of the polarization (thus we need not to worry about the volume of interest in the numerical calculation but just get the physical quantities per unit volume), we make the following definitions:

$$\begin{aligned} \mathbf{M}_\mu^{ex} &= \mathbf{M}_o S_\mu\sqrt{\frac{V}{d}} \\ &= \mathbf{M}_o\widetilde{S}_\mu\frac{V}{da_o^2}, \end{aligned} \quad (3.21)$$

where

$$\widetilde{S}_\mu=a_o S_\mu=\frac{a_o}{\sqrt{N_z}}\int dz\psi^\mu(\boldsymbol{\rho}=0,z,z),$$

where $\psi^\mu(\boldsymbol{\rho},z,z)$ is defined in Eq. (2.15). The main purpose of this re-definition and other definitions is to effect the removal of the factor of $1/V$ in the definition of polarization. With

Reproduced with permission of the copyright owner. Further reproduction prohibited without permission.

these factors gone, the above elements are easily computed and the equations of motion can be solved on the computer.

Now, we make the following definitions:

$$\begin{aligned} \langle B_\mu \rangle (\tau/\omega_B) &= \frac{e}{\mathbf{M}_o^*}\sqrt{\frac{V}{d}}K_\mu(\tau)e^{-i\omega_\mu^0 t}, \\ \left\langle B_\mu^\dagger B_\nu \right\rangle (\tau/\omega_B) &= \frac{e^2}{|\mathbf{M}_o|^2}\frac{V}{d}K_\mu^* K_\nu(\tau)e^{i\left(\omega_\mu^0-\omega_\nu^0\right)t} \end{aligned} \tag{3.22}$$

where $\tau = \omega_B t$. This makes $K_\mu(\tau)$ and $K_\mu^* K_\nu(\tau)$ into slowly-varying quantities suitable for solving on a computer using a Runge Kutta procedure. Finally, we define

$$\Gamma_\mu = \omega_B T_\mu$$

with similar definitions for the other dephasing times. Using these definitions in equations of motion (3.19) and (3.20), we obtain:

$$\begin{aligned} \frac{dK_\mu}{d\tau} + \frac{1}{\Gamma_\mu}K_\mu &= i\mathbf{E}(\mathbf{t})e^{-i\left(\omega_c-\omega_\mu^0\right)t}\cdot\widetilde{S}_\mu\frac{|\mathbf{M}_o|^2}{e\hbar\omega_B a_o} \\ &\quad + i\frac{\langle \mathbf{E}_{intra}\rangle}{\hbar\omega_B}\cdot\sum_{\mu'}\mathbf{G}_{\mu',\mu}^* K_{\mu'}e^{i\left(\omega_{\mu'}^0-\omega_\mu^0\right)t} \end{aligned} \tag{3.23}$$

and

$$\begin{aligned} \frac{dK_\mu^* K_\nu}{d\tau} &= -\frac{1}{\Gamma_{\mu\nu}}K_\mu^* K_\nu - i\mathcal{E}^*(t)e^{i\left(\omega_c-\omega_\mu^0\right)t}\cdot\widetilde{S}_\mu^*\frac{|\mathbf{M}_o|^2}{e\hbar\omega_B a_o}K_\nu \\ &\quad + i\mathbf{E}(\mathbf{t})e^{i\left(-\omega_c+\omega_\nu^0\right)t}\cdot\widetilde{S}_\nu\frac{|\mathbf{M}_o|^2}{e\hbar\omega_B a_o}K_\mu^* \\ &\quad - i\frac{\langle \mathbf{E}_{intra}\rangle}{\hbar\omega_B}\cdot\sum_{\mu'}\Big(\mathbf{G}_{\mu',\mu}K_{\mu'}^* K_\nu e^{i\left(\omega_{\mu'}^0-\omega_\mu^0\right)t} \\ &\quad - \mathbf{G}_{\mu',\nu}^* K_\mu^* K_{\mu'}e^{-i\left(\omega_{\mu'}^0-\omega_\nu^0\right)t}\Big). \end{aligned} \tag{3.24}$$

Reproduced with permission of the copyright owner. Further reproduction prohibited without permission.

In terms of these quantities, the intraband polarization is given by

$$\begin{aligned}\langle \mathbf{P}^{ex}_{intra} \rangle (\tau) &= \frac{1}{V} \sum_{\nu\mu} G^{ex}_{\mu\nu} \left\langle B^{\dagger}_{\mu} B_{\nu} \right\rangle \\ &= \frac{e^2}{|\mathbf{M}_o|^2 d} \sum_{\nu\mu} G^{ex}_{\mu\nu} K^{*}_{\mu} K_{\nu}(\tau) e^{i(\tilde{\omega}^0_{\mu} - \tilde{\omega}^0_{\nu})\tau}. \end{aligned} \tag{3.25}$$

Eqs. (3.23), (3.24) and (3.25) form the basic frame work for calculations of the 1s excitonic portion in the SCD Bloch oscillations in Chapter 5.

Reproduced with permission of the copyright owner. Further reproduction prohibited without permission.

Chapter 4

Dynamics of Free Electron-hole Pairs in Semiconductor Superlattice

In this chapter, we wish to account for the influence of the unbound continuum excitonic states on the 1s excitons as described on Chapter 3. However, calculating the dynamics of these continuum states would involve very intensive calculations due to the continuum nature of these unbound excitonic states. Therefore we will instead calculate the influence of free electron-hole pairs, i.e., pairs of non-interacting electrons and holes, to approximate these continuum states. Although it is known that the Coulomb interaction has a rather large effect on the linear optical properties of semiconductor, the goal here is to investigate the general feature of the interaction of 1s excitons with the continuum to obtain quantitative results. Thus we expect this approximation to be satisfactory for our purpose.

However, it is known that the electron-hole Coulomb interaction enhances the absorption due to continuum states [29]. To account for the influence of these carriers on the 1s excitons, we must first derive the equations of motion of the free electron-hole pairs. To obtain the equations of motion of these free electron-hole pairs in a superlattice, we need the full Hamiltonian of the system. In this chapter, we first derive the Hamiltonian for the free electron-hole pairs in the superlattice potential in the presence of the external optical, DC and terahertz electric fields. Using this, the equations of motion for electron-hole pairs are obtained by using the Heisenberg equations of motion. After that, the corresponding simplified and dimensionless equations

Reproduced with permission of the copyright owner. Further reproduction prohibited without permission.

that are favorable for numerical calculation are derived by defining new variables. Finally, some results in a few limiting cases are calculated to demonstrate the validity of numerical calculations by comparison with analytical results in these cases.

4.1 Hamiltonian for Electron-hole Pairs in External Optical and Terahertz fields

The full Hamiltonian of the system for free electron-hole pairs takes the form

$$H^f = H_o^f - V\mathbf{E}^f \cdot \mathbf{P}^f + V\frac{\mathbf{P}_{intra}^f \cdot \mathbf{P}_{intra}^f}{2\epsilon_0\epsilon}, \tag{4.1}$$

where $H_o^f = \sum_\mu \hbar\omega_\mu B_\mu^\dagger B_\mu$. This is identical to the definition of Hamiltonian for the excitonic case as in Eq. (3.13) except that we omit the Coulomb interaction between the electron and hole within each pair in H_o^f. As a result, the $B_\mu^\dagger$ are now free electron-hole pair creation operators. Correspondingly, the quantities such as ω_u^{ex}, M_μ^{ex} and G_{uv}^{ex} in the definitions of $\mathbf{P}^{ex}$, $\mathbf{P}_{inter}^{ex}$ and $\mathbf{P}_{intra}^{ex}$ in the excitonic case become ω_u^f, M_μ^f and G_{uv}^f in the free electron-hole pair case. Although these terms are similar in definitions, they are actually different and have to be re-calculated. Also, in the absence of the electron-hole Coulomb interaction, the along-axis in-plane motions decouple and we index a free pair state by double indices $\{n, \mathbf{k}\}$ rather than a single index μ as in excitonic case, where n labels the WSL index and $\mathbf{k}$ labels the in-plane relative wavevector.

The wavefunction for the free electron-hole pair (with zero center of mass momentum) corresponding to an eigenstate of H_0^f can be written as

$$\Psi_{n,\mathbf{k}}^f(z_e, z_h, \boldsymbol{\rho}) = \frac{1}{\sqrt{AN_z}} e^{i\mathbf{k}\cdot\boldsymbol{\rho}} \sum_m \chi_0^h(z_h - md)\chi_n^e(z_e - md), \tag{4.2}$$

where $\boldsymbol{\rho}$ refers to the two-dimensional position vector in the (x, y) plane, $\mathbf{k}$ is the two-dimensional in-plane wave vector, and A is the in-plane normalization area. The functions, $\chi_0^h(z_h)$ and $\chi_n^e(z_e)$ are WSL states, which have the same definitions as in Eqs. (2.3) and (2.4). The corresponding eigenenergy for the above wavefunction is

$$E_{n,\mathbf{k}} = \hbar\omega_0 + n\hbar\omega_B + \frac{\hbar^2 k^2}{2m_{||}}, \tag{4.3}$$

Reproduced with permission of the copyright owner. Further reproduction prohibited without permission.

where $\hbar\omega_0$ is the energy for $n=0, \mathbf{k}=0$ state, and $m_{\|}$ is defined as $\frac{1}{m_{\|}} = \frac{1}{m_{e\|}} + \frac{1}{m_{h\|}}$.

With the wavefunction defined in Eq. (4.2), the expression for the intraband dipole matrix element can thus be written as,

$$G^f_{nl}(\mathbf{k},\mathbf{k}') = \left\langle \Psi^f_{n,\mathbf{k}} | -e(z_e - z_h) | \Psi^f_{l,\mathbf{k}'} \right\rangle . \tag{4.4}$$

Inserting the wavefunction Eq. (4.2) into Eq. (4.4), we have,

$$\begin{aligned} G^f_{nl}(\mathbf{k},\mathbf{k}') &= \left\langle \Psi^f_{n,\mathbf{k}} | -e(z_e - z_h) | \Psi^f_{l,\mathbf{k}'} \right\rangle \\ &= -e\frac{1}{AN_z}\int d\Omega e^{i(\mathbf{k}'-\mathbf{k})\cdot\rho} \sum_{m,m'} \chi^{h*}_0(z_h - md)\chi^{e*}_n(z_e - md) \\ &\quad \cdot(z_e - z_h)\chi^h_0(z_h - m'd)\chi^e_l(z_e - m'd). \end{aligned} \tag{4.5}$$

Within the one-miniband approximation, the WSL eigenstates $\chi^h_0(z_h)$ and $\chi^e_n(z_e)$ can be expanded in the basis of the Wannier states, $a^\lambda(z)$, of the lowest minibands (superscript λ refers to electron or hole),

Inserting Eq.(2.3) and Eq. (2.4) into Eq.(4.5) gives,

$$\begin{aligned} G^f_{nl}(\mathbf{k},\mathbf{k}') &= -e\frac{1}{AN_z}\int d\Omega e^{i(\mathbf{k}'-\mathbf{k})\cdot\rho} \cdot \sum_{m,m',m'',m''',m_4,m_5} C^{h*}_{m''} a^{v*}(z_h - md - m''d) C^{e*}_{m'''-n} \\ &\quad \cdot a^{c*}(z_e - md - m'''d)(z_e - z_h) \\ &\quad \cdot C^h_{m_4} a^v(z_h - m'd - m_4 d) C^e_{m_5-l} a^c(z_e - m'd - m_5 d). \end{aligned} \tag{4.6}$$

After re-indexation, $m'' \to m'' - m$, $m''' \to m''' - m$, $m_4 \to m_4 - m'$ and $m_5 \to m_5 - m'$, Eq. (4.6) becomes,

Reproduced with permission of the copyright owner. Further reproduction prohibited without permission.

$$
\begin{aligned}
G^f_{nl}(\mathbf{k},\mathbf{k}') &= -e\frac{1}{AN_z}\int d\Omega e^{i(\mathbf{k}'-\mathbf{k})\cdot\rho}\cdot \sum_{m,m',m'',m''',m_4,m_5} C^{h*}_{m''-m}a^{v*}(z_h-m''d)\\
&\quad \cdot C^{e*}_{m'''-m-n}a^{c*}(z_e-m'''d)(z_e-z_h)\\
&\quad \cdot C^{h}_{m_4-m'}a^{v}(z_h-m_4d)C^{e}_{m_5-m'-l}a^{c}(z_e-m_5d)\\
&= -e\frac{1}{AN_z}\int d\rho e^{i(\mathbf{k}'-\mathbf{k})\cdot\rho}\cdot \sum_{m,m',m'',m''',m_4,m_5} C^{h*}_{m''-m}C^{e*}_{m'''-m-n}C^{h}_{m_4-m'}C^{e}_{m_5-m'-l}\\
&\quad \cdot\Big[\int_{-\infty}^{+\infty} dz_h a^{v*}(z_h-m''d)a^{v}(z_h-m_4d)\cdot\int_{-\infty}^{+\infty} dz_e a^{c*}(z_e-m'''d)\cdot z_e\cdot a^{c}(z_e-m_5d)\\
&\quad -\int_{-\infty}^{\infty} dz_e a^{c*}(z_e-m'''d)a^{c}(z_c-m_5d)\\
&\quad \cdot\int_{-\infty}^{+\infty} dz_h a^{v*}(z_h-m''d)\cdot z_h\cdot a^{v}(z_h-m_4d)\Big]. \qquad (4.7)
\end{aligned}
$$

In order to continue our derivation, we will first evaluate the integral with the following form by defining $z' = z - \frac{m+p}{2}d$,

$$
\begin{aligned}
\int_{-\infty}^{+\infty} dz a^*(z-md)za(z-pd) &= \int_{-\infty}^{+\infty} dz' a^*(z'+\frac{m+p}{2}d-md)\cdot(z'+\frac{m+p}{2}d)\\
&\quad \cdot a(z'+\frac{m+p}{2}d-pd)\\
&= \int_{-\infty}^{+\infty} dz' a^*(z'+\frac{p-m}{2}d)\cdot(z'+\frac{m+p}{2}d)\cdot a(z'-\frac{p-m}{2}d)\\
&= \int_{-\infty}^{+\infty} dz' a^*(z'+\frac{p-m}{2}d)\cdot\frac{m+p}{2}d\cdot a(z'-\frac{p-m}{2}d)\\
&= \frac{m+p}{2}d\delta_{pm}, \qquad (4.8)
\end{aligned}
$$

where integral $\int dz' a^*(z'+\frac{p-m}{2}d)\cdot z'\cdot a(z'-\frac{p-m}{2}d)$ must be zero as long as the miniband Wannier functions have definite parity. This will be true for superlattice potentials with inversion symmetry [34].

Using Eq. (4.8) and integrating over $d\Omega$, the intraband dipole moments Eq. (4.7) can be further simplified as,

Reproduced with permission of the copyright owner. Further reproduction prohibited without permission.

$$
\begin{aligned}
G^f_{nl}(\mathbf{k},\mathbf{k}') &= -e\frac{\delta_{\mathbf{k}\mathbf{k}'}}{N_z}\cdot \sum_{m,m',m'',m''',m_4,m_5} C^{h*}_{m''-m}C^{e*}_{m'''-m-n}C^{h}_{m_4-m'}C^{e}_{m_5-m'-l} \\
&\quad \cdot\left[m'''d\delta_{m''m_4}\delta_{m'''m_5} - m''d\delta_{m''m_4}\delta_{m'''m_5}\right] \\
&= -\frac{ed\delta_{\mathbf{k}\mathbf{k}'}}{N_z}\sum_{m,m',m'',m'''} C^{h*}_{m''-m}C^{e*}_{m'''-m-n}C^{h}_{m''-m'}C^{e}_{m'''-m'-l}(m'''-m''). \quad (4.9)
\end{aligned}
$$

Using the summation relations Eqs. (2.5) and (2.6) for expansion coefficients, we arrive at,

$$
\sum_n C^{e*}_{n-m}C^{e}_{n-m'} = \sum_{n'} C^{e*}_{n'}C^{e}_{n+m-m'} = \delta_{0,m-m'} = \delta_{m,m'},
$$

$$
\begin{aligned}
\sum_n nC^{h*}_{n-m}C^{h}_{n-m'} &= \sum_{n'}(n'+m)C^{h*}_{n'}C^{h}_{n'+m-m'} \\
&= \sum_{n'} n'C^{h*}_{n'}C^{h}_{n'+m-m'} + m\sum_{n'} n'C^{h*}_{n'}C^{h}_{n'+m-m'} \\
&= \frac{-1}{eF_o d}\left[\varepsilon^h_{m-m'} - \delta_{m-m',0}\varepsilon^h_0\right] + m\delta_{m,m'}.
\end{aligned}
$$

Thus we finally get the intraband dipole moments,

Reproduced with permission of the copyright owner. Further reproduction prohibited without permission.

$$
\begin{aligned}
G^f_{nl}(\mathbf{k},\mathbf{k}') &= -\frac{ed\delta_{\mathbf{kk}'}}{N_z}\sum_{m,m',m'''} C^{e*}_{m'''-m-n}C^{e}_{m5-m'-l}\left[m'''\delta_{m,m'}\right. \\
&\quad \left.+\frac{1}{eF_od}(\varepsilon^h_{m-m'}-\delta_{m-m',0}\varepsilon^h_0)+m\delta_{m,m'}\right] \\
&= -\frac{ed\delta_{\mathbf{kk}'}}{N_z}\left\{\sum_m\left[\frac{-1}{eF_od}(\varepsilon^e_{n-l}-\delta_{nl}\varepsilon^e_0)+n\delta_{nl}\right]\right. \\
&\quad \left.+\sum_{m,m'}\delta_{m+n,m'+l}\cdot\frac{\varepsilon^h_{m-m'}}{eF_od}-\sum_m\delta_{m+n,m+l}(\frac{\varepsilon^h_0}{eF_od}+m)\right\} \\
&= -\frac{ed\delta_{\mathbf{kk}'}}{N_z}\sum_m\left\{\frac{1}{eF_od}(\varepsilon^h_{l-n}-\varepsilon^e_{n-l})+\left[n+\frac{\varepsilon^e_0}{eF_od}-m-\frac{\varepsilon^h_0}{eF_od})\right]\delta_{nl}\right\} \\
&= \delta_{\mathbf{kk}'}\left\{-\frac{ed}{N_z}\sum_m\left[\frac{1}{eF_od}(\varepsilon^h_{l-n}-\varepsilon^e_{n-l})+(n+\frac{\varepsilon^e_0-\varepsilon^h_0}{eF_od})\delta_{nl}\right]\right\} \\
&= \delta_{\mathbf{kk}'}\left\{-ed\left[\frac{1}{eF_od}(\varepsilon^h_{l-n}-\varepsilon^e_{n-l})+(n+\frac{\varepsilon^e_0-\varepsilon^h_0}{eF_od})\delta_{nl}\right]\right\} \\
&\equiv \delta_{\mathbf{k},\mathbf{k}'}g_{nl}. \qquad (4.10)
\end{aligned}
$$

In the nearest tight-binding approximation, by using $\varepsilon^\lambda_n=\varepsilon^\lambda_0\delta_{n,0}+\frac{q_\lambda\Delta_\lambda}{4e}\delta_{n,n\pm1}$, where $\Delta_\lambda=\Delta_e+\Delta_h$, the matrix element g_{nl} in Eq. (4.10) can be further simplified as,

$$
g_{nl}=-ed\{\frac{\theta}{2}[\delta_{n,l-1}+\delta_{n,l+1}]+l\delta_{nl}\}, \qquad (4.11)
$$

where $\theta\equiv\theta_e-\theta_h$, $\theta_{e,h}\equiv\Delta_{e,h}/2q_{e,h}F_od$, where $\Delta_{e,h}$ is the bandwidth of the electron or hole miniband [34]. This result can also be obtained alternatively by a simple derivation using the nearest-neighbor tight-binding approximation. In this situation, the expansion coefficients in Eqs. (2.3) and (2.4) are replaced by Bessel function of the first kind of order m as in Eq. (2.7a).

Reproduced with permission of the copyright owner. Further reproduction prohibited without permission.

Therefore, we have,

$$\begin{aligned} g_{nl} &= -ed \cdot \sum_p p J_{p-n}(\theta) J_{p-l}(\theta) \\ &= -ed \cdot \sum_p J_{p-n}(\theta)[J_{p-l}(\theta)(p-l) + l J_{p-l}(\theta)] \\ &= -ed \cdot \sum_p J_{p-n}(\theta)\{\frac{\theta}{2}[J_{p-l+1}(\theta) + J_{p-l-1}(\theta)] + l J_{p-l}(\theta)]\} \\ &= -ed\{\frac{\theta}{2}[\delta_{n,l-1} + \delta_{n,l+1}] + l\delta_{nl}\}. \end{aligned} \tag{4.12}$$

However, for a more complete calculation, the matrix element g_{nl} defined in Eq. (4.10) rather than in Eq. (4.11) should be used.

By using the above intraband dipole matrix element Eq. (4.10), the intraband polarization per unit volume takes the form

$$\begin{aligned} \mathbf{P}^f_{intra}(\tau) &= \frac{1}{V} \sum_{n,\mathbf{k},n',\mathbf{k}'} G^f_{n\mathbf{k};n'\mathbf{k}'} B^\dagger_{n\mathbf{k}} B_{n'\mathbf{k}'} \\ &= \frac{1}{V} \sum_{n,\mathbf{k},n',\mathbf{k}'} \delta_{\mathbf{k},\mathbf{k}'} g_{nn'} B^\dagger_{n\mathbf{k}} B_{n'\mathbf{k}'} \\ &= \frac{1}{V} \sum_{n,\mathbf{k},n'} g_{nn'} B^\dagger_{n\mathbf{k}} B_{n'\mathbf{k}} \end{aligned} \tag{4.13}$$

and therefore the interacting Hamiltonian for an electron-hole pair and Terahertz field is written as,

$$\begin{aligned} H^f_T &= -V\mathbf{E}^f_{intra} \cdot \mathbf{P}^f_{intra} \\ &= -\mathbf{E}^f_{intra} \cdot \sum_{n,\mathbf{k},n'} g_{nn'} B^\dagger_{n\mathbf{k}} B_{n'\mathbf{k}}, \end{aligned} \tag{4.14}$$

where $\mathbf{E}^f_{intra} = -\frac{\mathbf{P}^f_{intra}}{\epsilon_0 \epsilon}$.

We now turn our attention to the interband polarization which can be written as

$$\mathbf{P}^f_{inter} = \frac{1}{V} \sum_{n,\mathbf{k}} \left(M^f_{n\mathbf{k}} B^\dagger_{n\mathbf{k}} + M^{f*}_{n\mathbf{k}} B_{n\mathbf{k}} \right), \tag{4.15}$$

Reproduced with permission of the copyright owner. Further reproduction prohibited without permission.

where $M^f_{n\mathbf{k}}$ has the similar definition as in Eq. (3.16) for exciton case but with $\psi^{\nu*}(z,z,0)$ as defined by Eq. (2.15) replaced by $\Psi^f_{n,\mathbf{k}}(z,z,0)$ as defined by Eq. (4.2). That is,

$$\begin{aligned} M^f_{n\mathbf{k}} &= \mathbf{M}_o \frac{1}{\sqrt{N_z}} \int dz \Psi^{f*}_{n,\mathbf{k}}(z,z,0) \\ &= \mathbf{M}_o \frac{1}{\sqrt{N_z}} \int dz e^{i\mathbf{k}\cdot 0} \sum_m \chi^{h*}_0(z_h - md) \chi^{e*}_n(z_e - md) \\ &= \mathbf{M}_o \frac{1}{\sqrt{N_z}} \int dz \sum_m \chi^{h*}_0(z_h - md) \chi^{e*}_n(z_e - md) \\ &\equiv M^f_n \end{aligned}$$

So we see that $M^f_{n\mathbf{k}}$ is actually independent of $\mathbf{k}$. Thus the interacting Hamiltonian with the optical field is written as

$$\begin{aligned} H^f_I &= -V\mathbf{E}_{opt}(t) \cdot \mathbf{P}^f_{inter} \\ &= -V\mathbf{E}_{opt}(t) \cdot \frac{1}{V} \sum_{n,\mathbf{k}} \left(M^f_n B^\dagger_{n\mathbf{k}} + M^{f*}_n B_{n\mathbf{k}} \right) \\ &= -\mathbf{E}_{opt}(t) \cdot \sum_{n,\mathbf{k}} \left(M^f_n B^\dagger_{n\mathbf{k}} + M^{f*}_n B_{n\mathbf{k}} \right). \end{aligned} \tag{4.16}$$

4.2 Equations of Motion for Free Electron-hole Pairs

By using the Hamiltonian defined in Eq. (4.1), the equations of motion for free electron-hole pairs can be derived from the Heisenberg equations of motion. The only extra ingredients we need are the commutation relations introduced in Eqs. (3.10) and (3.11). Neglecting the phase-space filling effects as we did for the excitonic case and through elementary but lengthy derivations, we obtain the following interband and intraband equations of motion,

$$i\hbar \frac{dB^\dagger_{n\mathbf{k}}}{dt} = -E_{n\mathbf{k}} B^\dagger_{n\mathbf{k}} + \mathbf{E}_{opt}(t) \cdot M^{f*}_n + \mathbf{E}_{intra} \cdot \sum_{n'} g_{n'n} B^\dagger_{n'\mathbf{k}}, \tag{4.17}$$

$$\begin{aligned} i\hbar \frac{dB^\dagger_{n\mathbf{k}} B_{m\mathbf{k}}}{dt} &= (E_{m\mathbf{k}} - E_{n\mathbf{k}}) B^\dagger_{n\mathbf{k}} B_{m\mathbf{k}} - \mathbf{E}_{intra} \cdot \sum_{n'} [g_{mn'} B^\dagger_{n\mathbf{k}} B_{n'\mathbf{k}} - g_{n'n} B^\dagger_{n'\mathbf{k}} B_{m\mathbf{k}}] \\ &\quad -\mathbf{E}_{opt}(t) \cdot [M^f_m B^\dagger_{n\mathbf{k}} - M^{f*}_n B_{m\mathbf{k}}]. \end{aligned} \tag{4.18}$$

Reproduced with permission of the copyright owner. Further reproduction prohibited without permission.

Eqs. (4.17) and (4.18) are the basic equations for studying the dynamic behavior of free electron-hole pairs. In the next section, we will try to simplify the equation within the rotating wave approximation and obtained the dimensionless equations suitable for numerical calculation.

4.3 Solving the Equations of Motion Numerically

4.3.1 Simplified Equations of Motion

Assuming that there is no external terahertz field and that the optical field consists of a pulse of the form

$$\mathbf{E}_{opt}(t) = \mathbf{E}(\mathbf{t})e^{-i\omega_c t} + c.c,$$

and including phenomenological damping, as was done for the 1s excitons, we obtain the following expressions for the equations of motion within the rotating wave approximation:

$$i\hbar\frac{d\langle B_{n\mathbf{k}}\rangle}{dt} + (E_{n\mathbf{k}} + \frac{i\hbar}{T_n(\mathbf{k})})\langle B_{n\mathbf{k}}\rangle = -\mathbf{E}(\mathbf{t})e^{-i\omega_c t}\cdot M^f_{n\mathbf{k}} - \langle \mathbf{E}_{intra}\rangle \cdot \sum_{n'} g^*_{n'n}\langle B'_{n'\mathbf{k}}\rangle, \quad (4.19)$$

$$\begin{aligned} i\hbar\frac{d\left\langle B^\dagger_{n\mathbf{k}}B_{m\mathbf{k}}\right\rangle}{dt} &= (E_{m\mathbf{k}} - E_{n\mathbf{k}} - \frac{1}{T_{nm}(\mathbf{k})})\left\langle B^\dagger_{n\mathbf{k}}\, B_{m\mathbf{k}}\right\rangle \\ &+\mathcal{E}^*(t)e^{i\omega_c t}\cdot M^{f*}_{n\mathbf{k}}\langle B_{m\mathbf{k}}\rangle - \mathbf{E}(\mathbf{t})e^{-i\omega_c t}M^f_{m\mathbf{k}}\left\langle B^\dagger_{n\mathbf{k}}\right\rangle \\ &+\langle \mathbf{E}_{intra}\rangle\cdot\sum_{n'}\left[g_{n'n}\left\langle B^\dagger_{n'\mathbf{k}}B_{m\mathbf{k}}\right\rangle - g^*_{n'm}\left\langle B^\dagger_{n\mathbf{k}}B_{n'\mathbf{k}}\right\rangle\right]. \quad (4.20) \end{aligned}$$

These are the sets of equations that need to be solved simultaneously to obtain the second order intraband polarization. Because the $\mathbf{k}$ in the above equations is a 2D vector, it therefore can be a big burden for numerical calculation. We will try to simplify the Eqs. (4.19) and (4.20) so as to make the problem more computationally tractable.

We begin by defining:

$$Y_{n,m} \equiv \sum_{\mathbf{k}}\left\langle B^\dagger_{n\mathbf{k}}B_{m\mathbf{k}}\right\rangle \quad (4.21)$$

Reproduced with permission of the copyright owner. Further reproduction prohibited without permission.

and

$$C_n(\varepsilon) \equiv \int_0^{2\pi} \langle B_{n\mathbf{k}} \rangle \, d\phi, \tag{4.22}$$

where $\mathbf{k} = (k, \phi)$. Now, we assume that $T_n(\mathbf{k}) \equiv T_n(k, \phi)$ is independent of ϕ and $T_{nm}(\mathbf{k})$ is independent of $\mathbf{k}$. This is a good approximation because it is reasonable to assume the scattering within the plane is isotropic, and for the relatively small k considered here, the dependence on k should be small. With the above assumptions, the number of equations to be solved is significantly reduced. Moreover, the intraband polarization is seen to depend only on $Y_{n,m}$:

$$\begin{aligned} \left\langle \mathbf{P}^f_{intra} \right\rangle(\tau) &= \frac{1}{V} \sum_{n,\mathbf{k},m,\mathbf{k}'} G^f_{n\mathbf{k};m\mathbf{k}'} \left\langle B^\dagger_{n\mathbf{k}} B_{m\mathbf{k}'} \right\rangle \\ &= \frac{1}{V} \sum_{n,m} g_{n,m} Y_{n,m} \end{aligned} \tag{4.23}$$

Using these definitions, Eqs. (4.19) and (4.20) become:

$$i\hbar \frac{dC_n(\varepsilon)}{dt} + \left(-\hbar\omega_{n\varepsilon} + \frac{i\hbar}{T_{n\varepsilon}} \right) C_n(\varepsilon) = -2\pi \mathbf{E}(\mathbf{t}) e^{-i\omega_c t} \cdot \mathbf{M}^f_n - \langle \mathbf{E}_{intra} \rangle \cdot \sum_{n'} \mathbf{g}^*_{n',n} C_{n'}(\varepsilon), \tag{4.24}$$

$$\begin{aligned} i\hbar \frac{dY_{n,m}}{dt} &= \left(\hbar\omega_m - \hbar\omega_n - \frac{i\hbar}{T_{nm}} \right) Y_{n,m} + \frac{A m_\parallel}{(2\pi)^2 \hbar^2} \int_0^\infty d\varepsilon [\mathcal{E}^*(t) e^{i\omega_c t} \cdot \mathbf{M}^{f*}_n C_m(\varepsilon) \\ &\quad - \mathbf{E}(\mathbf{t}) e^{-i\omega_c t} \mathbf{M^f}_m C^*_n(\varepsilon)] \\ &\quad + \langle \mathbf{E}_{intra} \rangle \cdot \sum_{n'} \left(\mathbf{g}_{n',n} Y_{n',m} - \mathbf{g}^*_{n',m} Y_{n,n'} \right), \end{aligned} \tag{4.25}$$

where

$$\hbar\omega_{n\varepsilon} = \hbar\omega_0 + n\hbar\omega_B + \varepsilon \tag{4.26}$$

and

$$\hbar\omega_n = n\hbar\omega_B,$$

where

$$\varepsilon = \frac{\hbar^2 k^2}{2m_\parallel} \tag{4.27}$$

Reproduced with permission of the copyright owner. Further reproduction prohibited without permission.

is the in-plane dispersion relation with $\frac{1}{m_{\|}} = \frac{1}{m_{e\|}} + \frac{1}{m_{h\|}}$. With the simplification made above, the number of differential equations to be solved is greatly reduced and hence makes the problem tractable. To proceed to use these equations in a computer program, they must first be put into dimensionless form and the time dependence factored out in a way similar to that which was done for the exciton equations.

4.3.2 Dimensionless Equations

We now wish to move to dimensionless equations which do not contain the factors of area A and volume V. We note that the volume is given by

$$V = AN_z d.$$

We begin by defining

$$\mathbf{M}_n^f = \mathbf{M}_o S_n \sqrt{\frac{V}{d}}.$$

In these definitions, $\mathbf{M}_o$ is the bulk dipole matrix element between the conduction and valence bands (units of charge times length) and

$$S_n = \frac{1}{\sqrt{N_z}} \int dz \Psi_{n,\mathbf{k}}^f(\boldsymbol{\rho} = 0, z, z),$$

with units of one over length, where $\Psi_{n,\mathbf{k}}^f(\boldsymbol{\rho} = 0, z, z)$ is defined in Eq. (4.2). Thus by defining

$$S_n = \frac{1}{\sqrt{A}} \widetilde{S}_n,$$

we obtain

$$\mathbf{M}_n^f = \mathbf{M}_o \widetilde{S}_n \sqrt{N_z}.$$

For simplicity, we will confine our calculations to the tight-binding approximation. In this case, $\chi_n(z)$ in Eq. (4.2) can be written as

$$\chi_n(z) = \sum_p J_{p-n}(\theta_\sigma) f_p^\sigma(z). \tag{4.28}$$

Reproduced with permission of the copyright owner. Further reproduction prohibited without permission.

and the redefined dimensionless interband dipole matrix can be simplified as,

$$\begin{aligned}
\tilde{S}_n &= \sum_{p,p'} J_{p-n}(\theta_e) J_{p'}(\theta_h) \int dz f_p^e(z - pd) f_{p'}^h(z - p'd) \\
&\approx \sum_{p,p'} J_{p-n}(\theta_e) J_{p'}(\theta_h) \delta_{pp'} \\
&= \sum_{p} J_{p-n}(\theta_e) J_p(\theta_h) \\
&= J_{-n}(\theta_e - \theta_h) \\
&\equiv J_{-n}(\theta), \qquad (4.29)
\end{aligned}$$

where $\theta \equiv \theta_e - \theta_h = \frac{\Delta_e}{2eF_0d} - (\frac{-\Delta_h}{2eF_0d}) = \frac{\Delta_e + \Delta_h}{2eF_0d}$.

Now, we make the following definitions to remove A and V from the equations and to remove fast time dependence:

$$C_n(\varepsilon = x\hbar\omega_B; t = \tau/\omega_B) \equiv \frac{ed}{\mathbf{M}_o^*} \sqrt{N_z} K_n(x, \tau) e^{-i\widetilde{\omega}_{nx}^0 t} \qquad (4.30)$$

and

$$Y_{n,m}(t = \tau/\omega_B) \equiv \frac{e^2 N_z A}{|\mathbf{M}_o|^2} X_{n,m}(\tau) e^{-i(m-n)t}, \qquad (4.31)$$

where $\tau = \omega_B t$, and

$$x \equiv \frac{\varepsilon}{\hbar\omega_B},$$

and

$$\begin{aligned}
\widetilde{\omega}_{nx} &\equiv \frac{\hbar\omega_{nx}}{\hbar\omega_B} \\
&\equiv \frac{\hbar\omega_{n\varepsilon}}{\hbar\omega_B} \\
&= \frac{\hbar\omega_0 + n\hbar\omega_B + \varepsilon}{\hbar\omega_B} \\
&\equiv \widetilde{\omega}_0 + n + x,
\end{aligned}$$

Reproduced with permission of the copyright owner. Further reproduction prohibited without permission.

where $\widetilde{\omega}_0 \equiv \frac{\omega_0}{\omega_B}$. Finally, we define

$$\begin{aligned}\Gamma_{nx} &= \omega_B T_n(x\hbar\omega_B), \\ \Gamma_{nm} &= \omega_B T_{nm}.\end{aligned}$$

Using these definitions in Eqs. (4.24) and (4.25), we obtain:

$$\begin{aligned}\frac{dK_n(x)}{d\tau} &= -\frac{1}{\Gamma_{nx}}K_n(x) + i2\pi\mathbf{E}(\mathbf{t})e^{-i(\widetilde{\omega}_c-\widetilde{\omega}_0-n-x)\tau}\cdot\frac{|\mathbf{M}_o|^2}{ed\hbar\omega_B}\widetilde{S}_n \\ &\quad +i\frac{\langle\mathbf{E}_{intra}\rangle}{\hbar\omega_B}\cdot\sum_{n'}\mathbf{g}^*_{n',n}K_{n'}(x)\,e^{-i(n'-n)\tau},\end{aligned} \tag{4.32}$$

$$\begin{aligned}\frac{dX_{n,m}}{d\tau} &= -\frac{1}{\Gamma_{nm}}X_{n,m} - i\frac{m_{\|}|\mathbf{M}_o|^2 d}{(2\pi)^2\hbar^2 e}\int_0^\infty dx\left[\mathcal{E}^*(t)e^{i(\widetilde{\omega}_c-\widetilde{\omega}_0-n-x)\tau}\widetilde{S}^*_n K_m(x)\right. \\ &\quad \left.-\mathbf{E}(\mathbf{t})e^{-i(\widetilde{\omega}_c-\widetilde{\omega}_0-m-x)\tau}\widetilde{S}_m K^*_n(x)\right] \\ &\quad -i\frac{\langle\mathbf{E}_{intra}\rangle}{\hbar\omega_B}\cdot\sum_{n'}\left(\mathbf{g}_{n',n}X_{n',m}e^{i(n'-n)\tau}-\mathbf{g}^*_{n',m}X_{n,n'}e^{-i(n'-m)\tau}\right).\end{aligned} \tag{4.33}$$

To solve these equations, it is necessary to discretize x. We let $x \equiv x_j = \frac{jx_{\max}}{M}$, where $j = 1, 2, ...M$, and $x_{\max}$ is the upper limit for the integral in Eq. (4.33). The appropriate value for $x_{\max}$ will be discussed in next section. Once the time-dependent reduced matrix elements $X_{n,m}$ and $K_n(x)$ are obtained by solving the above equations of motion, physical quantities such as interband and intraband polarization, absorption, etc., can be arrived at by straightforward calculations. We finally note that by using the definition in Eq. (4.31), the intraband polarization in Eq. (4.23) can be rewritten as,

$$\left\langle\mathbf{P}^f_{intra}\right\rangle(\tau) = \frac{e^2}{|\mathbf{M}_o|^2 d}\sum_{n,n'}g_{n,n'}X_{n,n'}e^{-i(n'-n)\tau}. \tag{4.34}$$

4.3.3 Solving the Dimensionless Equations for Free Electron-hole Pairs

Although it seems that the equations of motion for a free electron-hole pair are very similar to the exciton equations, there are some important differences. The tricky part of the problem is this: in the first-order exciton equation, the number of equations is same as the number of $\widetilde{S}_\mu$

Reproduced with permission of the copyright owner. Further reproduction prohibited without permission.

and the number of $\omega_c - \omega_\mu^0$, i.e. they are all indexed by the same index μ which runs from 1 to N, the total number of exciton states in the superlattice; however, this is not the case in free electron-hole pair. While the number of $\widetilde{S}_n$ remains the same as $\widetilde{S}_\mu$ in the exciton case, the number of equations and the number $\widetilde{\omega}_c - \widetilde{\omega}_0 - n - x_j$ are different from their exciton counterparts. Therefore, we must re-index the first-order free electron-hole pair equation so as to make them parallel with the exciton equations.

The number of equations for free electron-hole pairs is M times its excitonic counterpart. A good way to solve these equations is to transfer the two dimensional arrays indexed by n and j to one dimensional arrays indexed by

$$J \equiv (j-1)N + n, \tag{4.35}$$

where j runs from 1 to M and n runs from 1 to N. Another tricky problem in solving equations of motion lies in evaluating the integral part in Eq. (4.33). This will be addressed in the next section, where we will discuss the convergence and relevant numerical results for this integral.

4.4 Testing of the Numerical Method

4.4.1 The Convergence of the Integral in the Second-order Equation

Because the integral limits in the second-order equation (4.33) are from zero to infinity, we will first test the convergence of this integral so as to make sure our method is accurate.

We define a new variable:

$$W_n(x) \equiv \frac{K_n(x)}{\widetilde{S}_n},$$

Then we have:

$$\begin{aligned} \frac{dW_n(x)}{d\tau} &= -\frac{1}{\Gamma_{nx}} W_n(x) + i2\pi \mathbf{E}(\mathrm{t}) e^{-i(\widetilde{\omega}_c - \widetilde{\omega}_0 - n - x)\tau} \cdot \frac{|\mathbf{M}_o|^2}{ed\hbar\omega_B} \\ &\quad + i\frac{\langle \mathbf{E}_{intra} \rangle}{\hbar\omega_B} \cdot \sum_{n'} \mathbf{g}^*_{n',n} \frac{\widetilde{S}_{n'}}{\widetilde{S}_n} W_{n'}(x)\, e^{-i(n'-n)\tau}, \end{aligned} \tag{4.36}$$

Reproduced with permission of the copyright owner. Further reproduction prohibited without permission.

$$\begin{aligned}\frac{dX_{n,m}}{d\tau} &= -\frac{1}{\Gamma_{nm}}X_{n,m} - i\frac{m_{\|}\left|\mathbf{M}_o\right|^2 d}{(2\pi)^2\hbar^2 e}\int_0^\infty dx\left[\mathcal{E}^*(t)e^{i(\widetilde{\omega}_c-\widetilde{\omega}_0-n-x)\tau}\widetilde{S}_n^*\widetilde{S}_m W_m(x)\right.\\ &\left.-\mathbf{E}(\mathbf{t})e^{-i(\widetilde{\omega}_c-\widetilde{\omega}_0-m-x)\tau}\widetilde{S}_m\widetilde{S}_n^* W_n^*(x)\right]\\ &-i\frac{\langle\mathbf{E}_{intra}\rangle}{\hbar\omega_B}\cdot\sum_{n'}\left(\mathbf{g}_{n',n}X_{n',m}e^{i(n'-n)\tau}-\mathbf{g}_{n',m}^*X_{n,n'}e^{-i(n'-m)\tau}\right). \qquad (4.37)\end{aligned}$$

Note that in the absence of the THz field $\langle\mathbf{E}_{intra}\rangle$, the equations for all W_n are identical except for the shift of x by n. We define

$$f(\tau) = 2\pi\frac{\left|\mathbf{M}_o\right|^2}{ed\hbar\omega_B}\mathbf{E}(\mathbf{t})$$

and assume a Gaussian field of the form

$$\mathbf{E}(\mathbf{t}) = E\exp(i\phi)\exp\left(-\Omega^2\tau^2/2\right) \qquad (4.38)$$

such that

$$f(\tau) = f_o\exp(i\phi)\exp\left(-\Omega^2\tau^2/2\right), \qquad (4.39)$$

where

$$f_o = 2\pi\frac{E\left|\mathbf{M}_o\right|^2}{ed\hbar\omega_B} \qquad (4.40)$$

is a real constant, and Ω characterizes the exciting optical pulse width. Then, when there is no dephasing and no THz field, the solution of Eq. (4.36) is:

$$\begin{aligned}W_n(x,\tau) &= i\frac{\sqrt{2\pi}}{2\Omega}f_o\exp(i\phi)\exp\left[-\frac{(\widetilde{\omega}_c-\widetilde{\omega}_0-n-x)^2}{2\Omega^2}\right]\\ &\cdot\left[\mathrm{erf}\left(\frac{-\tau\Omega^2-i(\widetilde{\omega}_c-\widetilde{\omega}_0-n-x)}{\sqrt{2}\Omega}\right)-1\right]. \qquad (4.41)\end{aligned}$$

Reproduced with permission of the copyright owner. Further reproduction prohibited without permission.

Using this result, we see that the second term in Eq. (4.37) is proportional to

$$\begin{aligned}
T_2 &= -i\int_0^\infty dx\mathcal{E}^*(t)\left[e^{i(\widetilde{\omega}_c-\widetilde{\omega}_0-n-x)\tau}\widetilde{S}_n^*\widetilde{S}_m W_m(x,\tau)-\mathbf{E}(t)e^{-i(\widetilde{\omega}_c-\widetilde{\omega}_0-m-x)\tau}\widetilde{S}_m\widetilde{S}_n^* W_n^*(x,\tau)\right] \\
&= -i\exp\left(-\Omega^2\tau^2/2\right)\widetilde{S}_n\widetilde{S}_m\int_0^\infty dx\left[e^{i(\widetilde{\omega}_c-\widetilde{\omega}_0-n-x)\tau}W_m(x,\tau)-e^{-i(\widetilde{\omega}_c-\widetilde{\omega}_0-m-x)\tau}W_n^*(x,\tau)\right] \\
&= C\int_0^\infty dx\{e^{i(\widetilde{\omega}_c-\widetilde{\omega}_0-n-x)\tau}\exp\left[-\frac{\left(\widetilde{\omega}_c-\widetilde{\omega}_0-m-x\right)^2}{2\Omega^2}\right] \\
&\quad\cdot\left[\mathrm{erf}\left(\frac{-\tau\Omega^2-i\left(\widetilde{\omega}_c-\widetilde{\omega}_0-m-x\right)}{\sqrt{2}\Omega}\right)-1\right]+e^{-i(\widetilde{\omega}_c-\widetilde{\omega}_0-m-x)\tau} \\
&\quad\cdot\exp\left[-\frac{\left(\widetilde{\omega}_c-\widetilde{\omega}_0-n-x\right)^2}{2\Omega^2}\right]\left[\mathrm{erf}\left(\frac{-\tau\Omega^2+i\left(\widetilde{\omega}_c-\widetilde{\omega}_0-n-x\right)}{\sqrt{2}\Omega}\right)-1\right],
\end{aligned}$$

where C is a real constant. Now, for large values of $|z|$, the asymptotic form of the error function is:

$$\mathrm{erf}(z)=1-\frac{e^{-z^2}}{\sqrt{\pi}z}\left[1-\frac{1}{2z^2}+...\right].$$

Thus, in the limit that x becomes very large, the integrand above takes the form:

$$\begin{aligned}
I(x) &\simeq -\frac{e^{i(\widetilde{\omega}_c-\widetilde{\omega}_0-n-x)\tau}}{\sqrt{\pi}}\exp\left[-\frac{\left(\widetilde{\omega}_c-\widetilde{\omega}_0-m-x\right)^2}{2\Omega^2}\right] \\
&\quad\cdot\exp\left[-\left(\frac{-\tau\Omega^2-i\left(\widetilde{\omega}_c-\widetilde{\omega}_0-m-x\right)}{\sqrt{2}\Omega}\right)^2\right] \\
&\quad\cdot\left[\frac{-\tau\Omega^2-i\left(\widetilde{\omega}_c-\widetilde{\omega}_0-m-x\right)}{\sqrt{2}\Omega}\right]^{-1} \\
&\quad+\frac{e^{-i(\widetilde{\omega}_c-\widetilde{\omega}_0-m-x)\tau}}{\sqrt{\pi}}\exp\left[-\frac{\left(\widetilde{\omega}_c-\widetilde{\omega}_0-n-x\right)^2}{2\Omega^2}\right] \\
&\quad\cdot\exp\left[-\left(\frac{-\tau\Omega^2+i\left(\widetilde{\omega}_c-\widetilde{\omega}_0-n-x\right)}{\sqrt{2}\Omega}\right)^2\right] \\
&\quad\cdot\left[\frac{-\tau\Omega^2+i\left(\widetilde{\omega}_c-\widetilde{\omega}_0-n-x\right)}{\sqrt{2}\Omega}\right]^{-1} \\
&= -\exp\left[-\tau^2\Omega^2/2\right]\{\frac{e^{i(\widetilde{\omega}_c-\widetilde{\omega}_0-n-x)\tau}}{\sqrt{\pi}}\exp\left[-i\sqrt{2}\tau\Omega\left(\widetilde{\omega}_c-\widetilde{\omega}_0-m-x\right)\right] \\
&\quad\cdot\left[\frac{-\tau\Omega^2-i\left(\widetilde{\omega}_c-\widetilde{\omega}_0-m-x\right)}{\sqrt{2}\Omega}\right]^{-1}+\frac{e^{-i(\widetilde{\omega}_c-\widetilde{\omega}_0-m-x)\tau}}{\sqrt{\pi}} \\
&\quad\cdot\exp\left[i\sqrt{2}\tau\Omega\left(\widetilde{\omega}_c-\widetilde{\omega}_0-n-x\right)\right]\cdot\left[\frac{-\tau\Omega^2+i\left(\widetilde{\omega}_c-\widetilde{\omega}_0-n-x\right)}{\sqrt{2}\Omega}\right]^{-1}.
\end{aligned}$$

Reproduced with permission of the copyright owner. Further reproduction prohibited without permission.

Now, there is no problem with convergence of the terms which are proportional to $1/x^2$, however the terms which are proportional to $1/x$ would seem to pose a problem. Collecting those terms we have

$$\begin{aligned} I_2(x) &= i\frac{\sqrt{2}\Omega}{x}\exp\left[-\tau^2\Omega^2/2\right]\frac{1}{\sqrt{\pi}}\left\{e^{i(\widetilde{\omega}_c-\widetilde{\omega}_0-n-x)\tau}\exp\left[-i\sqrt{2}\tau\Omega\left(\widetilde{\omega}_c-\widetilde{\omega}_0-m-x\right)\right]\right. \\ &\left. -e^{-i(\widetilde{\omega}_c-\widetilde{\omega}_0-m-x)\tau}\exp\left[i\sqrt{2}\tau\Omega\left(\widetilde{\omega}_c-\widetilde{\omega}_0-n-x\right)\right]\right\}. \end{aligned}$$

The first term is proportional to

$$\exp\left[-i\left(1-\sqrt{2}\Omega\right)\tau x\right]/x.$$

This integral is convergent unless $\sqrt{2}\Omega = 1$, or $\tau = 0$. However, if $\tau = 0$ then we have

$$\begin{aligned} I_2(x) &= i\frac{\sqrt{2}\Omega}{x}\exp\left[-\tau^2\Omega^2/2\right]\frac{1}{\sqrt{\pi}}\{1-1\} \\ &= 0. \end{aligned}$$

If $\sqrt{2}\Omega = 1$, then we have

$$\begin{aligned} I_2(x) &= i\frac{1}{x}\exp\left[-\tau^2/4\right]\frac{1}{\sqrt{\pi}}\left\{e^{i(m-n)\tau}-e^{-i(m-n)\tau}\right\} \\ &= -2\frac{1}{x}\exp\left[-\tau^2/4\right]\frac{1}{\sqrt{\pi}}\sin\left[(n-m)\tau\right]. \end{aligned}$$

If $m \neq n$ and $\Omega = \frac{1}{\sqrt{2}}$, the integral will be divergent. But we are not in this situation. Therefore, we expect no convergence problems in our calculation.

4.4.2 Convergence Test by Numerical Calculation

Considering a GaAs/GaAlAs superlattice, we calculate the real part of the integral

$$\int_0^\infty dx\mathcal{E}^*(t)e^{i(\widetilde{\omega}_c-\widetilde{\omega}_0-x)\tau}K_m(x)$$

in Eq. (4.33) with the related parameters in Table 4.1. Here, F_0 is the applied static field; d is the period of the superlattice; ε_c is the energy (relative to the $n = 0$ Stark ladder) corresponding

Reproduced with permission of the copyright owner. Further reproduction prohibited without permission.

F_0(kV/cm)	$d(10^{-10}\text{m})$	ε_c(meV)	E_{op}(GV/m)	T_1	T^f_{2inter}	T^f_{2inter}
15	84	0	1×10^{-3}	∞	20	10

Table 4.1: Parameters for Testing Integral Convergence

to the exciting center laser frequency; E_{op} is the exciting optical field strength of the exciting laser pulse; T^f_{2inter} and T^f_{2inter} are respectively the interband and intraband dephasing constants for free electron-hole pairs; T_1 denote the population decay constant for both excitons and free electron-hole pairs. Other parameters that are applicable to all the calculations in this work include: dielectric constant ϵ is taken as 12.5 for the GaAS/GaAlAs superlattice system; the parameter characterizing the optical pulse width Ω is 0.964; the transverse electron and hole effective masses ($m_{e\|}$ and $m_{h\|}$) are respectively 0.0665 and 0.115 (in units of free electron mass), from which the layer-dependent transverse electron-hole-reduced effective mass $m_{\|}$ can be calculated by using Eq. (2.12).

As shown in Fig. 4-1, we evaluate the real part of the integral $\int_0^\infty dx\mathcal{E}^*(t)e^{i(\tilde{\omega}_c-\tilde{\omega}_0-x)\tau}K_m(x)$ at $\tau = 14$ for all the states m using a trapezoidal rule. In the program, the optical pulse is introduced at time point $\tau = 10$ and then the pulse has passed at the evaluation time point $\tau = 14$. The integrals converge very well as long as the upper limit is beyond 126 meV. In the remainder of this work we use $x_{\max} = 130$meV. It is found that the number of discretized points should be more than 50 for convergence. In the computer program, we take this number as 102. Finally, we find that the imaginary part of the integral also converges very well.

4.4.3 Testing the Numerical Calculation in a Coherent Limit

The numerical results will be tested by assuming there is no dephasing, i.e., in the coherent limit. In this situation, $Y_{n,m}$ defined in Eq. (4.21) takes the form,

$$\begin{aligned} Y_{n,m} &= \sum_{\mathbf{k}} \left\langle B^\dagger_{n\mathbf{k}} B_{m\mathbf{k}} \right\rangle \\ &= \sum_{\mathbf{k}} \left\langle B^\dagger_{n\mathbf{k}} \right\rangle \langle B_{m\mathbf{k}} \rangle \\ &\approx \int_0^\infty dk \cdot k \int_0^{2\pi} d\phi \left\langle B^\dagger_{n\mathbf{k}} \right\rangle \langle B_{m\mathbf{k}} \rangle \cdot \frac{A}{(2\pi)^2}. \end{aligned} \tag{4.42}$$

Reproduced with permission of the copyright owner. Further reproduction prohibited without permission.

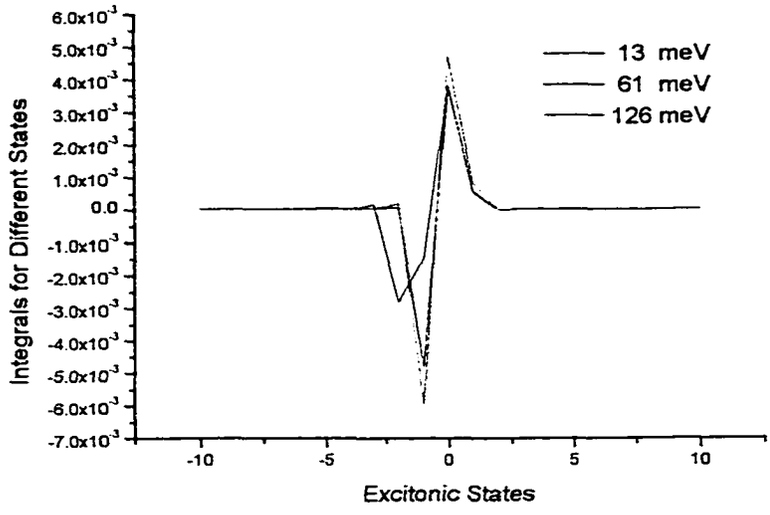

Figure 4-1: Integral evaluations for different excitonic states for diffrent $x_{\max}$

Using the definition for $C_n(\varepsilon)$, Eq. (4.22), we may also get,

$$\begin{aligned} C_n^*(\varepsilon)\, C_m(\varepsilon) &= \int_0^{2\pi} d\phi \left\langle B_{n\mathbf{k}}^\dagger, \phi \right\rangle \int_0^{2\pi} d\phi' \left\langle B_{m\mathbf{k}}, \phi' \right\rangle \\ &= 2\pi \int_0^{2\pi} d\phi \left\langle B_{n\mathbf{k}}^\dagger \right\rangle \langle B_{m\mathbf{k}} \rangle . \end{aligned} \tag{4.43}$$

Combining the above two equations, we have,

$$\begin{aligned} Y_{n,m} &= \int_0^\infty dk \cdot k C_n^*(\varepsilon)\, C_m(\varepsilon) \cdot \frac{A}{(2\pi)^3} \\ &= \frac{A}{(2\pi)^3} \int_0^\infty dk \cdot k \frac{(ed)^2}{|\mathbf{M}_o|^2} N_z K_n^*(x,\tau) K_m(x,\tau) e^{i(\tilde{\omega}_{nx}^0 - \tilde{\omega}_{mx}^0)t} \\ &= \frac{e^2 N_z A}{|\mathbf{M}_o|^2} X_{n,m}(\tau) e^{i(\tilde{\omega}_{nx}^0 - \tilde{\omega}_{mx}^0)t}, \end{aligned} \tag{4.44}$$

Reproduced with permission of the copyright owner. Further reproduction prohibited without permission.

F_0(kV/cm)	$d(10^{-10}\text{m})$	ε_c(meV)	E_{op}(GV/m)	T_1	T_{2inter}^f	T_{2inter}^f
15	84	0	1×10^{-3}	∞	∞	∞

Table 4.2: Parameters for Testing Eq. (4.45) in the Coherent Limit

where the definitions in Eqs. (4.30) and (4.31) have been used. Finally we arrive at,

$$\begin{aligned} X_{n,m} &= \frac{d^2}{(2\pi)^3}\int_0^\infty dk\cdot kK_n^*(x,\tau)K_m(x,\tau) \\ &= \frac{m_{\|}\omega_B d^2}{\hbar(2\pi)^3}\int_0^\infty dx\cdot K_n^*(x,\tau)K_m(x,\tau), \end{aligned} \tag{4.45}$$

where we use

$$\begin{aligned} dx &= \frac{d\varepsilon}{\hbar\omega_B} \\ &= \frac{d}{\hbar\omega_B}(\frac{\hbar k^2}{2m_{\|}}) \\ &\Longrightarrow\ dk\cdot k = dx\cdot\frac{m_{\|}\omega_B}{\hbar}, \end{aligned} \tag{4.46}$$

where $m_{\|}$ is the reduced mass of the electron and hole in the plane. We can use Eq. (4.45) to test the numerical calculation. The RHS of Eq. (4.45), which can be obtained by integrating over the results from solving first-order equation of motion, should be equal to the LHS of the equation which is obtained by solving the second-order equation. The following are some examples for such verification.

Considering the same GaAs/GaAlAs superlattice discussed in Section 4.4.2, we calculate the real parts of the RHS and LHS of Eq. (4.45) with the related parameters in Table 4.2. As shown in Fig. 4-2, after the optical is gone, [here we take the RHS and LHS of the Eq. (4.45) at time point $\tau = 94$; the exciting optical pulse is at time point $\tau = 10.$], the curves corresponding to the real parts of the LHS and RHS of Eq. (4.45) are exactly overlapped to within the plot resolution and hence demonstrate the numerical validity in calculating both first-order and second-order equations of motion in the coherent limit (similar results can be obtained for imaginary parts). Note that we compare the two 2D arrays by transforming them into 1D arrays.

If we do not choose the coherent limit case but calculate with the parameters in Table 4.1.

Reproduced with permission of the copyright owner. Further reproduction prohibited without permission.

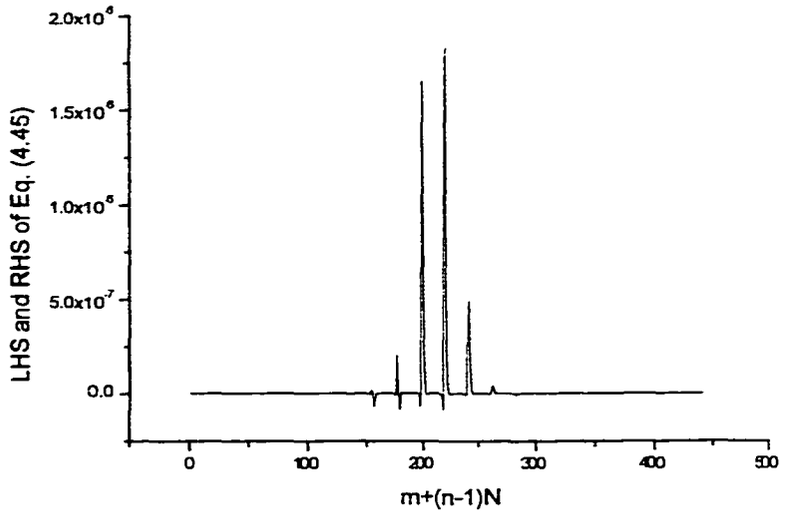

Figure 4-2: LHS and RHS of Eq. (4.45)

i.e. with dephasing, then we can not get the same results as in Eq. 4.45. As shown in Figs. 4-3 and 4-4, the calculated LHS and RHS of Eq.(4.45) are quite different.

4.4.4 Comparing the Analytical and Numerical Results for the Population in A Limiting Case

Under some circumstances, analytical results can be obtained by solving the equations of motion. We may compare these analytical results with the numerical ones in these situations and thereby check the numerical methods employed in the computer program. When there is no dephasing and no Terahertz field, we may get the analytical results for the electron-hole pair population long after the optical pulse has passed.

We assume that the optical field takes the Gaussian form,

$$\mathbf{E(t)} = E_{op} e^{-(\frac{\tau}{\gamma})^2}. \tag{4.47}$$

Note that here we use γ, rather than Ω in Eq. (4.38), to characterize the optical pulse width so as to be consistent with the parameter used in the computer program. The relation between γ

Reproduced with permission of the copyright owner. Further reproduction prohibited without permission.

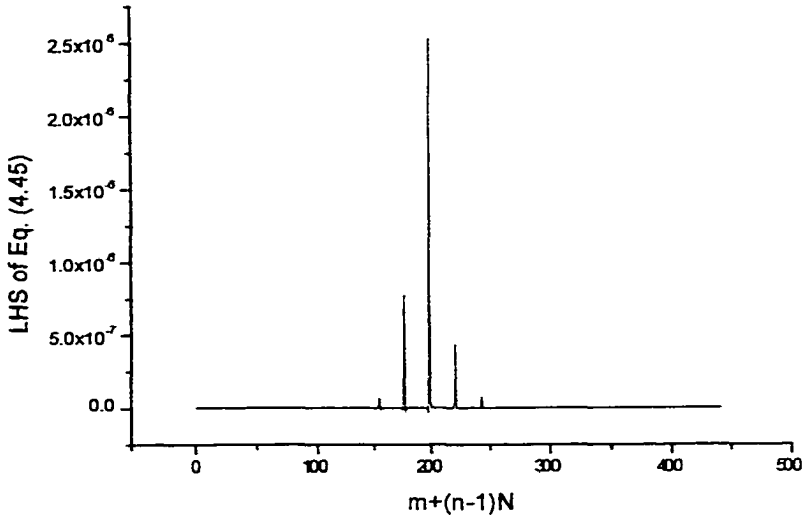

Figure 4-3: LHS of Eq. (4.45)

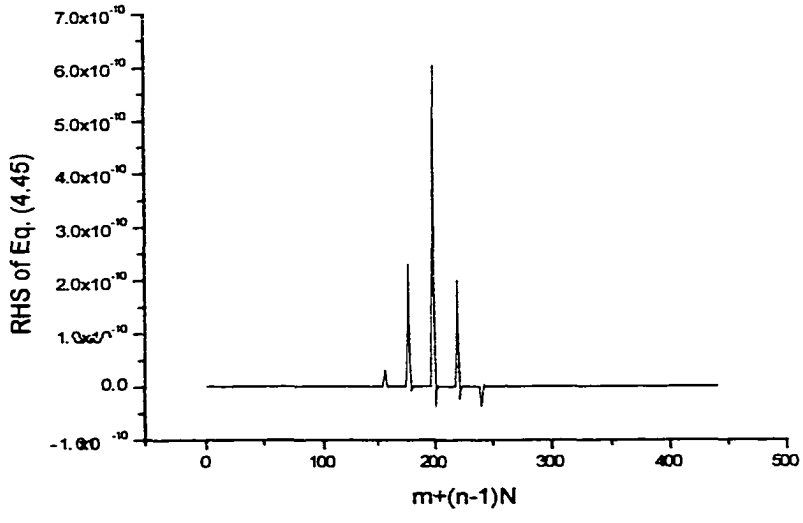

Figure 4-4: RHS of Eq. (4.45)

Reproduced with permission of the copyright owner. Further reproduction prohibited without permission.

and Ω is

$$\frac{\Omega^2}{2} = \frac{1}{\gamma^2}. \tag{4.48}$$

Then, when there are no dephasing and no Terahertz field, the first-order equation of motion becomes,

$$\frac{dK_n(x)}{d\tau} = i2\pi E_{op} e^{-(\frac{\tau}{\gamma})^2} e^{-i(\widetilde{\omega}_c - \widetilde{\omega}_0 - n - x)\tau} \cdot \frac{|\mathbf{M}_o|^2}{ed\hbar\omega_B} \widetilde{S}_n. \tag{4.49}$$

The solution for $K_n(x)$ long after the optical pulse has passed is,

$$K_n(x) = \int_{-\infty}^{\infty} d\tau \cdot i2\pi E_{op} e^{-(\frac{\tau}{\gamma})^2} e^{-i(\widetilde{\omega}_c - \widetilde{\omega}_0 - n - x)\tau} \cdot \frac{|\mathbf{M}_o|^2}{ed\hbar\omega_B} \widetilde{S}_n, \tag{4.50}$$

where we integrate from minus infinity to plus infinity because the system has experienced a whole Gaussian pulse rather than a half one as when we let the integral limits to be from zero to plus infinity. Now we continue to evaluate the solution for $K_n(x)$ by changing variables,

$$\begin{aligned}
K_n(x) &= \frac{i2\pi E_{op} |\mathbf{M}_o|^2 \widetilde{S}_n}{ed\hbar\omega_B} \int_{-\infty}^{\infty} \gamma d\tau' \cdot e^{-\tau'^2} e^{-i(\widetilde{\omega}_c - \widetilde{\omega}_0 - n - x)\gamma\tau'} && (\frac{\tau}{\gamma} \longrightarrow \tau') \\
&= \frac{i2\pi E_{op} |\mathbf{M}_o|^2 \widetilde{S}_n}{ed\hbar\omega_B} \int_{-\infty}^{\infty} \sqrt{\pi}\gamma d\tau \cdot e^{-\pi\tau^2} \cdot e^{-i(\widetilde{\omega}_c - \widetilde{\omega}_0 - n - x)\sqrt{\pi}\gamma\tau} && (\tau' \longrightarrow \gamma\sqrt{\pi}) \\
&= \frac{i2\pi E_{op} |\mathbf{M}_o|^2 \widetilde{S}_n}{ed\hbar\omega_B} \int_{-\infty}^{\infty} \sqrt{\pi}\gamma d\tau \cdot e^{-\pi\tau^2} \cdot e^{-i2\pi\tau(\widetilde{\omega}_c - \widetilde{\omega}_0 - n - x)\frac{\gamma}{2\sqrt{\pi}}} \\
&= \frac{i2\pi E_{op} |\mathbf{M}_o|^2 \widetilde{S}_n \sqrt{\pi}\gamma}{ed\hbar\omega_B} \int_{-\infty}^{\infty} d\tau \cdot e^{-\pi\tau^2} \cdot e^{-i2\pi\tau s} \\
&= \frac{i2\pi E_{op} |\mathbf{M}_o|^2 \widetilde{S}_n \sqrt{\pi}\gamma}{ed\hbar\omega_B} e^{-\pi s^2},
\end{aligned} \tag{4.51}$$

where $s = (\widetilde{\omega}_c - \widetilde{\omega}_0 - n - x)\frac{\gamma}{2\sqrt{\pi}}$. Therefore, the population of the free electron-hole pair per

Reproduced with permission of the copyright owner. Further reproduction prohibited without permission.

unit volume in this situation has the form,

$$
\begin{aligned}
Pop &= \frac{1}{V}\sum_{n,\mathbf{k}}\left\langle B^{\dagger}_{n\mathbf{k}}B_{n\mathbf{k}}\right\rangle \\
&= \frac{e^2}{|\mathbf{M}_o|^2 d}\sum_n X_{nn} \qquad (4.52)\\
&= \frac{e^2}{|\mathbf{M}_o|^2 d}\cdot\frac{4m_{\|}\omega_B d^2}{\hbar(2\pi)^3}\sum_n\int_0^{\infty}|K_n(x)|^2\,dx \\
&= \frac{m_{\|}E_{op}^2|\mathbf{M}_o|^2\widetilde{S}_n^2\gamma^2}{2d\hbar^3\omega_B}\sum_n\int_0^{\infty}e^{-\frac{\gamma^2}{2}(\widetilde{\omega}_c-\widetilde{\omega}_0-n-x)^2}dx \\
&= \frac{\sqrt{2}m_{\|}E_{op}^2|\mathbf{M}_o|^2\widetilde{S}_n^2\gamma}{2d\hbar^3\omega_B}\sum_n\int_0^{\infty}e^{-[\frac{\gamma}{\sqrt{2}}(\widetilde{\omega}_c-\widetilde{\omega}_0-n-x)]^2}\cdot d\frac{\gamma}{\sqrt{2}}(\widetilde{\omega}_c-\widetilde{\omega}_0-n-x)\,x \\
&= \frac{\sqrt{2}m_{\|}E_{op}^2|\mathbf{M}_o|^2\widetilde{S}_n^2\gamma}{2d\hbar^3\omega_B}\sum_n\int_{-\infty}^{\frac{\gamma}{\sqrt{2}}(\widetilde{\omega}_c-\widetilde{\omega}_0-n)}e^{-y^2}\cdot dy \\
&= \frac{\sqrt{2\pi}m_{\|}E_{op}^2|\mathbf{M}_o|^2\widetilde{S}_n^2\gamma}{4d\hbar^3\omega_B}\sum_n\begin{cases}1+\mathrm{erf}\frac{\gamma}{\sqrt{2}}[(\widetilde{\omega}_c-\widetilde{\omega}_0)-n] & \widetilde{\omega}_c-\widetilde{\omega}_0>n\\ 1 & \widetilde{\omega}_c-\widetilde{\omega}_0=n\\ 1-\mathrm{erf}\frac{\gamma}{\sqrt{2}}[n-(\widetilde{\omega}_c-\widetilde{\omega}_0)] & \widetilde{\omega}_c-\widetilde{\omega}_0<n\end{cases} \qquad (4.53)
\end{aligned}
$$

The results obtained with the above analytical expression are in agreement with the one obtained by numerical calculation to within roughly 0.01%. As shown in Fig. 4-5, the analytical and numerical results for a population of free electron-hole pairs excited with different $\omega_c = E_c/\hbar$ are exactly overlapped to within the plot resolution. The numerical calculations are made by using the same physical parameters as in Table 4.2 except that $E_{op} = 4\times10^{-4}$(GV/cm) here. Because the superlattice is only optically excited and therefore the population of free electron-hole pairs is proportional to the photo-current induced in the superlattice, the curve in Fig. 4-5 provides actually the "background" photo-current spectra underlying the excitonic photocurrent spectra.

We have presented in this chapter the basic derivations of the equations of motion for free electron-hole pairs. Some examples were also provided to check the validity of these equations. In next chapter, these equations will be used to study the behavior of free electron-hole pairs and their interaction with excitons.

Reproduced with permission of the copyright owner. Further reproduction prohibited without permission.

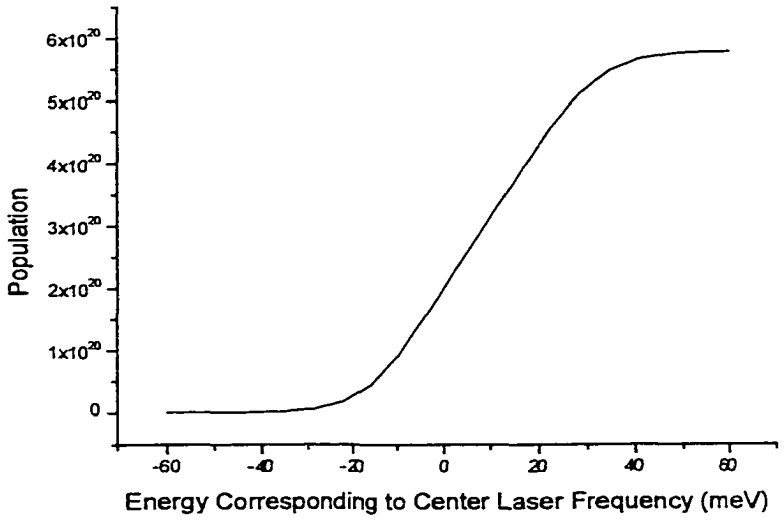

Figure 4-5: Population as function of center laser frequency

Reproduced with permission of the copyright owner. Further reproduction prohibited without permission.

Chapter 5

Interaction of Excitons and Free Electron-hole Pairs

With the theories concerning excitons in chapter 3 and free electron-hole pairs in chapter 4, we now turn our attention to the study of the interaction between these two sets of charge carriers and its consequences. The SCD effect, in which the electric fields due to the charge carriers interact with these carriers themselves, is the main subject of this chapter. Some experimental results for which we make our theoretical models will be introduced first. Then the SCD phenomena in the coherent regime will be studied in detail, from which some basic mechanisms of SCD will be discussed and demonstrated. Finally, we will apply our theory to the more realistic case, in which there is dephasing.

5.1 Experimental Results and Proposed Theoretical Models

As already discussed in Chapter 1, terahertz radiation is given off by the oscillating charge carriers such as excitons and free electron-hole pairs in a superlattice system. It is through the terahertz fields due to this radiation that different types of charge carriers interact with one another and substantially change their individual behavior. The first experiment demonstrating the existence of terahertz radiation due to intraband polarization was made by *Waschke et al* [26]. In other work, the self-induced terahertz fields were shown to be able to shift the energy level of the original WSL [27, 28]. However, in this work, we will focus on accounting for the

Reproduced with permission of the copyright owner. Further reproduction prohibited without permission.

Shapiro effect in the semiconductor superlattice system. In this effect, the BO were found to be accompanied by a coherent quasi-DC current that was attributed to the interaction of the charge carriers with the self-induced field [48]. This was observed by an apparently quasi-linear change in the intraband polarization.

The observed quasi-linear change in the intraband polarization of 1s excitons must require the transfer of energy between the coherent 1s excitons and the fields due to other types of charge carriers. The net energy transfer, however, needs a phase shift between the polarization due to 1s excitons and the fields driving them, as will be shown in next section. In this work, we will model two types of carriers (1s excitons and free electron-hole pairs) and then study their interaction. We will use a full quantum-mechanical model for both the 1s excitons and the free electron-hole pairs. Although this work is motivated by the experimental results described above, it is not limited to this situation. With our model, some other phenomena can be predicted in a photoexcited superlattice system. Moreover, a clearer physical picture on the basic interaction mechanisms among different types of carriers can be obtained by this model.

5.2 Full Hamiltonian of the interacting System

The full Hamiltonian of the interacting system when both excitons and free pairs are considered is

$$\begin{aligned} H &= H^{ex} + H^{f} + H^{f-ex} \\ &= H_o^{ex} + H_o^{f} - V\mathbf{E}(t)\cdot(\mathbf{P}^{ex}+\mathbf{P}^{f}) + V\frac{\mathbf{P}_{intra}\cdot\mathbf{P}_{intra}}{2\epsilon_0\epsilon}, \end{aligned} \tag{5.1}$$

where all the terms have been defined in either Chapter 3 or 4 except that $\mathbf{P}_{intra}$ here is defined by

$$\mathbf{P}_{intra} \equiv \mathbf{P}_{intra}^{ex} + \mathbf{P}_{intra}^{f}. \tag{5.2}$$

$\mathbf{E(t)}$ is the sum of exciting optical field and external terahertz field, i.e., $E(t)= \mathbf{E}_{op}(\mathbf{t}) + \mathbf{E}_{TH}^{ext.}(\mathbf{t})$. In the following sections, we will use the above Hamiltonian and the equations of motions defined in Chapters 3 and 4 to study the interaction of excitons and free electron-hole pairs in a photoexcited superlattice system.

Reproduced with permission of the copyright owner. Further reproduction prohibited without permission.

5.3 SCD Phenomena in the Coherent Regime

Although there is seldom such a case as a perfectly coherent system, much can be learned about the dynamics by studying this case. For example, solving the equations of motion for two-level system in the coherent limit can account for many aspects of the phenomena such as Rabi oscillation, photon echo, etc. Moreover, as can be seen in this section, the study of SCD phenomena in the coherent limit will help us to understand the basic principles underlying the SCD Bloch Oscillations that may be obscured when the dephasing is introduced.

5.3.1 Simplified Interpretation of SCD BO with a Semiclassical Model

Before we go into the details of the study of SCD BO with the quantum-mechanical model, we will first present a semiclassical model so as to have a simple but general understanding of the SCD BO. The basic tasks in the study of SCD BO are to explore such phenomena as energy exchange, driving mechanism etc. between different types of charge carriers. As mentioned in Chapter 1 (Page 10), although the validity of a semiclassical approach for derivations of the electronic motion is very limited for various reasons, it does provide an intuitive way of understanding the basic principles of BO and is useful in estimating the most important features of a system before complete analysis is followed.

We assume the polarization due to one type of charge carriers to be a classical dipole that is oscillating with time, and has some sort of natural frequency. Then, we take the THz field due to the other charge carriers to be an external field which drives this dipole. Consider now that the polarization is simply a sinusoidal function of time with frequency ω_B,

$$p = p_o \sin(\omega_B t), \tag{5.3}$$

and the THz field is also sinusoidal with the same frequency, and a relative phase shift, ϕ,

$$E(t) = E_o \sin(\omega_B t + \phi). \tag{5.4}$$

Reproduced with permission of the copyright owner. Further reproduction prohibited without permission.

In this case, the rate at which work is done by the field on the dipole is simply

$$\begin{aligned} \frac{dW}{dt} &= F\frac{dz}{dt} \\ &= -eE\frac{dz}{dt} \\ &= E\frac{dp}{dt}, \end{aligned} \tag{5.5}$$

where $F = -eE$ is the applied force, E is the associated electric field, and p is the dipole moment. Using the above expressions for the field and polarization, we obtain

$$\frac{dW}{dt} = E_o p_o \omega_B \cos(\omega_B t) \sin(\omega_B t + \phi). \tag{5.6}$$

Now, we take the time averaged power by averaging the above expression over one BO period:

$$\begin{aligned} \left\langle \frac{dW}{dt} \right\rangle &= E_o p_o \frac{(\omega_B)^2}{2\pi} \int_o^{2\pi/\omega_B} dt \cos(\omega_B t) \sin(\omega_B t + \phi) \\ &= \frac{E_o p_o \omega_B}{2} \sin(\phi). \end{aligned} \tag{5.7}$$

Thus, we see that as long as the phase difference between the polarization and the driving field is not zero or a multiple of π, then work will be done on the dipole. Depending on the value of ϕ, work may be done on the dipole or work may be done by the dipole on the field. However, from Eq. (5.7) we note that if there is no phase difference between the field and the oscillating dipole, then there will be no net energy exchanged between the two types of charge carriers. *As a result, the field due to the polarization of one type of charge carrier will do no net work on these carriers themselves since* $E(t) = -\frac{p}{\epsilon\epsilon_0}$. Work can only be done if ϵ is dispersive, in which case a phase shift is introduced between excitons and free electron-hole pairs. In Ref. [48], it was assumed that this shift can arise from the screening effect of the continuum carriers on the excitonic polarization. Here we take the effect of these carriers into account through their full dynamics.

The above simple semiclassical model of an oscillating dipole appears to be similar to a harmonic oscillator. However, there are a number of key differences. The most important one is that the effect of doing work on the BO carriers is not to increase the amplitude of the

Reproduced with permission of the copyright owner. Further reproduction prohibited without permission.

oscillations, but rather to change the average magnitude of the polarization. Thus, when work is done by the field, we may expect that the time-dependent function of either polarization or energy acquire an overall slope in its average value. The sign of this slope determines whether work is being done on the polarization by the field or on the field by the polarization.

5.4 Energy Conservation in SCD Bloch Oscillations

Checking energy conservation in some special cases is a good way to test the validity of both the theoretical models and the numerical methods being used. Moreover, this is also helpful in understanding the essence of the SCD effect. Energy conservation in the coherent limit will be studied in this section.

When there is no external terahertz field, the optical part in the full Hamiltonian in Eq. (5.1) depends explicitly on time. Therefore, the system is not conserved if this optical part is included. However, because the excited pulse is much shorter than the time span of interest, we may study the energy conservation after the optical pulse has passed. In this case and also in the coherent limit, the Hamiltonian in Eq. (5.1) is conservative. The total energy per unit volume of the SCD system then has the form,

$$\frac{E}{V} = \frac{1}{V}\sum_{\alpha}\left\langle B_{\alpha}^{\dagger}B_{\alpha}\right\rangle E_{\alpha} + \frac{\left\langle \mathbf{P}_{intra}^{2}\right\rangle}{2\epsilon_{0}\epsilon}, \tag{5.8}$$

where α refers to excitons and free electron-hole pairs. $\langle \mathbf{P}_{intra}\rangle$ is total polarization due to excitons and free electron-hole pairs. The specific forms of the first term in Eq. (5.8) for excitons and free pairs in the coherent limit are respectively,

$$\begin{aligned}\frac{E_{ex}}{V} &= \sum_{\mu}\hbar\omega_{\mu}\left\langle B_{\mu}^{\dagger}\right\rangle\langle B_{\mu}\rangle \\ &= \frac{e^{2}}{|\mathbf{M}_{o}|^{2}d}\sum_{\mu}\hbar\omega_{\mu}|K_{\mu}|^{2},\end{aligned} \tag{5.9}$$

Reproduced with permission of the copyright owner. Further reproduction prohibited without permission.

F_0(kV/cm)	$d(10^{-10}\text{m})$	ε_c(meV)	E_{op}(GV/m)	T_{2inter}	T_{2intra}	T_1	T^f_{2inter}	T^f_{2inter}
15	84	0	1×10^{-3}	∞	∞	∞	∞	∞

Table 5.1: Parameters for Calculations in the Coherent Case

$$\begin{aligned}\frac{E_f}{V} &= \sum_{n,\mathbf{k}} \hbar\omega_{n,\mathbf{k}} \left\langle B^\dagger_{n,\mathbf{k}} B_{n,\mathbf{k}} \right\rangle \\ &= \frac{1}{V}\sum_{n,\mathbf{k}} (n\hbar\omega_B + \frac{\hbar^2k^2}{2m_\parallel}) \left\langle B^\dagger_{n,\mathbf{k}} \right\rangle \langle B_{n,\mathbf{k}} \rangle \\ &= \frac{m_\parallel \omega_B^2 e^2 d}{|\mathbf{M}_o|^2 (2\pi)^3} \sum_n \left\{ \int_0^\infty n\,|K_n(x)|^2\,dx + \int_0^\infty x\,|K_n(x)|^2\,dx \right\}, \end{aligned} \tag{5.10}$$

where relations (3.22), (4.22), (4.27) and (4.30) have been used.

Considering a GaAs/GaAlAs superlattice and using the parameters as in Table, 5.1, we get the numerical results for energy conservation shown in Fig. 5-1. Here, T_{2inter} and T_{2intra} are respectively the interband and intraband dephasing constants for excitons. Other parameters are the same as described in Section 4.4.2. Parameters in Table 5.1 will be used for all the calculations in the coherent limit in Section 5.3, except that ε_c may change in some calculations.

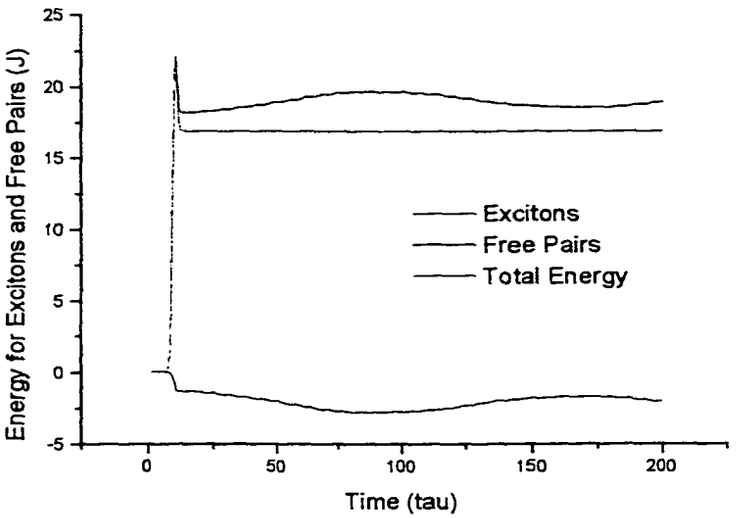

Figure 5-1: Energy conservation of self-driving system

Reproduced with permission of the copyright owner. Further reproduction prohibited without permission.

As can be seen from Fig. 5-1, the two sets of carriers drive each other and therefore their energies vary with time. We will turn to this point shortly. However, the total energy of the system is conserved after the optical pulse has passed at time point 10. This is expected when $\mathbf{E}_{opt}(t) = 0$ and the Hamiltonian is conserved.

5.4.1 Bloch Oscillations Driven by Fields due to Different Types of Charge Carriers

To examine the physical mechanism of SCD Bloch oscillation, three driving sources will be studied separately in detail in the following three subsections: the excitonic polarization, the polarization due to free electron-hole pairs, and the total polarization. The most important conclusion arrived is: in Bloch oscillations, the energy of a certain kind of charge carriers can not be driven up or down by the field induced by themselves, i.e., the energy is a constant. However, the different kinds of charge carriers can drive one another up or down in energy.

Driving by Polarization of Excitons only

When both excitons and free electron-hole pairs are driven by the field induced by excitons only, we obtain following results. The energy of excitons is constant after the optical pulse is gone, with or without the driving force, as shown in Fig. 5-2. Note the two curves are overlapped exactly to within the plot resolution.

The energy of free electron-hole pairs behaves differently as compared to excitons when the external driving force is only from excitonic polarization. The excitonic polarization field, $\langle E^{ex}_{intra} \rangle$, causes the free pair energy to oscillate as shown in Fig. 5-3. The crucial point here is that there is a phase shift between the oscillating free electron-hole pairs and the field from excitons. It is this phase shift that causes the energy change of free electron-hole pairs, as we discussed in the semiclassical model in Section 5.3.1. Moreover, this phase shift also varies with time in the driving process because the oscillating frequencies for the two sets of charge carriers are not equal. Thus excitons and free electron-hole pairs exchange energy time-dependently as shown in Fig. 5-3. The polarization due to excitons with or without driving by $\langle E^{ex}_{intra} \rangle$ are shown in Fig. 5-4. From Fig. 5-4, it can be seen that the polarization of excitons, unlike energy, is affected by SCD field. Also we note that the driven polarization does not maintain

Reproduced with permission of the copyright owner. Further reproduction prohibited without permission.

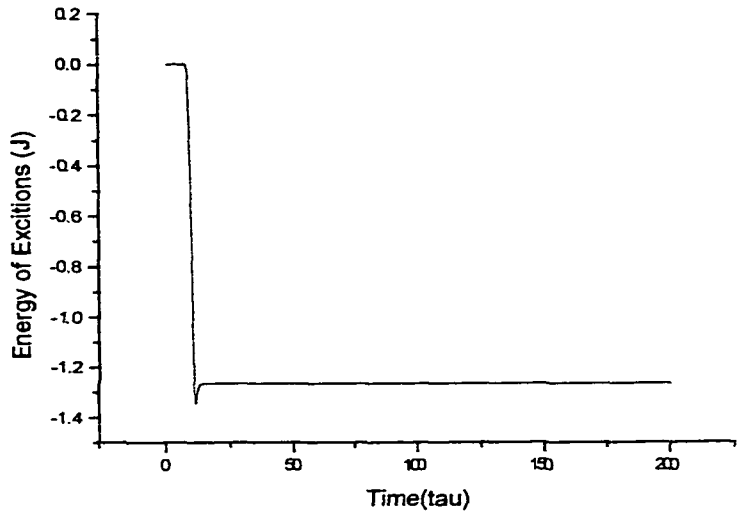

Figure 5-2: Excitons energy with or without self-driving from excitons

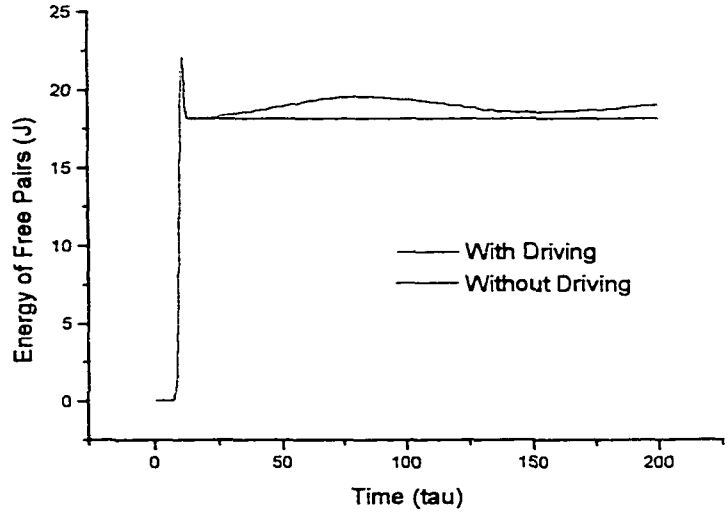

Figure 5-3: Energy of free pairs with or without driving from excitons

Reproduced with permission of the copyright owner. Further reproduction prohibited without permission.

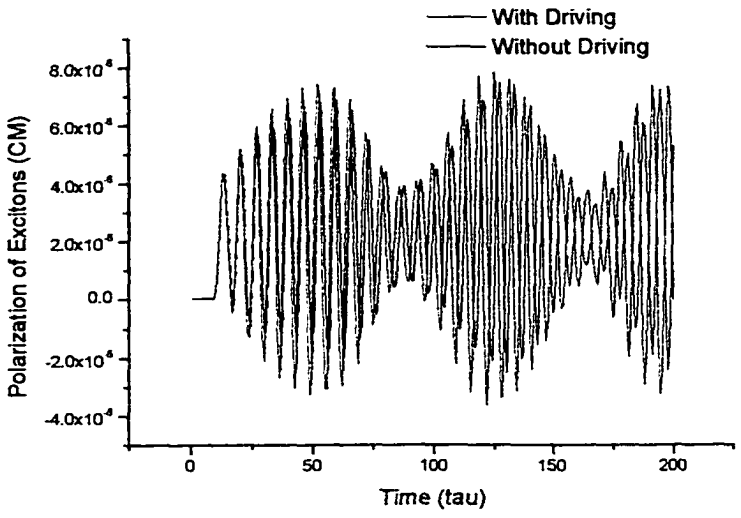

Figure 5-4: Polarization of excitons with or without driving from excitons

a slope relative to the non-driven polarization within the beating period. However, this is not the case for free electron pairs when they are driven by excitons, as in Fig. 5-5. That is, the driven polarization of free electron pairs keeps a big slope relative to the non-driven one when they are driven by excitons, rather than themselves. Thus, we arrive at the following general conclusions: in Bloch oscillations, the energy of a given type of charge carrier remains constant if the driving field is only due to their own polarization. The energy only changes when the charge carriers are driven by the other group of charge carriers. The polarization, however, changes even with the driving field due to themselves, although the driving effect is not as appreciable as when driven by other types of charge carriers. These general conclusions will be further verified in the next subsections.

Driving by Polarization of Free Electron-hole Pairs only

When both excitons and free electron-hole pairs are driven by the field induced by free electron-hole pairs only, $\left\langle E^{f}_{intra} \right\rangle$, the energy of excitons is no longer a constant after the optical pulse is gone but oscillates as in Fig. 5-6. Unlike the case when driven by the field due to excitons themselves (Fig. 5-2), the energy of excitons now changes due to the driving from the field due

Reproduced with permission of the copyright owner. Further reproduction prohibited without permission.

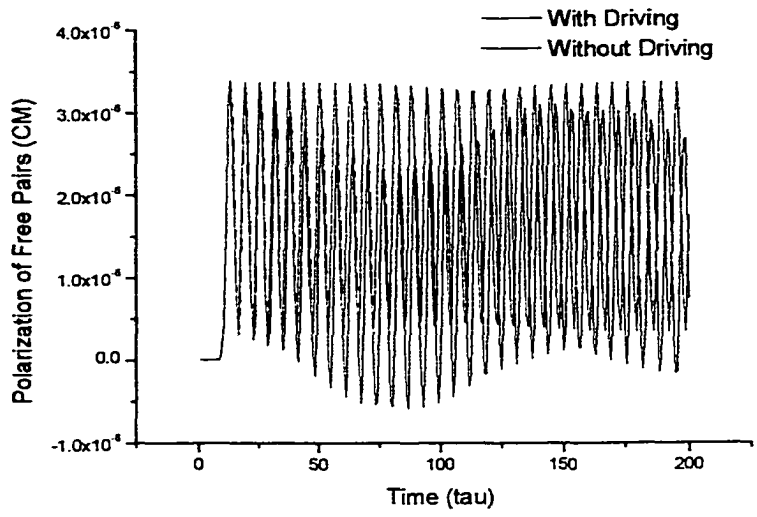

Figure 5-5: Polarization of free pairs with or without driving from excitons

to the free electron-hole pairs. Again the reason for such a change is that there is an phase shift between the oscillating excitons and the field from free electron-hole pairs, as we discussed in Section 5.3.1 and Section 5.4.1. This time-dependent phase shift (due to the different frequencies of the two sets of carriers) causes the energy of excitons to oscillate as shown in Fig. 5-6. The energy of free electron-hole pairs, however, remains as a constant when driven by $\left\langle \mathbf{E}^{f}_{intra} \right\rangle$, as shown in Fig. 5-7. Also note that the two curves for driven and non-driven cases overlap exactly to within the plot resolution. As for polarization, unlike the results in Section 5.4.1, the polarization due to excitons with or without driving behaves much differently because it is driven now by polarization due to the other type of charge carriers rather than due to themselves, as in Fig. 5-8. As predicted, the polarization due to free electron-hole pairs with SCD field does not change much as shown in Fig. 5-9. Now we are further convinced of the conclusion we arrived at in the last subsection. The energy or polarization of a given type of charge carrier can not be modified significantly by the field induced by themselves. This is simply a consequence of the fact that the uncoupled Hamiltonians for an exciton and a free electron-hole pair are both conservative. Any appreciable changes in energy or in the shape of the intraband polarization will be due to the fields from other types of charge carriers, rather

Reproduced with permission of the copyright owner. Further reproduction prohibited without permission.

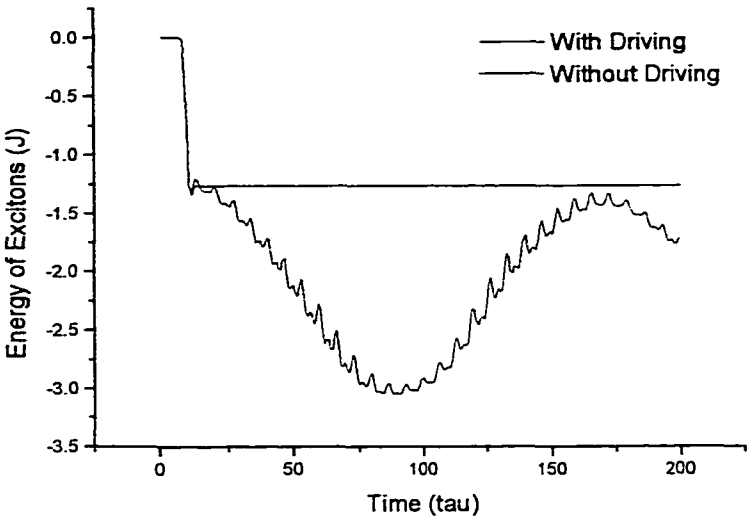

Figure 5-6: Energy of excitons with or without driving from free pairs

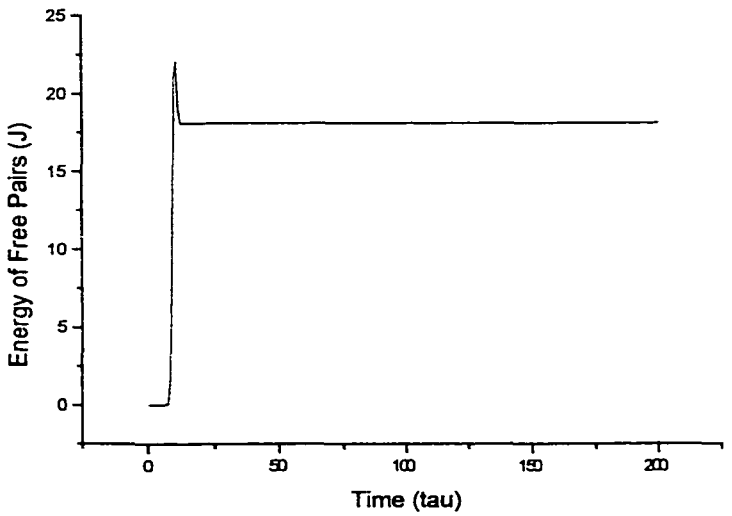

Figure 5-7: Energy of free pairs with and without driving from free pairs

Reproduced with permission of the copyright owner. Further reproduction prohibited without permission.

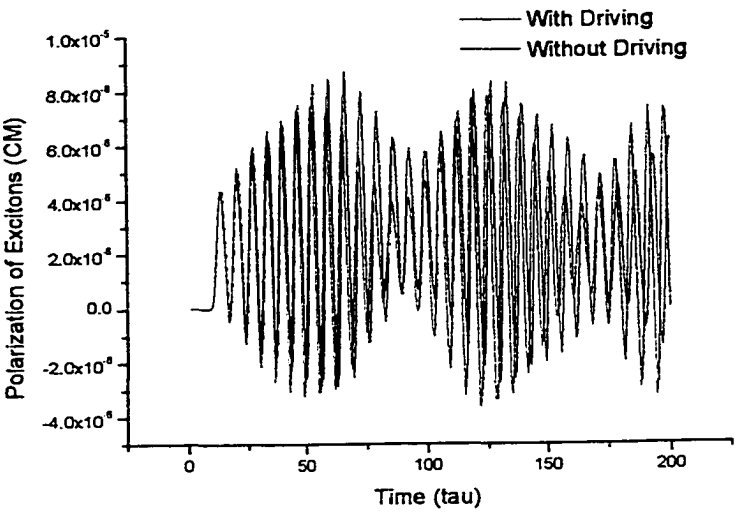

Figure 5-8: Polarization of excitons with and without driving from free pairs

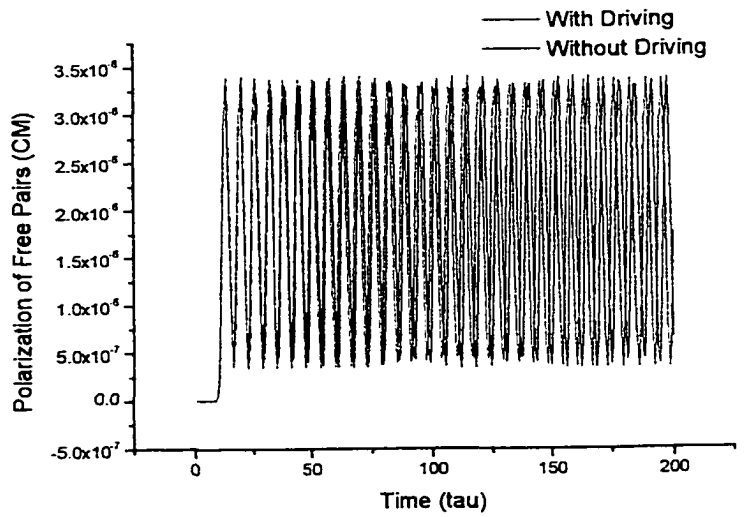

Figure 5-9: Polarization of free pairs with and without driving from free pairs

Reproduced with permission of the copyright owner. Further reproduction prohibited without permission.

than themselves.

Driving by Polarization due to Both Excitons and Free Electron-hole Pairs

Finally, we turn to the case in which charge carriers are driven by the total fields induced by both excitons and free electron-hole pairs. Because the field due to one type of carriers does not affect these carriers too much as compared to the field due to other types of carriers, the total polarization when driven by fields induced by both excitons and free pairs is similar to the combination of the results of the last two subsections. For instance, the polarization of free electron pairs with the driving of fields from both excitons and free pairs is much similar to that driven by the field from excitons only. Similar results can also be obtained for the polarization of excitons. We have shown all these are true by numerical calculations. The following figures include the effects of the total polarization due to both excitons and free electron-hole pairs. The polarization of excitons, free electron-hole pairs and their combination are shown in Fig. 5-10, all with driving fields due to both types of charge carriers. The total polarization with and without driving fields is shown in Fig. 5-11. As can be seen from Fig. 5-11, the total polarization with self-induced driving field does not maintain an appreciable slope as compared to the total polarization without self-induced driving field. This is different from the case where the polarization of either free electron-hole pairs or excitons is considered individually. In the later case, the polarization of either excitons or free electron-hole pairs with driving has a slope as compared to the polarization without driving, as shown in Figs. 5-5 and 5-8. This can be understood by the energy conservation relation shown in Fig. 5-1. Although the energy of either excitons or free electron-hole pairs is not conserved due to the driving force from other types of charge carriers, the total energy of excitons and free electron-hole pairs after the optical pulse is gone maintains a constant. Therefore the total polarization with driving does not have a slope in comparison with the total polarization without driving.

Of central importance here is the fact that the average dipole of each of the two sets of carriers and energy are changing in time as seen in Figs. 5-1 and 5-10. Thus there is a quasi-DC current due to the excitons which is opposed by a similar current due to the free electron-hole pairs. Recall that in the experiments by *F. Löser et al* [48], the average intraband polarization appears to change quasi-linearly in time. One hypothesis for this experimental result is that,

Reproduced with permission of the copyright owner. Further reproduction prohibited without permission.

because the continuum carriers are in "contact" with the doped reservoirs at the superlattice ends, no quasi-linear polarization develops due to these carriers. Thus one only observes the polarization due to excitons, which does have a quasi-linear component. This explanation has to be investigated via future experiments.

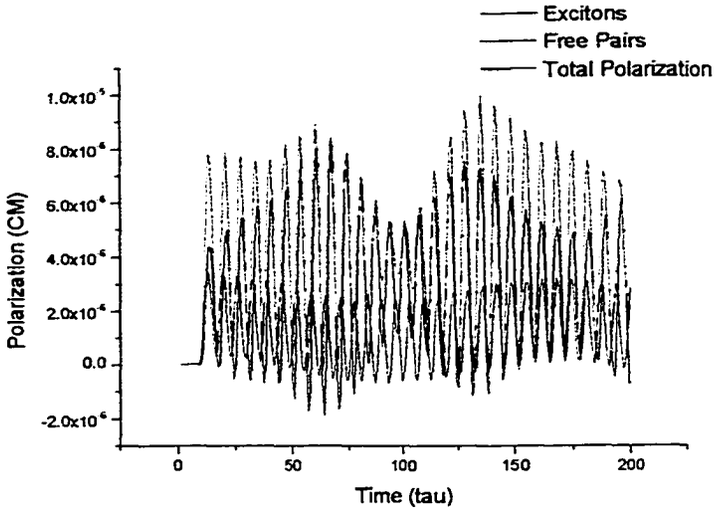

Figure 5-10: Polarizations of excitons, free pairs and their combination

5.4.2 Influence of the Different Positions of Central Frequency of the Laser

Because the population of charge carriers in the system of interest strongly depends on the exciting center laser frequency E_c and the E_c-dependences for excitons and free pairs are different (as shown in Fig. 5-12), different E_c must have an important influence on the interaction of the two sets of charge carriers. Moreover, different E_c will also strongly influence the average amplitude of BO as studied by *Dignam*, *Sipe* and *Shah* in 1994 [6]. They found that when neglecting the Coulomb interaction between electron-hole pairs, a different value of E_c may cause the amplitude of BO to vary between zero (breathing mode) and the value predicted by a semiclassical model. When the Coulomb interaction is included, the results are still valid except that there exists no such "breathing mode". Combining the above influences of different E_c on both population and BO amplitude of charge carriers, we know that E_c must have a strong

Reproduced with permission of the copyright owner. Further reproduction prohibited without permission.

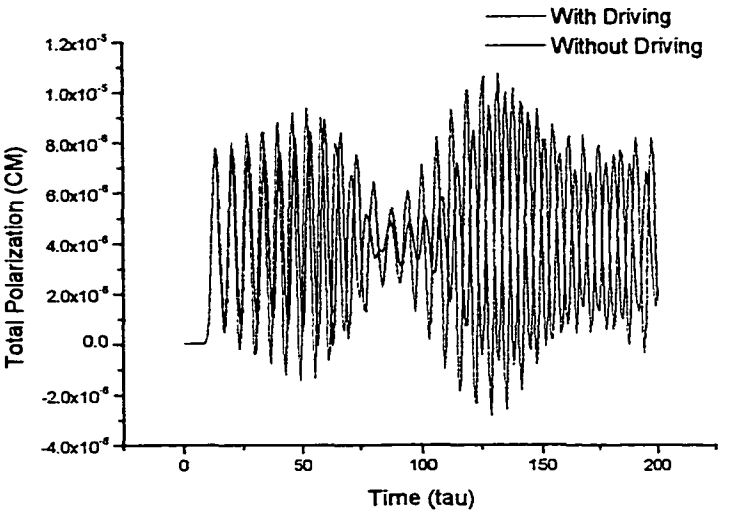

Figure 5-11: Total polarization with or without driving from excitons and free pairs

influence on the interaction between the two sets of charge carriers. As can be seen in Fig. 5-13, for the system parameters as described in Table 5.1, the exciton energy is driven appreciably only when the center laser frequency is near the $n = 0$ Stark-ladder state. When the laser frequency goes to the higher end of the excitonic states, the polarization due to free pairs does not drive the excitons so much although the free pairs gain appreciably in population. This is due to the fact that the total dipole amplitude created by free pairs is also a strong function of E_c, as is true for excitons discussed earlier. In the following sections, we will focus on the cases in which E_c is near zero WSL state, since we are interested in large interactions.

One important point that should be noticed is that in Fig. 5-13, the slope (if there is one) of the time-dependent energy curve takes only negative values regardless of the E_c value. Thus, the corresponding slope of the time-dependent polarization curve takes only positive values for different E_c. This is not in agreement with the experimental results as described in Ref. [48], where a change of slope sign was observed. This lack of sign change is due to two cancelling factors for the system studied. First the sign of $\omega_B - \tilde{\omega}^{ex}$ changes as E_c changes sign, where $\tilde{\omega}^{ex}$ is the average excitonic BO frequency. This would be expected to change the sign of the average phase shift in $\phi(t)$ in excitonic BO. However, $\langle \mathbf{P}^{ex}_{intra} \rangle$ also undergoes a π phase shift

Reproduced with permission of the copyright owner. Further reproduction prohibited without permission.

when E_c changes sign [34]. These two effects cancel each other to give no change in sign. We note that the coincidence of these two effects may not occur in all systems. This may be a partial explanation of the experiments reported in Ref. [48].

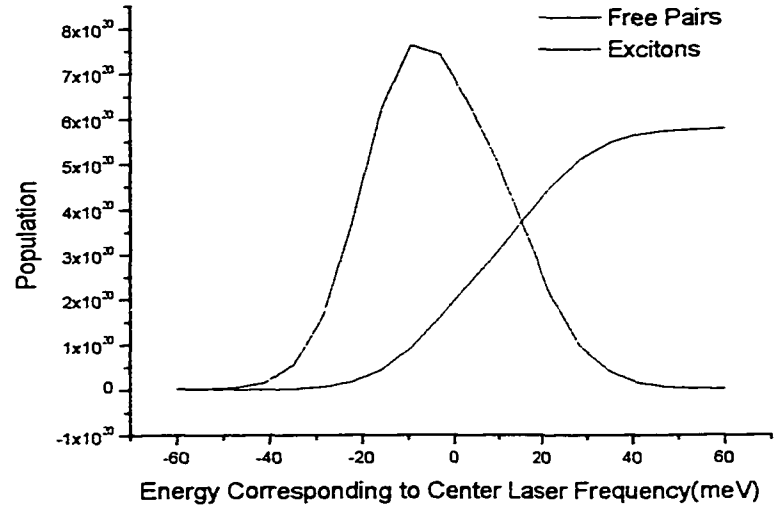

Figure 5-12: Population for excitons and free pairs vs laser central frequency

5.4.3 Influence of the Relative Phase Shift between Excitons and Free Pairs

We now turn to an interesting SCD phenomenon in which the self-induced driving field due to free electron-hole pairs can drive the time-dependent energy or polarization of excitons in different directions. This phenomenon is related to such experiments as the Shapiro effect etc, as we already discussed in Chapter 1 [48]. This can be realized by introducing different phase shifts between the polarizations of excitons and free electron-hole pairs. In the time domain, this is equivalent to introducing different time delays respectively in the optical fields exciting the excitons and free electron-hole pairs. These optical fields that can excite charge carriers dominated by either 1s excitons or free electron-hole pairs can be achieved by using pulse-shaping technique. For example, we may introduce a time delay T_s in the optical field exciting free electron-hole pairs: $\mathbf{E}^f_{opt}(t) = \mathcal{E}^f(t-T_s)e^{-i\omega_c t} + c.c$, where $\mathcal{E}^f(t-T_s)$ is usually a Gaussian form as in Eq. (4.47). In the coherent limit, we simulate this situation by using the same system

Reproduced with permission of the copyright owner. Further reproduction prohibited without permission.

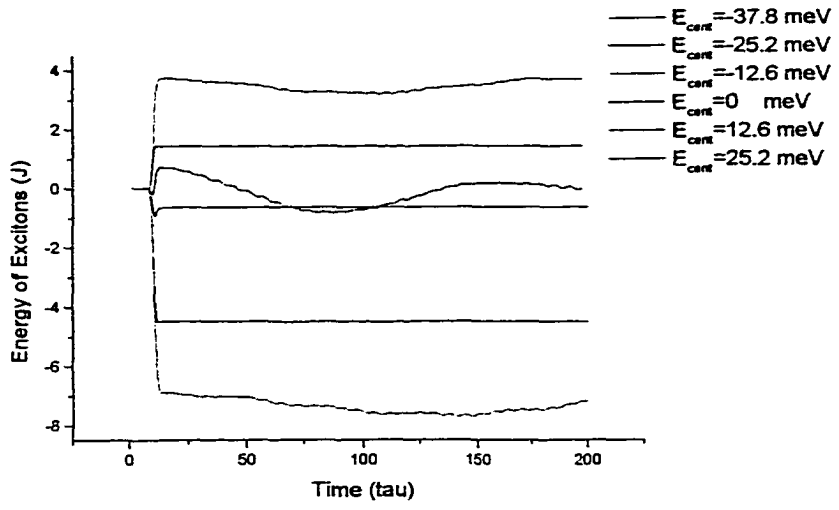

Figure 5-13: Energy of excitons excited by different laser frequency

F_0(kV/cm)	$d(10^{-10}\text{m})$	ε_c(meV)	E_{op}(GV/m)	T_{2inter}	T_{2intra}	T_1	T^f_{2inter}	T^f_{2inter}
15	84	0	1×10^{-3}	20	10	∞	20	10

Table 5.2: Parameters for Calculations in Non-coherent Case

parameters as in Table 5.1. For different time delay $T_s = -3, -2, -1, 0$, we get the energies of excitons as functions of time as shown in Fig. 5-14. Obviously, the time-dependent energies of excitons are driven by free electron-hole pairs in different directions (with different slopes). The slopes of time-dependent energy curves for $T_s = -3$ and $T_s = 0$ cases are even opposite in sign. Their corresponding polarizations are also driven in different directions as shown in Fig. 5-15.

5.5 SCD Phenomena in Systems with Dephasing Mechanism

In this section, we turn to the more realistic cases of SCD Bloch Oscillations in the systems with dephasing. We will use the parameters as in Table 5.2 for our numerical calculations. As can be seen, the dephasing time constants for both excitons and free pairs are introduced.

Reproduced with permission of the copyright owner. Further reproduction prohibited without permission.

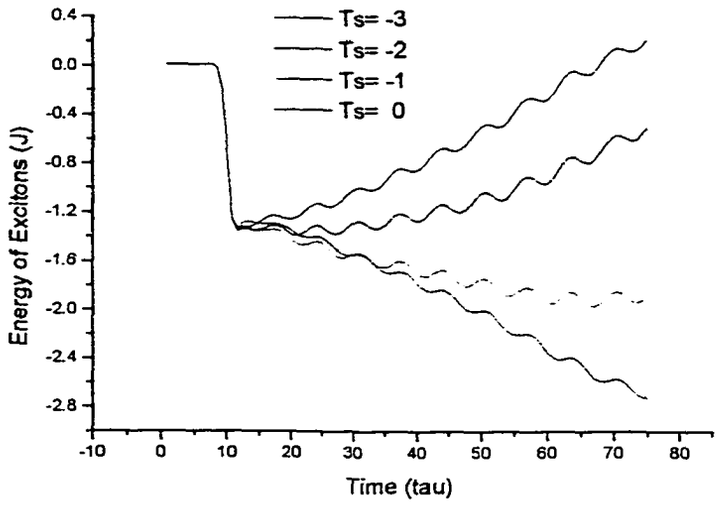

Figure 5-14: Energy of excitons driven by polarization of free pairs with different Ts

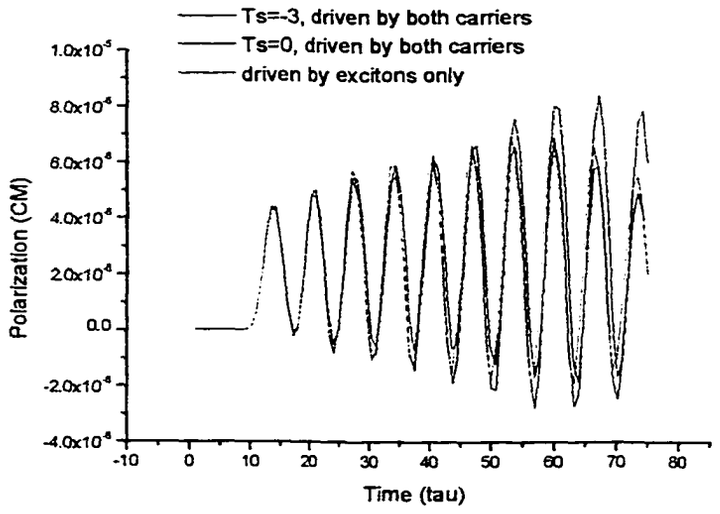

Figure 5-15: Polarization of excitons driven by free pairs with different Ts

Reproduced with permission of the copyright owner. Further reproduction prohibited without permission.

5.5.1 Choosing the Best Basis States to Solve the Equations of Motion when There Is Dephasing

In order to solve Eqs. (3.23) and (3.24) for excitons, Eqs. (4.32) and (4.33) for free electron-hole pairs, we need to choose an appropriate set of basis states. As discussed in Chapters 3 and 4, we choose the basis states to be the exciton or free electron-hole pair eigenstates in a superlattice potential with an applied DC field F_0. Consider the case in which the applied DC field is F_{app} and the SCD field is

$$\langle \mathbf{E}_{intra} \rangle (t) = -\frac{\langle \mathbf{P}_{intra} \rangle}{\epsilon_0 \epsilon}.$$

Under many conditions, when the optical field is strong, there will be an induced DC field arising from the excitonic intraband polarization. In this case, $\langle \mathbf{E}_{intra} \rangle (t)$ can be written as

$$\langle \mathbf{E}_{intra} \rangle (t) = \mathbf{E}_{DC} + \mathbf{E}_{AC}(t).$$

In the absence of dephasing, we could choose

$$F_0 = F_{app} \quad \text{and } E_{coup}(t) \equiv \langle E_{intra} \rangle (t) = E_{DC} + E_{AC}(t)$$

as we did in the previous sections. Alternatively, we could choose

$$F_0 = F_{app} + E_{DC} \text{ and } \mathbf{E}_{coup}(t) = \mathbf{E}_{AC}(t)$$

and the results would be the same when there is no dephasing since the same fundamental basis of two-well exciton states would be used in both cases. However, this freedom concerning the choice of basis states has to be restricted when dephasing is introduced.

If we have the full Hamiltonian then the basis does not matter as long as it is complete, even if dephasing is introduced. However, given that we will never know the full Hamiltonian and will likely have to introduce some phenomenological dephasing and decay constants, it is important that we choose a basis which best approximates the eigenstates of the excited system. This way, it is reasonable to assume that the populations will relax to some sort of quasi-equilibrium distribution on a time scale of T_1 and that the coherences between the eigenstates will decay

Reproduced with permission of the copyright owner. Further reproduction prohibited without permission.

on some other (faster) time scale. It is clear that the eigenstates of the SL in the applied field are not good approximations to the system if the induced DC field is large. In such a case, it seems that it would be preferable to choose the basis states to be the eigenstates of the total DC field.

The first thing we need to do is to arrive at a definition of the total DC field that we wish to use. We will try to determine the DC field at the time just after the optical pulse has passed. This is non-trivial as there is a THz portion in addition to the DC portion of the induced field. Let τ_i $(i = 1, 2, 3, ...)$ be the times at which $\langle \mathbf{P}_{intra} \rangle (t)$ achieves its various extrema, where $\tau_{i+1} > \tau_i$. We shall take the DC portion of the induced field to be the average of the field between the times τ_2 and τ_3. This ensures that the average is being taken over one oscillation after the optical pulse has passed. Let us call this calculated field $\mathbf{E}_{DC}$:

$$\mathbf{E}_{DC} \equiv \frac{-1}{\epsilon\epsilon_o} \int_{\tau_2}^{\tau_3} \frac{\langle \mathbf{P}_{intra} \rangle (\tau)}{\tau_3 - \tau_2} d\tau.$$

Now, we calculate a new set of excitonic basis states, which are the eigenstates of the SL in the total DC field:

$$F_0 = F_{app} + \mathbf{E}_{DC}. \tag{5.11}$$

We use this basis, with the newly calculated energies, $\hbar\omega_\mu$, and matrix elements, $G_{\mu\nu}$ and S_μ to calculate the full evolution. In doing so we must also modify the equations of motion so that the SCD field becomes:

$$\langle \mathbf{E}_{intra} \rangle (t) = -\frac{\langle \mathbf{P}_{intra} \rangle}{\epsilon\epsilon_o} - \mathbf{E}_{DC}. \tag{5.12}$$

This solution is not perfect in that we are not sure that we have the correct DC field, and we are not treating the effects of the AC field on the phenomenological decay. However, we find that in practice it works well over a range of $\mathbf{E}_{DC}$ values.

Now we consider a specific example to show the importance of basis choice. We use the same parameters as in Table 5.2 except that here we assume a big optical field strength $E_{op} = 3 \times 10^{-3}$(GV/m). As can be shown by the numerical calculation, the total induced DC electric field is around -4.07(GV/m). This induced DC electric field can appreciably modify the eigenstates

Reproduced with permission of the copyright owner. Further reproduction prohibited without permission.

of the superlattice system and thus cause the problem we described above. As shown in Figs. 5-16 and 5-17, the time-dependent polarization and energy of excitons are both continuously driven by the free electron-hole pairs even long after the typical dephasing time. While the coherences should die out due to dephasing, they do not because of the wrong basis we are using. In this basis, the population (which does not decay since $T_1 = \infty$) can be transformed into coherences and therefore we get the permanent driving situation that is obviously a non-physical phenomenon. However, if we modify the basis by considering the induced static electric field and modify F_0 and $\langle \mathbf{E}_{intra} \rangle (t)$ according to Eqs. (5.11) and (5.12) respectively, we may get the time-dependent energy and polarization of excitons as shown in Figs. 5-18 and 5-19. As already mentioned, the solutions in the modified basis are not the exact solutions because we are not sure that we have the correct DC field, and we are not treating the effects of the AC field on the phenomenological decay. However, to do so probably requires a full treatment of the dephasing/decay mechanisms. Note that E_{op} is very large here. The problem is not so obvious for lower optical field strength.

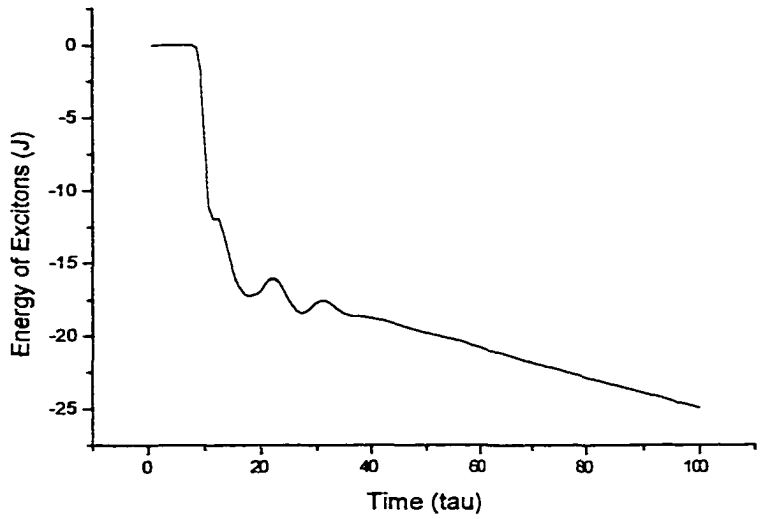

Figure 5-16: Energy of excitons in the wrong basis

Reproduced with permission of the copyright owner. Further reproduction prohibited without permission.

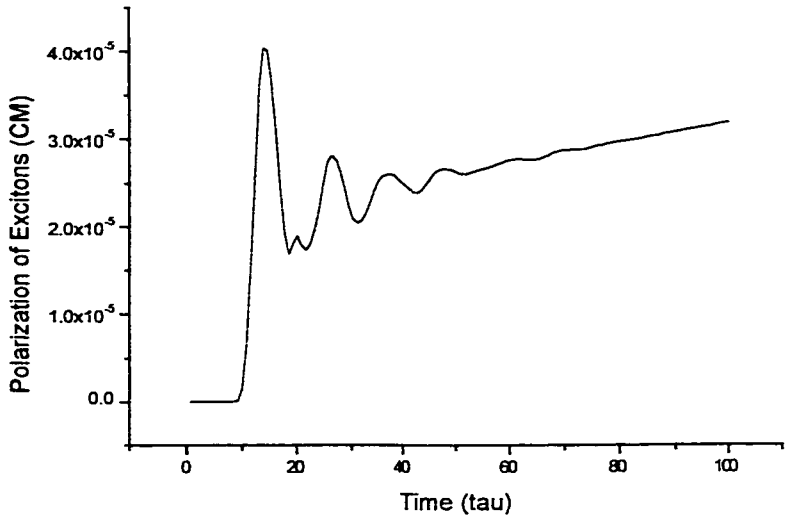

Figure 5-17: Polarization of excitons in the wrong basis

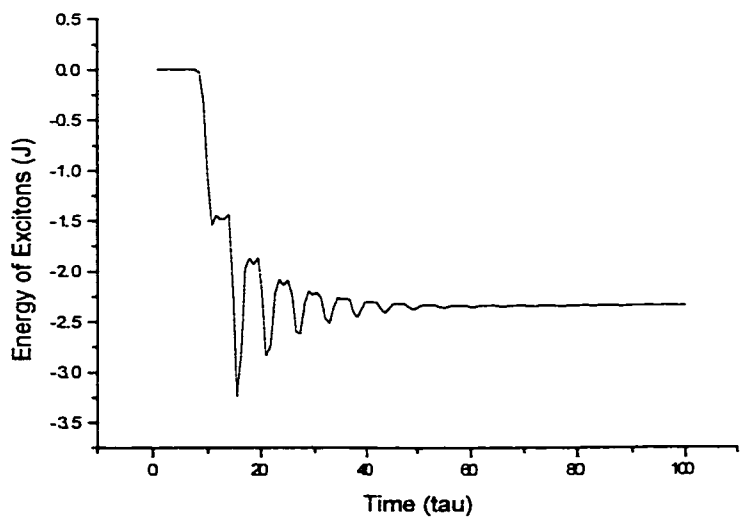

Figure 5-18: Energy of excitons in the modified basis

Reproduced with permission of the copyright owner. Further reproduction prohibited without permission.

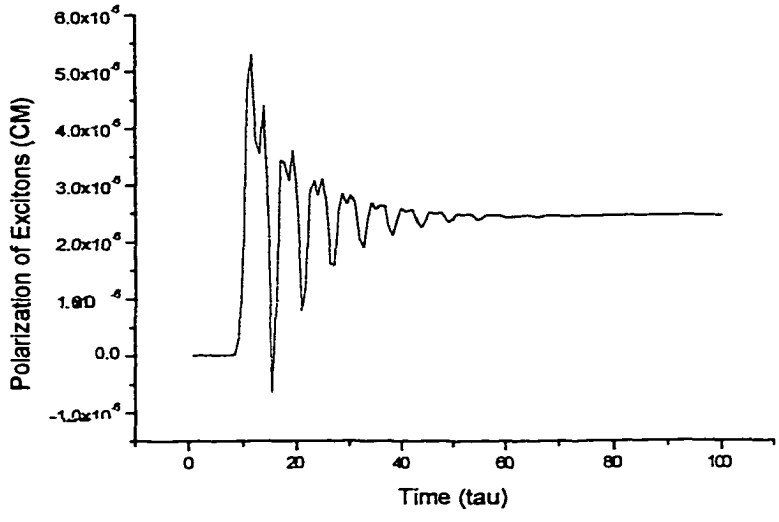

Figure 5-19: Polarization of excitons in the modified basis

5.5.2 Energy Evolution in Non-Coherent Case

When the dephasing factor is introduced, it is obvious from the Heisenberg equation that the total energy is not conserved. However, we may study the evolution of energy to verify the validity of our equations. In the coherent limit, what we have done about energy conservation can be used to verify the validity of the first-order equations. This is because only first-order equations are involved when calculating energy in the coherent limit. Next, energy evolution in the non-coherent case will be studied *to verify the second-order equations*. For simplicity, only the energy evolution for excitons will be studied in detail. The study of energy evolution for free electron-hole pairs is very similar to the excitonic case if some new definitions are made.

Consider the energy term of excitons:

$$E_o = \frac{e^2}{|\mathbf{M}_o|^2 d} \sum_{\mu} \tilde{\omega}_{\mu}^0 \left\langle K_{\mu}^{\dagger} K_{\mu} \right\rangle \hbar \omega_B. \tag{5.13}$$

Note that E_o is not the total energy of excitons; the missing interacting energy between excitons and self-induced field will be included later. Also, when there is dephasing, $\left\langle K_{\mu}^{\dagger} K_{\mu} \right\rangle$ can no

Reproduced with permission of the copyright owner. Further reproduction prohibited without permission.

longer be written as $\left\langle K_\mu^\dagger \right\rangle \langle K_\mu \rangle$, as in the coherent limit. Let us look at the time derivative of this term once the optical pulse is gone but with population decay. Using Eq. (3.24), we get,

$$\begin{aligned}
\frac{dE_o}{d\tau} &= -\frac{ie^2 \langle \mathbf{E}_{intra} \rangle}{|\mathbf{M}_o|^2 d} \cdot \sum_{\mu\mu'} \tilde{\omega}_\mu^0 \left(\mathbf{G}_{\mu',\mu} \left\langle K_{\mu'}^\dagger K_\mu \right\rangle e^{i\left(\omega_{\mu'}^0 - \omega_\mu^0\right)t} \right. \\
&\quad \left. -\mathbf{G}_{\mu',\mu}^* \left\langle K_\mu^\dagger K_{\mu'} \right\rangle e^{-i\left(\omega_{\mu'}^0 - \omega_\mu^0\right)t} \right) - \frac{E_o}{T_1} \\
&= \frac{2e^2 \langle \mathbf{E}_{intra} \rangle}{|\mathbf{M}_o|^2 d} \cdot \mathrm{Im} \left\{ \sum_{\mu\mu'} \tilde{\omega}_\mu^0 \mathbf{G}_{\mu',\mu} \left\langle K_{\mu'}^\dagger K_\mu \right\rangle e^{i\left(\omega_{\mu'}^0 - \omega_\mu^0\right)t} \right\} - \frac{E_o}{T_1},
\end{aligned}$$

where we assume that population decay constants for different excitonic states are the same, i.e., T_1. Now consider the time derivative of the intraband polarization for excitons in Eq.(3.25):

$$\begin{aligned}
\frac{d\langle \mathbf{P}_{intra} \rangle}{d\tau} &= \frac{e^2}{|\mathbf{M}_o|^2 d} \sum_{\nu\mu} \left\{ G_{\mu\nu} \frac{d\left\langle K_\mu^\dagger K_\nu \right\rangle}{d\tau} e^{i(\tilde{\omega}_\mu^0 - \tilde{\omega}_\nu^0)\tau} + i\left(\tilde{\omega}_\mu^0 - \tilde{\omega}_\nu^0\right) G_{\mu\nu} \left\langle K_\mu^\dagger K_\nu \right\rangle e^{i(\tilde{\omega}_\mu^0 - \tilde{\omega}_\nu^0)\tau} \right\} \\
&= \frac{e^2}{|\mathbf{M}_o|^2 d} \sum_{\nu\mu} \left\{ G_{\mu\nu} \frac{d\left\langle K_\mu^\dagger K_\nu \right\rangle}{d\tau} e^{i(\tilde{\omega}_\mu^0 - \tilde{\omega}_\nu^0)\tau} + 2\,\mathrm{Im}\left\{ \tilde{\omega}_\nu^0 G_{\mu\nu} \left\langle K_\mu^\dagger K_\nu \right\rangle e^{i(\tilde{\omega}_\mu^0 - \tilde{\omega}_\nu^0)\tau} \right\} \right\} \\
&= \frac{e^2}{|\mathbf{M}_o|^2 d} \sum_{\nu\mu} \left\{ G_{\mu\nu} \frac{d\left\langle K_\mu^\dagger K_\nu \right\rangle}{d\tau} e^{i(\tilde{\omega}_\mu^0 - \tilde{\omega}_\nu^0)\tau} \right\} + \frac{1}{\mathbf{E}_{THz}} \frac{dE_o}{d\tau} + \frac{1}{\mathbf{E}_{THz}} \frac{E_o}{T_1} \\
&= \frac{1}{\mathbf{E}_{THz}} \frac{dE_o}{d\tau} + \frac{e^2}{|\mathbf{M}_o|^2 d} \sum_{\nu\mu} G_{\mu\nu} e^{i(\tilde{\omega}_\mu^0 - \tilde{\omega}_\nu^0)\tau} \left\{ -\frac{1}{\Gamma_{\mu\nu}} \left\langle K_\mu^\dagger K_\nu \right\rangle i \frac{\langle \mathbf{E}_{intra} \rangle}{\hbar\omega_B} - i \frac{\langle \mathbf{E}_{intra} \rangle}{\hbar\omega_B} \cdot \right. \\
&\quad \left. \sum_{\mu'} \left(\mathbf{G}_{\mu',\mu} \left\langle K_{\mu'}^\dagger K_\nu \right\rangle e^{i\left(\omega_{\mu'}^0 - \omega_\mu^0\right)t} - \mathbf{G}_{\mu',\nu}^* \left\langle K_\mu^\dagger K_{\mu'} \right\rangle e^{-i\left(\omega_{\mu'}^0 - \omega_\nu^0\right)t} \right) \right\} + \frac{1}{\mathbf{E}_{THz}} \frac{E_o}{T_1} \\
&= \frac{1}{\mathbf{E}_{THz}} \frac{dE_o}{d\tau} + + \frac{1}{\mathbf{E}_{THz}} \frac{E_o}{T_1} \\
&\quad + \frac{e^2}{|\mathbf{M}_o|^2 d} \sum_{\nu\mu} G_{\mu\nu} \left\{ -\frac{1}{\Gamma_{\mu\nu}} \left\langle K_\mu^\dagger K_\nu \right\rangle e^{i(\tilde{\omega}_\mu^0 - \tilde{\omega}_\nu^0)\tau} \right. \\
&\quad \left. - i \frac{\langle \mathbf{E}_{intra} \rangle}{\hbar\omega_B} \cdot \sum_{\mu'} \left(\mathbf{G}_{\mu',\mu} \left\langle K_{\mu'}^\dagger K_\nu \right\rangle e^{i\left(\omega_{\mu'}^0 - \omega_\nu^0\right)t} - \mathbf{G}_{\mu',\nu}^* \left\langle K_\mu^\dagger K_{\mu'} \right\rangle e^{-i\left(\omega_{\mu'}^0 - \omega_\mu^0\right)t} \right) \right\}
\end{aligned}$$

Thus using the factorization $\left\langle \mathbf{P}_{intra}^2 \right\rangle = \langle \mathbf{P}_{intra} \rangle \langle \mathbf{P}_{intra} \rangle$, which is consistent with our fac-

Reproduced with permission of the copyright owner. Further reproduction prohibited without permission.

torized equations of motion, we have:

$$\begin{aligned}
\frac{d}{d\tau}\left[E_o+\frac{\langle \mathbf{P}_{intra}^2\rangle}{2\epsilon_0\epsilon}\right] &= \frac{dE_o}{d\tau}-\mathbf{E}_{THz}\frac{d\langle \mathbf{P}_{intra}\rangle}{d\tau} \\
&= \frac{e^2\langle \mathbf{E}_{intra}\rangle}{|\mathbf{M}_o|^2 d}\cdot\sum_{\nu\mu}\frac{G_{\mu\nu}}{\Gamma_{\mu\nu}}\left\langle K_\mu^\dagger K_\nu\right\rangle e^{i(\tilde{\omega}_\mu^0-\tilde{\omega}_\nu^0)\tau}-\frac{E_o}{T_1}+i\frac{e^2\langle \mathbf{E}_{intra}\rangle}{|\mathbf{M}_o|^2 d\hbar\omega_B} \\
&\quad\cdot\sum_{\mu\nu\mu'}\left(\mathbf{G}_{\mu',\mu}G_{\mu\nu}\left\langle K_{\mu'}^\dagger K_\nu\right\rangle e^{i\left(\omega_{\mu'}^0-\omega_\nu^0\right)t}\right. \\
&\quad\left.-\mathbf{G}_{\mu',\nu}^* G_{\mu\nu}\left\langle K_\mu^\dagger K_{\mu'}\right\rangle e^{-i\left(\omega_{\mu'}^0-\omega_\mu^0\right)t}\right) \\
&= \frac{e^2\langle \mathbf{E}_{intra}\rangle}{|\mathbf{M}_o|^2 d}\cdot\sum_{\nu\mu}\frac{G_{\mu\nu}}{\Gamma_{\mu\nu}}\left\langle K_\mu^\dagger K_\nu\right\rangle e^{i(\tilde{\omega}_\mu^0-\tilde{\omega}_\nu^0)\tau}-\frac{E_o}{T_1}+i\frac{e^2\langle \mathbf{E}_{intra}\rangle}{|\mathbf{M}_o|^2 d\hbar\omega_B} \\
&\quad\cdot\sum_{\nu\mu'}\left(\mathbf{G}_{\mu'\nu}^2\left\langle K_{\mu'}^\dagger K_\nu\right\rangle e^{i\left(\omega_{\mu'}^0-\omega_\nu^0\right)t}-\mathbf{G}_{\mu',\nu}^2\left\langle K_\nu^\dagger K_{\mu'}\right\rangle e^{-i\left(\omega_{\mu'}^0-\omega_\nu^0\right)t}\right) \\
&= \frac{e^2\langle \mathbf{E}_{intra}\rangle}{|\mathbf{M}_o|^2 d}\cdot\sum_{\nu\mu}\frac{G_{\mu\nu}}{\Gamma_{\mu\nu}}\left\langle K_\mu^\dagger K_\nu\right\rangle e^{i(\tilde{\omega}_\mu^0-\tilde{\omega}_\nu^0)\tau}-\frac{E_o}{T_1} \\
&\quad-\frac{2e^2\langle \mathbf{E}_{intra}\rangle}{|\mathbf{M}_o|^2 d\hbar\omega_B}\cdot\mathrm{Im}\left\{\sum_{\nu\mu}\left(\mathbf{G}_{\mu\nu}^2\left\langle K_\mu^\dagger K_\nu\right\rangle e^{i(\omega_\mu^0-\omega_\nu^0)t}\right)\right\}.
\end{aligned}$$

But

$$\begin{aligned}
\left\{\sum_{\nu\mu}\left(\mathbf{G}_{\mu\nu}^2\left\langle K_\mu^\dagger K_\nu\right\rangle e^{i(\omega_\mu^0-\omega_\nu^0)t}\right)\right\}^* &= \left\{\sum_{\nu\mu}\left(\mathbf{G}_{\mu\nu}^2\left\langle K_\nu^\dagger K_\mu\right\rangle e^{-i(\omega_\mu^0-\omega_\nu^0)t}\right)\right\} \\
&= \left\{\sum_{\nu\mu}\left(\mathbf{G}_{\mu\nu}^2\left\langle K_\mu^\dagger K_\nu\right\rangle e^{i(\omega_\mu^0-\omega_\nu^0)t}\right)\right\}
\end{aligned}$$

and hence

$$\mathrm{Im}\left\{\sum_{\nu\mu}\left(\mathbf{G}_{\mu\nu}^2\left\langle K_\mu^\dagger K_\nu\right\rangle e^{i(\omega_\mu^0-\omega_\nu^0)t}\right)\right\}=0.$$

Thus, we have

$$\frac{d}{d\tau}\left[E_o+\frac{\langle \mathbf{P}_{intra}^2\rangle}{2\epsilon_0\epsilon}\right]=\frac{e^2\langle \mathbf{E}_{intra}\rangle}{|\mathbf{M}_o|^2 d}\cdot\sum_{\nu\mu}\frac{G_{\mu\nu}}{\Gamma_{\mu\nu}}\left\langle K_\mu^\dagger K_\nu\right\rangle e^{i(\tilde{\omega}_\mu^0-\tilde{\omega}_\nu^0)\tau}-\frac{E_o}{T_1}, \tag{5.14}$$

where $E_0+\frac{\langle \mathbf{P}_{intra}^2\rangle}{2\epsilon_0\epsilon}$ is the total energy of excitons. For the case where there is no dephasing or

Reproduced with permission of the copyright owner. Further reproduction prohibited without permission.

decay, then we have

$$\frac{d}{d\tau}\left[E_o + \frac{\langle \mathbf{P}^2_{intra} \rangle}{2\epsilon_0 \epsilon}\right] = 0,$$

which is what was found in Section 5.4.

Now, we turn to general case in which dephasing or decay time constants are finite. Under this situation, we must use the Eq. (5.14) to study the energy evolution of excitons. Fig. 5-20 is obtained in such a case, in which we can see the two curves corresponding to LHS and RHS of the Eq. (5.14) are exactly overlapped to within the plot resolution after the optical pulse is gone. Thus we can use Eq. (5.14) to understand the energy evolution in different cases.

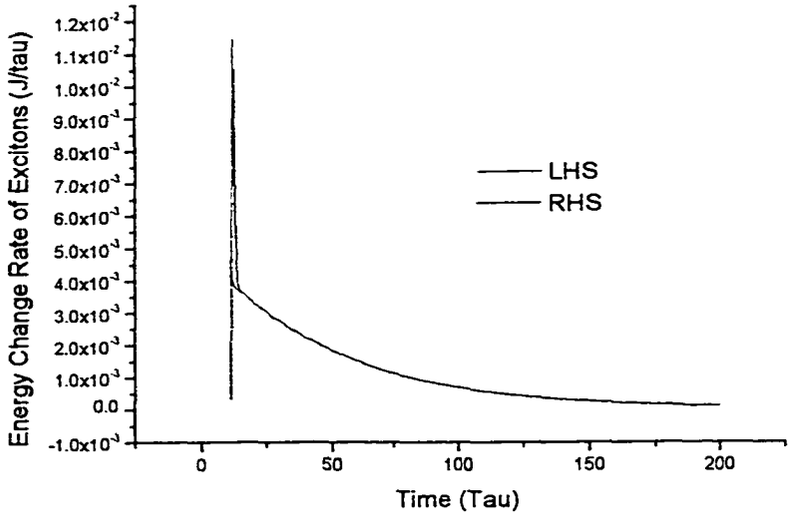

Figure 5-20: Rate of change of excitonic energy

Finally, we will try to get some more insight relevant to basis choice that has been already mentioned in Section 5.5.1. For this purpose, we set $T_1 = \infty$ but T_{2intra} is finite, which is more appropriate for real superlattice system. Using Eq. (5.14), we have,

Reproduced with permission of the copyright owner. Further reproduction prohibited without permission.

$$\frac{d}{d\tau}\left[E_o+\frac{\langle \mathbf{P}^2_{intra}\rangle}{2\epsilon_0\epsilon}\right] = \frac{e^2}{|\mathbf{M}_o|^2 dT_{2intra}}\sum_{\nu\neq\mu} G_{\mu\nu}\left\langle K^\dagger_\mu K_\nu\right\rangle e^{i(\tilde{\omega}^0_\mu-\tilde{\omega}^0_\nu)\tau}$$
$$= \frac{\langle \mathbf{E}_{intra}\rangle \langle \mathbf{P}_{THz}\rangle}{T_{2intra}}, \tag{5.15}$$

where

$$\langle \mathbf{P}_{THz}\rangle \equiv \frac{e^2}{|\mathbf{M}_o|^2 d}\sum_{\nu\neq\mu} G_{\mu\nu}\left\langle K^\dagger_\mu K_\nu\right\rangle e^{i(\tilde{\omega}^0_\mu-\tilde{\omega}^0_\nu)\tau}$$

is the Terahertz portion of the intraband polarization. That is, it is the portion coming from the intraband *coherences rather than populations*. Eq. (5.15) can be further written as,

$$\frac{dE_{Tot}}{d\tau} = \frac{e^2\langle \mathbf{E}_{intra}\rangle}{|\mathbf{M}_o|^2 dT_{2intra}}\cdot\sum_{\nu\neq\mu} G_{\mu\nu}\left\langle K^\dagger_\mu K_\nu\right\rangle e^{i(\tilde{\omega}^0_\mu-\tilde{\omega}^0_\nu)\tau}.$$
$$= \frac{\langle \mathbf{E}_{intra}\rangle}{T_{2intra}}\cdot\langle \mathbf{P}_{THz}\rangle. \tag{5.16}$$

From Eq. (5.16), we may see that if the coherences do not die out due to the basis problem as we already discussed in Section 5.5.1, then $\langle \mathbf{P}_{THz}\rangle$ in Eq. (5.16) will not disappear and will drive the excitonic energy forever. This is obviously a non-physical phenomenon.

5.6 Influence of the Relative Phase Shift between Excitons and Free Pairs

We have investigated the influence of a relative phase shift between excitons and free pairs in the coherent limit in Section 5.4.3. Now we examine the similar influence in cases where there is dephasing. Assuming the $E_{op} = 1.5\times10^{-3}$(GV/m) (other parameters are the same as those in Table 5.2), we may get the polarization of excitons with the different time delays T_s (This amounts to a phase difference in frequency space as we discussed in Section 5.4.3) as shown in Fig. 5-21.

From Fig. 5-21, it can be seen that the polarizations of excitons are driven in different directions due to the different phase shifts between excitons and free electron-hole pairs. This is similar to the results in the coherent limit discussed in Section 5.4.3. Thus we may finally

Reproduced with permission of the copyright owner. Further reproduction prohibited without permission.

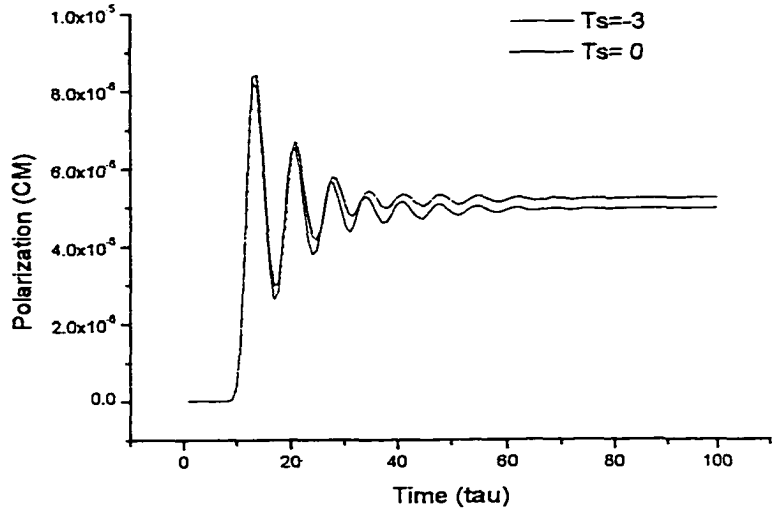

Figure 5-21: Polarization of excitons driven by polarization of free pairs with different Ts in dephasing system

arrive at whether in the coherent or non-coherent case, the 1s excitons and free electron-hole pairs do exchange energies when an average phase shift between them. Such an effect could perhaps be observed experimentally, and would be a nice way to investigate the interaction. Note, however, that the shift of the polarization is quite small as compared to those of Fig. 5-15. The same thing is found when the effect of E_c is investigated (not shown). This is essentially due to the effect of rapid dephasing, which quickly kills the energy exchange. The shifts shown appear to be smaller than the experimentally obtained ones by almost an order of magnitude. It is not clear why the experimentally observed polarization changes are so large relative to the calculated results.

Reproduced with permission of the copyright owner. Further reproduction prohibited without permission.

Chapter 6

Conclusions

In this work, the Self-consistent driven Bloch oscillations due to different types of charge carriers in a photoexcited semiconductor superlattice were investigated. The emphasis was placed on the study of SCD BO with the full dynamics of these charge carriers and their interactions. After examining the advantages and disadvantages of a variety of approaches such as SBEs and DCTs, we based our calculations on a recently-developed Quasi-bosonic treatment by which we could study the SCD BO to infinite order in optical field and without loosing the crucial intraexcitonic electron-hole correlations.

In Chapter 4, we presented a model to account for the influence of the unbound continuum excitonic states on the 1s excitons as described in Chapter 3. In this model, the influence of free electron-hole pairs were calculated to represent the influence of unbound continuum excitonic states. Some reasonable approximations were made to simplify the very intensive calculations due to the continuum nature of these unbound excitonic states. Using Heisenberg equation of motion, we derived the equations of motion for the electron-hole pairs with the Hamiltonian for electron-hole pairs in the superlattice potential in the presence of the external optical and terahertz electric fields. Some results in a few limiting cases were calculated to demonstrate the validity of numerical calculations by comparison with analytical results in these cases.

With the theories concerning excitons in chapter 3 and free electron-hole pairs in chapter 4, the SCD BO were studied in Chapter 5. The main purpose of this chapter was to study the interaction between excitons and free electron-hole pairs, and then connect the theoretical model with the experimental results recently reported. Before the study of the superlattice

Reproduced with permission of the copyright owner. Further reproduction prohibited without permission.

system with dephasing, we first focused on the SCD phenomena in the coherent regime, from which some basic mechanisms of SCD were obtained and discussed. We showed that 1s excitons can exchange energy with the electric fields due to other types of charge carriers, eg., the free electron-hole pairs discussed in this work. One direct conclusion we may draw from this result is that the average dipole of the two sets of charge carriers (1s excitons and free electron-hole pairs) can vary in time due to the exchange of energy. This was demonstrated by numerical calculations in this work. Thus a quasi-DC current due to the excitons can be generated which is opposed by a similar current due to the free electron-hole pairs. If the continuum carriers are assumed to be in contact with the doped reservoirs at the superlattice ends, then no quasi-DC polarization will build up due to these carriers to oppose the polarization due to the 1s excitons. We postulate that this is the mechanism that causes the quasi-linear change in the intraband polarization that is evidenced in recent experiments [48]. With the full quantum-mechanical model, we also studied the influence of different exciting laser frequencies. It is shown that the free electron-hole pairs excited by different laser frequencies do drive the polarization due to 1s excitons in different directions. However, the slope of these directions does not change signs as in the experiment. In the present, we can not account for such a disagreement and are still in the process of trying to solving this problem. Also in the coherent limit, we studied the polarization of 1s excitons driven by the electric fields from free electron-hole pairs that have an average phase shift relative to the 1s excitons. In this case, the electric fields due to free pairs can drive the polarization of 1s excitons in the directions with the slopes of different signs. This is a promising avenue for future experimental work. Finally, we turned to the more realistic case of the superlattice systems with dephasing. In such systems, energy evolution of the system was investigated and was shown to be in agreement with the analytical solutions in some cases. All other SCD BO phenomena studied in the coherent limit are generally applicable in non-coherent cases.

Although this work was mainly motivated by the recently reported experimental results of *F. Löser et al.* [48], the work we presented goes beyond that situation and provides some useful points in understanding the dynamics of interaction mechanisms of different types of charge carriers in a photoexcited superlattice system. Future work may include, among others, the study of the problem of driving directions as mentioned earlier; the interaction of 1s excitons

Reproduced with permission of the copyright owner. Further reproduction prohibited without permission.

with other types of carriers, eg. excitons beyond 1s excitons, scattering phonons etc; the all quantum-mechanical treatment of the dephasing time constants and DFWM results.

Reproduced with permission of the copyright owner. Further reproduction prohibited without permission.

Bibliography

[1] F. Bloch, Z. Phys. **52**, 555 (1928).

[2] C. Zener, Proc. R. Soc. London Ser. A **145**, 523 (1934).

[3] N. W. Ashcroft and N. D. Mermin, Solid State Physics (Holt, Rinehart, and Winston, Philadelphia, 1976), pp. 213-225.

[4] H. M. James, Phys. Rev. **76**, 1611 (1949).

[5] Fritz Henneberger, Stefan Schmitt-Rink and Ernst O. Göbel, *Optics of Semiconductor Nanostructures*(Akademie Verlag GmbH, Berlin, 1993), pp 186.

[6] M. Dignam, J. E. Sipe, and J. Shah, Phys. Rev. B **49**, 10502 (1994).

[7] G. H. Wannier, Phys. Rev. **117**, 432 (1969).

[8] Ortiz and Martin, Phys. Rev. B **43,** 14202 (1994).

[9] King-Smith and Vanderbilt, Phys. Rev. B **47,** 1651 (1993).

[10] A. G. Chynoweth, G. H. Wannier, R. A. Logan, and D. E. Thomas, Phys. Rev. Lett. **5**, 57 (1960).

[11] V. S. Vavilov, V. B. Stopachinskii, and V. S. Chanbarisov, Sov. Phys. Sol. States **8**, 2126 (1967).

[12] S. Maekawa, Phys. Rev. Lett. **24**, 1175 (1970).

[13] R. W. Koss, and L. M. Lambert, Phys. Rev. **B5**, 1479 (1972).

Reproduced with permission of the copyright owner. Further reproduction prohibited without permission.

[14] L. Esaki and R. Tsu, IBM J. Res. and Dev. **14**, 61 (1970).

[15] L. Esaki and R. Tsu, IBM J. Res. and Dev. **61**, 61 (1970).

[16] P. W. A. McIlroy, J. Appl. Phys. **59**, 3532 (1986).

[17] E. Cota, J. V. José, and G. Monsiváis, Phys. Rev. **B35**, 8929 (1987).

[18] E. E. Mendez, F. Agulló-Rueda, and J. M. Hong, Phys. Rev. Lett. **60**, 2426 (1988).

[19] P. Voisin, J. Bleuse, C. Bouche, S. Gaillard, C. Alibert, and A. Regreny, Phys. Rev. Lett. **61**, 1639 (1988).

[20] J. Bleuse, P. Voisin, M. Allovon, and M. Quillec, Appl. Phys. Lett. **53**, 2632 (1988).

[21] M. M. Dignam, and J. E. Sipe, Phys. Rev. **B43,** 4097 (1991).

[22] G. Bastard and R. Ferreira, in Spectroscopy of Semiconductor Microstructures, Vol. **206** of NATO Advance Study Institute, Series B: Physics, eds. G. Fasol and A. Fasolino, 333 (Plenum Press, New York 1989).

[23] G. von Plesson and P. Thomas, Phys. Rev. B45, 9185 (1992).

[24] J. Feldmann, K. Leo, J. Shah, D. A. B. Miller, J. E. Cunningham, T. Meier, G. von Plessen, A. Schulze, P. Thomas, and S. Schmitt-Rink, Phys. Rev. B **46**, 7252 (1992).

[25] K. Leo, P. Haring Bolivar, F. Brüggemann, R. Schwedler, and K.Köhler, Solid State Comm. **84**, 943 (1992).

[26] C. Waschke, H. G. Roskos, R. Schwedler, K. Leo, H. Kurz, and K. Köhler, Phys. Rev. Lett. **70**, 3319 (1993).

[27] V. G. Lyssenko, G. Valusis, F. Löser, T. Hasche, K. Leo, M. M. Dignam, and K. Köhler, Phys. Rev. Lett. **79**, 301 (1997).

[28] M. Sudzius, V. G. Lyssenko, F. Löser, K. Leo, M. M. Dignam, and K. Köhler, Phys. Rev. **B57**, 12673 (1998).

Reproduced with permission of the copyright owner. Further reproduction prohibited without permission.

[29] See *e.g.,* H. Haug and S. W. Koch, *Quantum Theory of the Optical and Electronic Properties of Semiconductors* (World Scientific, Singapore, 1994), Third Edition.

[30] Jörg Hader, Torsten Meier, Stephan W. Koch, Fausto Rossi, and Norbert Linder, Phys. Rev. B **55**, 13799 (1997).

[31] T. Meier, G. von Plessen, P. Thomas, and S. W. Koch, Phys. Rev. Lett. **73**, 902 (1994).

[32] T. Meier, G. von Plessen, P. Thomas, and S. W. Koch, Phys. Rev. B **51**, 14490 (1995).

[33] T. Meier, F. Rossi, P. Thomas, and S. W. Koch, Phys. Rev. Lett. **75**, 2558 (1995).

[34] M. M. Dignam, Phys. Rev. **B59**, 5770 (1999).

[35] T. Meier *et al.*, Physics of Low-Dimensional Structures **3/4**, 1 (1998).

[36] V. M. Axt, and A. Stahl, Z. Phys. **B93**, 195 (1994).

[37] K. Victor, V. M. Axt, and A. Stahl, Phys. Rev. B **51**, 14164 (1995).

[38] V. M. Axt, G. Bartels, and A. Stahl, Phys. Rev. Lett. **76**, 2543 (1996).

[39] J. Schlösser, C. Neumann, and A. Stahl, J. Phys. : Cond. Matter **4**, 121 (1992).

[40] S. Schmitt-Rink *et al.*, Phys. Rev. **B46**, 10460 (1992).

[41] U. Siegner *et al.*, Phys. Rev. **B46**, 4564 (1992).

[42] M. Lindberg, R. Binder, and S. W. Koch, Phys. Rev. Rev. **A45**, 1865 (1992).

[43] M. Wegner, D. S. Chemla, S. Schmitt-Rink, W. Schäfer, Phys. Rev. **A42**, 5675 (1990).

[44] P. H. Bolivar, F. Wolter, A. Müller, H. G. Roskos, and H. Kurz, Phys. Rev. Lett. **78**, 2232 (1997).

[45] Margaret Hawton and Delene Nelson, Phys. Rev. B **57**, 4000 (1998).

[46] J. M. Lachaine, Margaret Hawton, J.E. Sipe, and M. M. Dignam, Phys. Rev. **B62**, R4829-4832 (2000).

[47] M. M. Dignam, M. Hawton, and Sawlor, to be submitted.

Reproduced with permission of the copyright owner. Further reproduction prohibited without permission.

[48] F. Lõser, M. M. Dignam, Yu. A. Kosevich, K. Köhler, and K. Leo, Phys. Rev. Lett. **85**, 4763 (2000).

[49] Paula Feuer, Phys. Rev. **88**, 92 (1952).

[50] J. Bleuse, G. Bastard, and P. Voisin, Phys. Rev. Lett. **60**, 220 (1988).

[51] J. P. Hagon, and M. Jaros, Phys. Rev. **B41**, 2900 (1990).

[52] B. Soucail *et al.*, Phys. Rev. **B41**, 8568 (1990).

[53] F. Bentosela, *et al.*, Commun. Math. Phys. **88**, 387 (1983).

[54] D. Emin, and C. F. Hart, Phys. Rev. **B36**, 7353 (1987).

[55] Leonard Kleinman, ibid. **41**, 3857 (1990).

[56] D. Emin2, C. F. Hart, ibid. **41**, 3859 (1990).

[57] A. Nenciu, and G. Nenciu, Phys. Rev. **B40**, 3622 (1989).

[58] M. M. Dignam, and J. E. Sipe, Phys. Rev. Lett. **64**, 1797 (1990).

[59] M. M. Dignam, and J. E. Sipe, Phys. Rev. **B41**, 2865 (1990).

[60] R. H. Yan, F. Laruelle, and L. A. Coldren, Appl. Phys. Lett. **55**, 2002 (1989).

[61] D. M. Whittaker, Phys. Rev. **B41**, 3238 (1990).

[62] D. M. Whittaker *et al.*, Phys. Rev. **B42**, 3591 (1990).

[63] F. Agulló-Rueda, J. A. Brum, E. E. Mendez, and J. M. Hong, Phys. Rev. **B41**, 1676 (1990).

[64] F. Agulló-Rueda, E. E. Mendez, and J. M. Hong, Phys. Rev. **B40**, 1357 (1989).

[65] E. E. Mendez, F. Agulló-Rueda, E. E. Mendez, and J. M. Hong, Appl. Phys. Lett. **56**, 2545(1990).

[66] R. P. Leavitt, and J. W. Little, Phys. Rev. **B41**, 5174 (1990).

Reproduced with permission of the copyright owner. Further reproduction prohibited without permission.

[67] Xide Xie, Dong Lu, *Energy Band Theory of Solids* (Fudan University Press, Shanghai, 1998).

[68] G. H. Wannier, in: Elements of Solid State Theory, Cambridge Univ. Press., 1959, p. 190.

[69] R. F. Kazarinov, and R. A. Suris, Sov. Phys. Semicond. **6**, 120 (1972).

[70] R. Tsu, and G. Döhler, Phys. Rev. **B12**, 680 (1975).

[71] C. Y. Fong, R. F. Gallup, L. Esaki, and L. L. Chang, Superlatt. and Microstruct. **7**, 147 (1990).

[72] J. B. Xia, and K. Huang, J. Phys.: Condens. Matter **3**, 4639 (1991).

[73] M. H. Degani, Appl. Phys. Lett. **59**, 57 (1991).

[74] Walter L. Bloss, J. Appl. Phys. **65**, 4789 (1989).

[75] J. A. Brum, and F. Agulló-Rueda, Surf. Sci. **229**, 472 (1990).

[76] R. P. Leavitt, and J. W. Little, Phys. Rev. **B42**, 11784 (1990).

[77] N. W. Ashcroft and N. D. Mermin, Solid State Physics (Holt, Rinehart, and Winston, Philadelphia, 1976), pp. 176-190.

[78] D. M. Whittaker, Europhys. Lett. **31**, 55 (1995).

[79] N. Linder, Phys. Rev. **B55**, 13664 (1997).

[80] S. Glutsch, P. Lefebvre, and D. S. Chemla, Phys. Rev. **B 55**, 15786 (1997).

[81] T. Kuhn, F. Rossi, Phys. Rev. **B46**, 7496 (1992).

[82] S. Schmitt-Rink, D. S. Chemla, Phys. Rev. Lett. **57**, 2752 (1986).

[83] C. Stafford, S. Schmitt-Rink, W. Schäfer, Phys. Rev. **B41,** 10000 (1990).

[84] E. Hanamura, and H. Haug, Phys. Rep. **33**, 210 (1977).

[85] T. Usui, Prog. Theor. Phys. **23**, 787 (1960).

Reproduced with permission of the copyright owner. Further reproduction prohibited without permission.